Geoscience BC Publication 2024-07

Characterization and Bench Scale Testing of Rare Earth Elements from East Kootenay Coalfields

V.K. Kuppusamy, M.L. Mackay, P. Aboagye, M.E. Holuszko, NBK Institute of Mining Engineering, The University of British Columbia, Vancouver, British Columbia.

Table of Contents

Characterization and Bench Scale Testing of Rare Earth Elements from East Kootenay Coalfields

V.K. Kuppusamy, NBK Institute of Mining Engineering, The University of British Columbia, Vancouver, British Columbia, vinothkumar@alumni.ubc.ca

M.L. Mackay, NBK Institute of Mining Engineering, The University of British Columbia, Vancouver, British Columbia

P. Aboagye, NBK Institute of Mining Engineering, The University of British Columbia, Vancouver, British Columbia

M.E. Holuszko, NBK Institute of Mining Engineering, The University of British Columbia, Vancouver, British Columbia

---

Abstract

As global society moves towards a low-carbon economy, secure access to raw materials becomes the key bottleneck in achieving a green transition. Alternative resources such as coal-based materials have been evaluated for rare earth production in recent years to reduce import dependence. This study has been conducted to evaluate the potential of using metallurgical coal-based materials from the East Kootenay coalfields in British Columbia as a source for rare earth elements. Further, enrichment of REE in the plant feed sample was also conducted using bench-scale physical separation techniques including density separation, wet high intensity magnetic separation, gravity separation using Knelson concentrator, and flotation. Finally, preliminary evaluation of REE extraction from the plant feed sample was also tested using direct acid leaching and acid baking followed by water leaching technique.

The investigation involved the collection of more than 100 raw coal samples to develop a database for identifying potentially elevated REE contents in East Kootenay coalfields. Further, plant samples were also collected from coal preparation plant to assess the concentration of REE from coal related feed material. It was found that the concentration of REE in the samples tested is enriched relative to the average crustal abundance. The samples in this dataset contain a higher proportion of Light REE than Heavy REE. Out of 17 REE, the five elements (Ce, La, Nd, Y and Sc) accounted for more than 77% of the total REE present in these samples. When subjected to flotation, most of the REE (by wt.%) were deported to waste streams such as middlings and tailings due to the inorganic (mineral matter) association

of REE in the sample. Mineralogical examination identified more than one rare earth bearing mineral in the sample including apatite, monazite, xenotime, and zircon. Among the different physical separation technique tested in this study, flotation exhibited the most promising technique for concentration of REE in the samples tested. Further, direct extraction of REE using leaching was also conducted and presented in the study.

1.0 Introduction

To slow global warming and build resilience to climate change, 196 countries have adopted the Paris Agreement in 2015 to limit warming to 1.5 degree Celsius (United Nations, 2015). In this regard, energy transition to renewables and related technologies have become a key solution to tackle the climate emergency as well as to achieve energy security for sustaining and growing the economies around the world. According to International Renewable Energy Agency (IRENA), six technological avenues can help us to achieve 2050 carbon emission target to meet the Paris accord which includes: 1) Renewables: electricity generation from wind, solar, hydro etc., 2) Energy conservation and efficiency: Reducing energy demand and increasing the energy efficiency of end-use applications 3) End-use Electrification: direct use of clean electricity in heat & transport applications 4) Hydrogen: use of green hydrogen as fuel for shipping, steel, aviation etc., 5) Bioenergy: use of biomass coupled with carbon capture in power & industrial sector 6) Carbon capture and storage: Capturing and storing of CO_2 emissions in cement, steel industries etc.

To meet the Paris Agreement targets, the installed generation capacity of renewable energy will need to expand by about ten-fold from around 2.8 terawatt (TW) in 2020 to over 27.7 TW in 2050 (IRENA, 2021). This energy transition at global scale can increase the demand for certain minerals and metals in a substantial way. For example, the demand for Rare Earth Elements (REE), which includes 15 lanthanides and 2 transition elements Scandium and Yttrium, will increase by sevenfold in 2040 (IEA, 2022). The role of critical minerals in clean energy transition is described in detail elsewhere (IEA, 2022).

The increased supply risk of certain raw materials to meet the future demand due to increased geopolitical, geological, environmental risks, and complex market dynamics are termed as critical elements (Nieto & Zhang, 2013; Pavel et al., 2017). REE are classified as critical elements by various countries including United States of America, Countries of Europe, United Kingdom, and Canada (European Commission, 2020; National Resources Canada, 2021; U.S. Department of Energy, 2022;

British Geological Survey, 2021). To mitigate the risk, both public and private entities are looking to find the alternate resource and supply chain dynamics.

Coal deposits are known to contain most of the elements in the periodic table in trace amounts (Swaine, 1990). Due to certain favourable conditions, some of the coal deposits contains enriched concentration of specific valuable trace elements, which are termed as coal hosted metal deposits or metalliferous coal (Dai et al., 2016; Seredin & Finkelman, 2008). During early 90's, the enriched concentrations of REE in far Eastern Russian Coal deposits were first documented (Seredin, 1996). Since then, various coal deposits with enriched concentrations of REE have been discovered around the world (Birk & White, 1991; Dai et al., 2007, 2008; Hower et al., 1999).

Among the various unconventional resources, coal and related products have been viewed as a potential source for REE to meet the future demand (Dai & Finkelman, 2018). More specifically, the assessment of select United States (US) coal deposits using United States Geological Survey (USGS) coal database have shown that coal and associated waste materials have the potential to be viable source for REE (Bryan et al., 2015). Based on the initial assessment findings, US Department of Energy (USDOE) has initiated multi-year research and development program to demonstrate the technical and economic feasibility of extracting and recovering REE from US based coal resource materials with the program funding of at least 15 million US dollars every year since 2015 (US Department of Energy, n.d.).

In 2021, Canada produced around 42 million tonnes of coal, and most of the production is used for metallurgical purposes. More than 95% of the production came from three Western provinces: British Columbia (48%), Alberta (32%), and Saskatchewan (16%). Among the provinces, British Columbia produces the most steel-making coal of metallurgical quality, and it represents a value of about $12.2 billion in 2022, which accounts for around 67% of the total mineral revenue in the province. There is a potential opportunity to use the already being mined metallurgical coal deposits of British Columbia (BC) as a source for co-extracting REE. Data indicating the presence of REE in some Canadian coal deposits, especially in BC coalfields exists (Goodarzi, 1988; Birk and White, 1991; Goodarzi et al., 2009), however, there is no proper quantification, characterization, and extraction process currently available for developing coal deposits in BC or for other coal deposits across Canada.

Co-extraction of REE from coal-based source materials offer additional benefits compared to traditional rare earth ore deposits including reduced land disturbance, decreased environmental impact due to lower radionuclide concentration in the coal source, and also providing economic advantage with no additional

mining cost due to co-production with coal (Alipanah et al., 2020; Eterigho-Ikelegbe et al., 2021; W. Zhang et al., 2020).

2.0 Objectives

The main purpose of this study is to characterize and quantify the REE and their mode of occurrence in the East Kootenay coal deposits and to study the possible extraction of these elements using bench scale testing methods. **Figure 1** shows the location of East Kootenay Coalfield in Southeast (S.E) British Columbia. The assessment will be performed by creating a MS Access database of REE distribution, one similar to USGS COALQUAL database, but simplified version focusing on REE in the study area. To achieve the objective, the following sub-objectives are proposed:

- To compile the data base of rare earth concentration in East Kootenay coalfield by analyzing the field collected samples.

- To enrich the REE in the select coal related feed source using bench scale physical separation methods.

3.0 Material and Methods

3.1 Study Area

In this study, samples were collected from East Kootenay coalfield. The East Kootenay coalfield is located in southeastern British Columbia (Figure 1) and extends from the Montana-British Columbia border to the Elk lakes, some 30km north of Elkford, BC (Mills et al., 2016). It is comprised of three separate coalfields: Elk Valley coalfield, Crowsnest coalfield, and Flathead coalfield (Grieve, 1993).

Coal seams in the East Kootenay coalfields are largely of metallurgical quality, and predominantly classified as medium volatile bituminous coals with volatile matter that ranges from 20.7 to 33%. Furthermore, these coals are characterized by a low Sulphur content (Gibson, 1985; Holuszko, 1994). It is estimated that the mineable coal resource in the Kootenay coalfield is 8 billion tonnes (BC Ministry of Energy, Mines and Low Carbon Innovation, 2021).

3.2 Samples and Preparation

Samples used in this assessment were obtained from a variety of seam exposures and coal preparation plants. The samples were gathered from operating mines and plants by site geologists and plant operators.

For raw coal samples, approximately 10 to 20 kg were collected, whereas for plant samples approximately 50 kg were gathered for this study. To develop the REE database, coal seam samples were collected along with respective roof and floor samples. Total of more than 100 samples were collected and they were double bagged, sealed, and shipped to the Coal and Mineral Processing laboratory at the University of British Columbia in Vancouver. **Figure 2** shows the sampling locations at the plant.

For raw coal samples, top particle size was generally below 75 mm (3") for most of the samples. For the samples collected from plant, the particle size of samples was grouped into 3 categories: coarse (-50 + 1mm), medium (-1 mm + 0.15 mm) and fine (-0.15 mm) depending on the beneficiation technique used in the coal preparation plant. It should be noted that the particle size of the plant samples was general guideline but does not reflect the actual size ranges adopted in the processing plant.

Representative samples were obtained for testing following the standard procedure for coal sample preparation D2013/D2013M-12 (ASTM, 2012a). The sample preparation is explained below and schematically shown in **Figure 3**. In short, raw coal samples were screened using 1" inch (25.4 mm) sieve. The samples coarser than 1" inch (25.4 mm) size was crushed using Jaw crusher (**Figure 4A**) to obtain 100% passing 1" inch (25.4 mm) size. **Figure 4B** shows the crusher plates of the jaw crusher used in this study. The crushed sample was mixed the remaining samples and homogenized by mixing the samples thoroughly. The homogenized sample was split into 2 portions using riffle splitter. Except for the samples which were further processed, the remaining samples were double bagged and stored in a closed bucket to avoid sample degradation for future use.

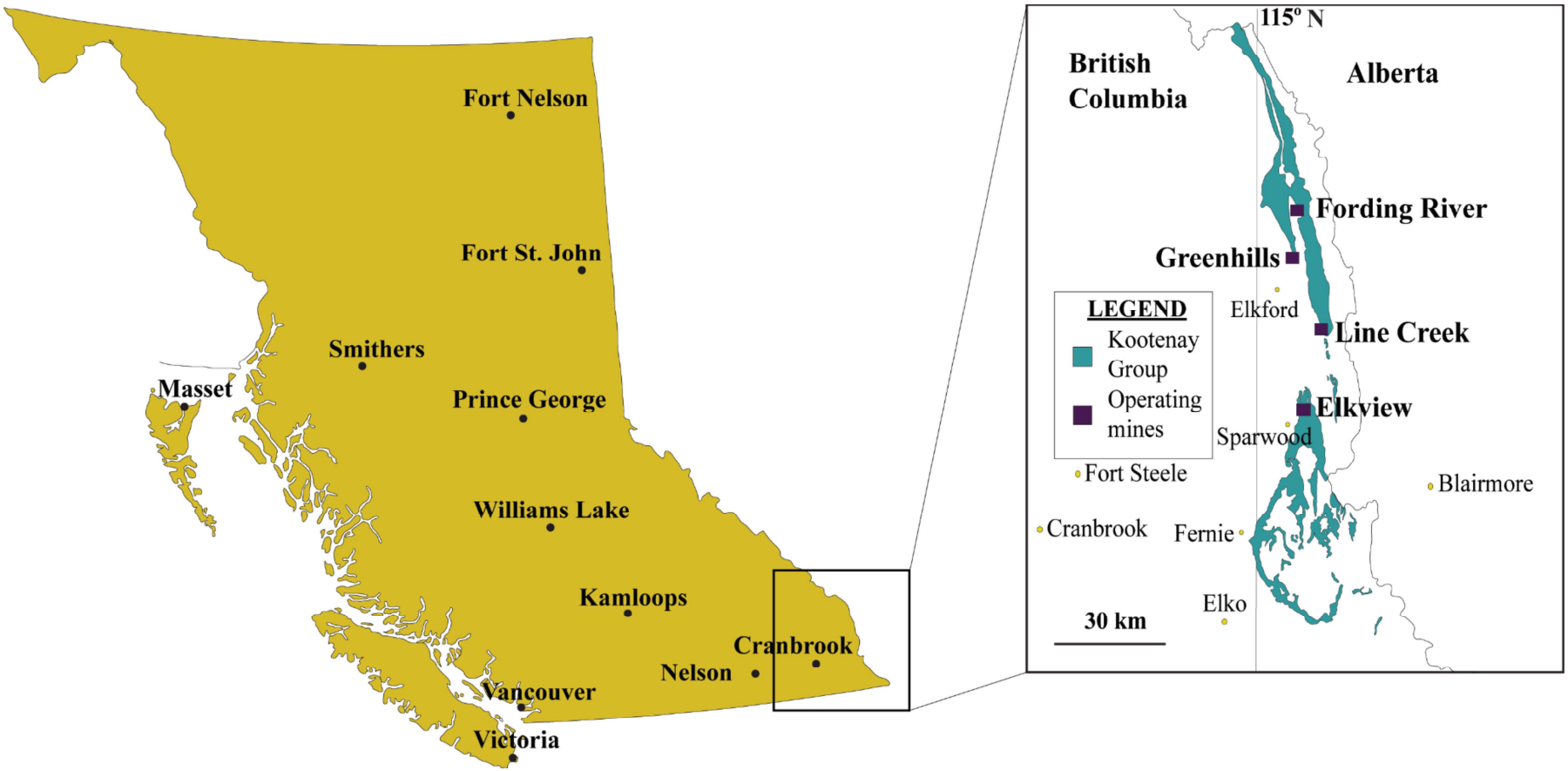

Figure 1 Location of East Kootenay coalfields and coal mines in the Southeastern BC (Adapted from BC Ministry of Energy and Mines, 2015 and BC Ministry of Energy and Mines, 2016)

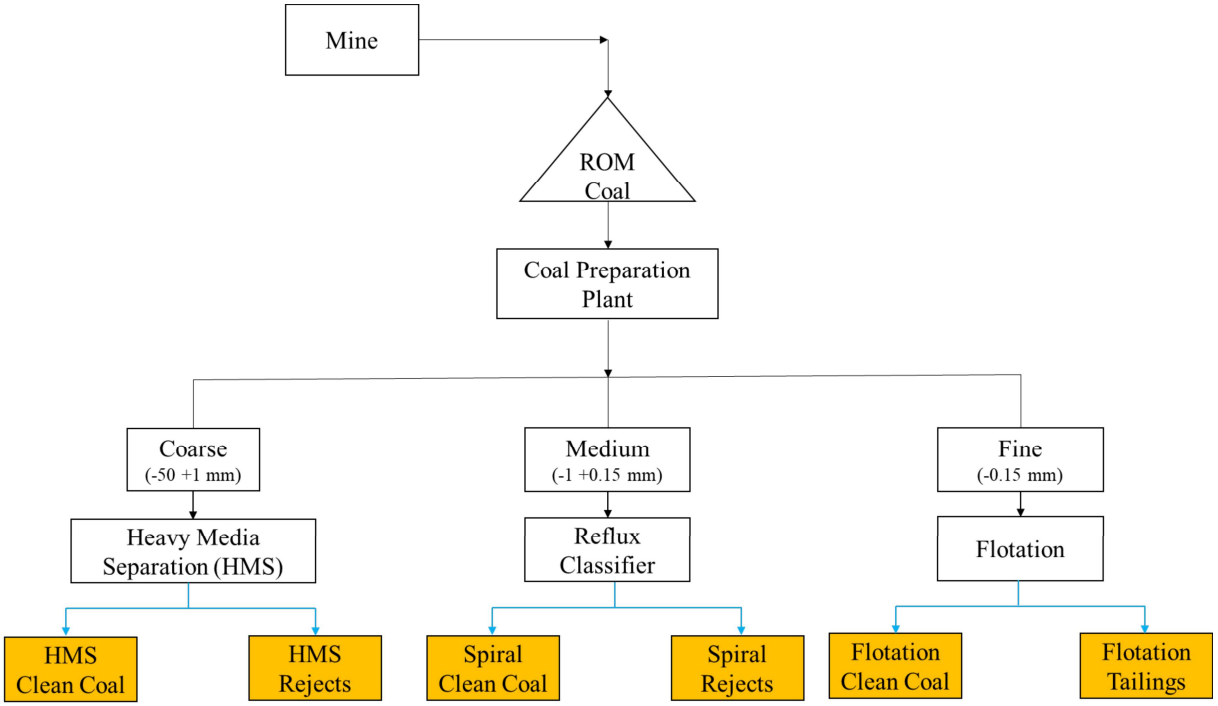

Figure 2. Sampling points at the coal preparation plant

The -1" inch (25.4 mm) sample were further crushed using hammer mill (**Figure 4C**) passing 4.75 mm and riffle spilt into 5 kg representative sample batches. Each was labeled appropriately, double bagged, and stored in closed buckets for use. Depending on the requirements, these 5 kg sample batches were further crushed or split to obtain representative sample of required size for analysis.

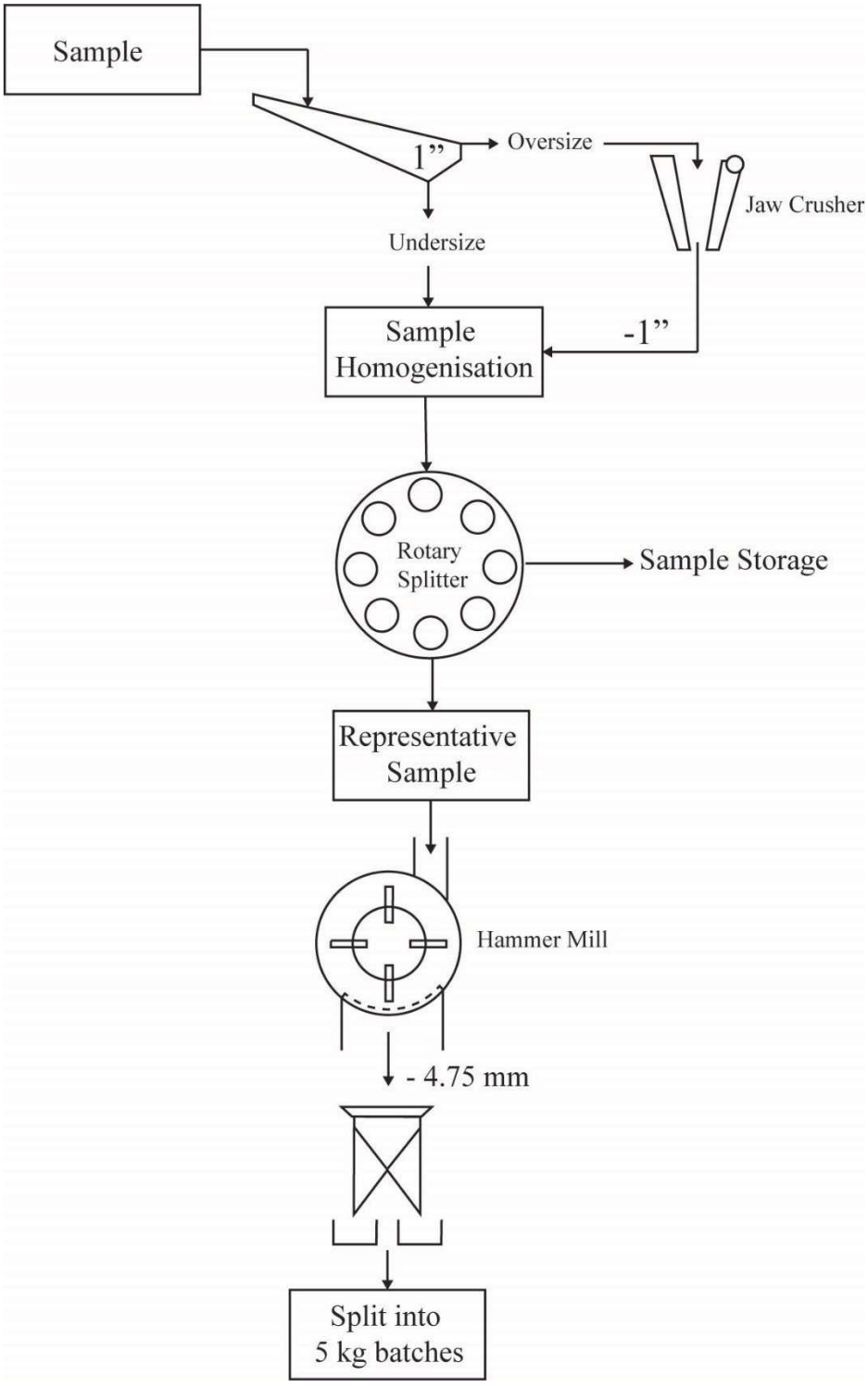

Figure 3 Schematics of sample preparation for analysis

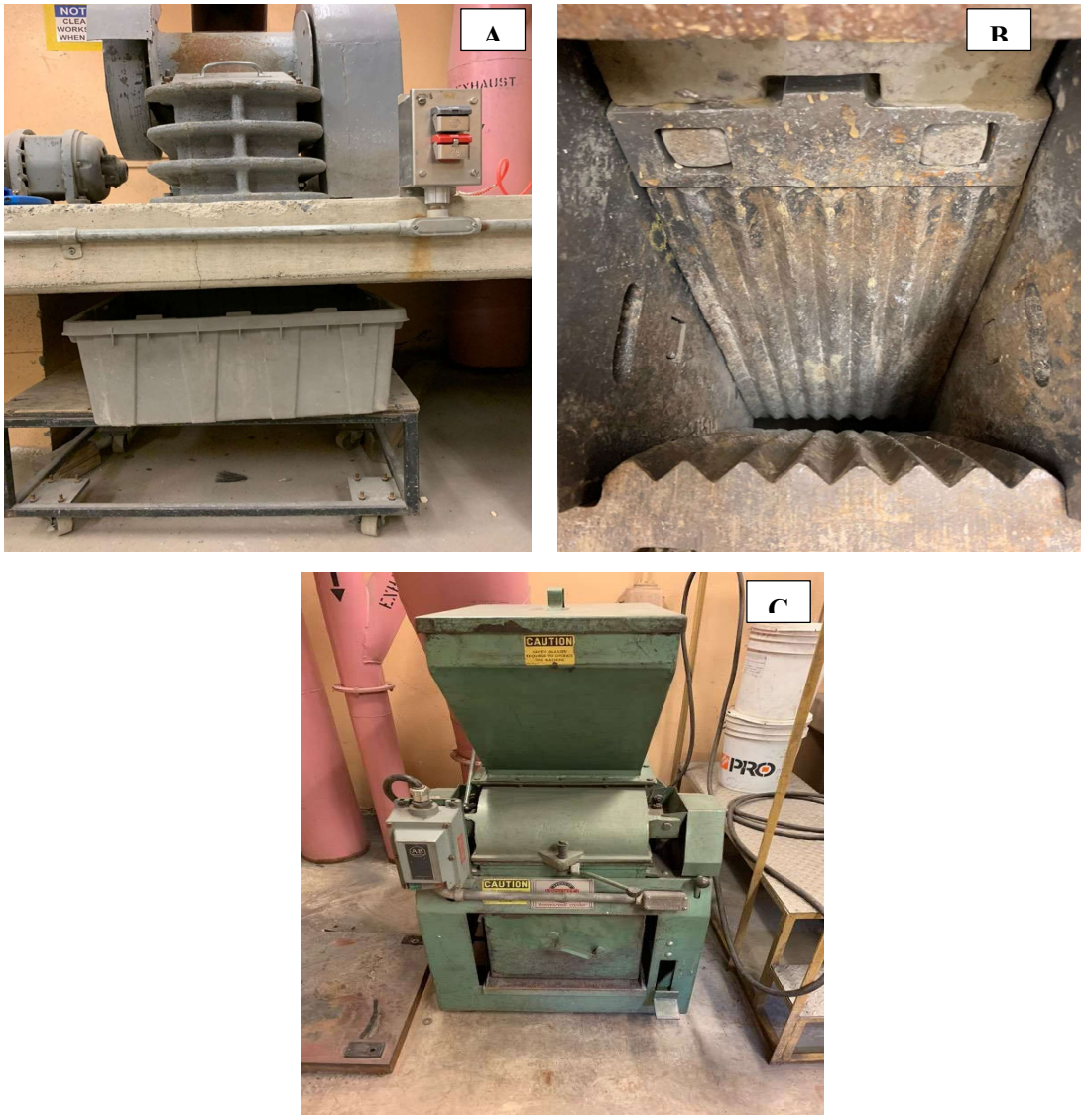

Figure 4. Crusher used in the sample preparation: A) Jaw crusher B) Jaw crusher plates C) Hammer mill

3.3 Sample Characterization

3.3.1 Proximate Analysis

Proximate analysis was conducted on representative samples in duplicates using the ASTM standard methods (ASTM, 2012b, 2013, 2017a, 2017b) for all the samples listed in the database.

The moisture content of the sample was determined by weight loss resulting from oven-drying of a 1 g sample in a dry crucible at 104 – 110 ˚C for 1 hour. The moisture content was calculated as follows:

Moisture content (%): $(\frac{W_i - W_f}{W_i})*100$

Where W_i represents the initial weight of the sample used (g), and W_f denotes the weight of the sample after heating (g).

To determine the ash content, the dried sample from the moisture analysis was gradually heated in a ventilated furnace to reach a temperature of 500 $\pm$ 10 ˚C at the end of 1 hour. Further, the temperature of the furnace was increased to reach 750 $\pm$ 15 ˚C at the end of 2 hour. The sample was maintained at 750 $\pm$ 15 ˚C for an additional 2 hours, or until the mass of the residue reached constant weight. The mass of the residue was divided by the initial dried sample mass to obtain the ash content. The ash content of the sample was computed as follows:

Ash content (%): $(\frac{W_c - W_e}{W_s})*100$

Where W_c represents the weight of capsule, cover, and ash (g), W_e denotes the weight of the empty capsule and cover (g), and W_s is weight of sample used for analysis.

The volatile matter of the sample was determined by mass loss resulting from heating 1 g sample in a dry crucible at 950 $\pm$ 20˚C for 7 min. The calculated mass loss was corrected for moisture content to obtain volatile matter. The volatile matter of the sample was determined as follows:

Mass loss (%): $(\frac{W_i - W_f}{W_i - W_e})*100$

Where W_e denotes the weight of the empty capsule and cover (g), W_i represents the weight of capsule, cover, and sample before heating (g), and W_f is weight of capsule, cover, and sample after heating (g).

Volatile matter (%): Mass loss (%) – Moisture content (%)

Fixed carbon was calculated by subtracting the percentages of moisture, ash, and volatile matter from 100. The relation used for computing fixed carbon is shown below:

Fixed carbon (%): 100 – [Moisture (%) + Ash (%) + Volatile matter (%)]

3.3.2 Tree Release Analysis

The tree release analysis procedure can be used to generate a theoretical optimum separation performance curve for the flotation process, which is used for cleaning fine coal (Mohanty et al., 1998). This procedure was followed from the Australian Standards AS 4156.2.2 – 1998 (R2013) (Standards Australia, 1998). In this analysis, the coal is floated to obtain a clean coal concentrate and tailings. The flotation products (concentrate and tailings) are subjected to flotation individually to obtain successive concentrates and tailings in branches (see **Figure 5**). The ash content and yield of the final products are experimentally determined and presented as cumulative yield vs. ash plot. By increasing the number of branches, the

accuracy of the separation curve is increased (Laskowski, 2001; Mohanty et al., 1998). The resulting samples will be represented by a series of products from a low- to high-ash content, which will provide an assessment of the floatability of the coal. The release analysis is carried out under an ideal condition (reagent addition is in excess) and coal is floated to exhaustion to obtain the cleanest, middle range and dirtiest in terms of ash particles in the consecutive products. In that sense it is treated as the methodology to assess migration of REE in the flotation by products. In this study, these products are analyzed for REE contents which will provide information on the association of the REE with the ash-forming minerals and possible enrichment, if any, in the flotation product streams, which is crucial information for the extraction of the REE from the coal.

Tree Release analysis was conducted for selected samples. For each test, a 300 g representative feed sample was crushed to obtain -500 μm with P_{80} (the size where 80% of particles in the sample are smaller than this size) of feed samples is 350 - 360 μm, which represents typical feed size to flotation at the plants. **Figure 6** shows the flotation setup used for TREE release analysis. Flotation tests were conducted in the 2-liter Denver laboratory cell with an initial solid content of 14.3%. pH of the natural slurry was used in the coal flotation test without any modification, which was generally in the range of 8 to 8.5. Coal was conditioned for 5 min with an impeller speed of 1300 rpm. Flotation reagent emulsion of 25 g/t of MIBC and 50 g/t of kerosene in 200mL of water was made using a high-speed laboratory blender and added to the flotation cell. Further, the coal slurry with reagents was conditioned for 15 min followed by another 25 g/t of frother addition and conditioning for 1 minute.

Oily collectors such as diesel and kerosene are used in the flotation of hydrophobic materials like coal, molybdenite etc. These oil-based reagents are insoluble in water and found to be not efficient in dispersing in slurry and adsorbing on particle surfaces, which results in high reagent consumption, long conditioning time and decreased flotation performance. Dispersing oily collectors into fine droplets through emulsification before being added to flotation cell has been found beneficial to improving flotation performance, reducing reagent consumption, and shortening flotation conditioning time (Yu et al., 1990, Chen and Peng, 2022). Hence, emulsification strategy was adopted in this study.
Using an aeration rate of 4-5 L/min of air, the concentrate was collected until the froth was barren, which was usually between 3 to 5 min of froth collection time. The initial products were successively floated individually into three levels of branches to obtain eight products as shown in **Figure 5**. The final products from the tree analysis were dried at 65˚C and weighed to obtain yield data and analyzed for ash content, as described in section 3.3.1. For each feed sample, the tree analysis was conducted in duplicates. Based on the ash content of the products, three products were selected with low-, medium-, and high-ash to find REE concentration in the flotation products.

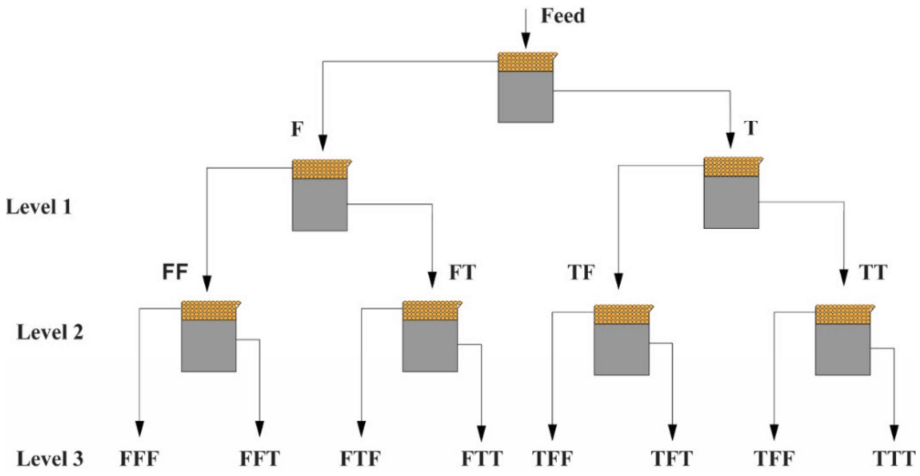

Figure 5. Schematic diagram of tree analysis procedure. In this test, coal sample (Feed) was first separated using flotation into Float (F) and Tailings T) (Level 1). In the second stage (Level 2), both Float (F) and Tailings (T) were re-floated separately to obtain 4 products: Float (FF), Tailings (FT), and Float (TF), Tailings (TT) respectively. In the third stage (Level 3), the 4 products from the second stage were again floated to obtain final Products (FFF to TTT). Yellow bubble and grey portion in the figure represent froth and tailings obtained during flotation respectively.

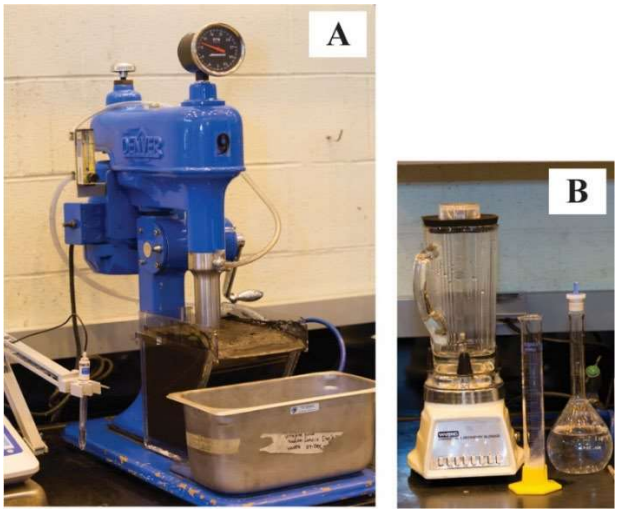

Figure 6. Flotation set up used for TREE release analysis A) Denver cell and B) High speed blender used for emulsion preparation

3.3. Sequential Extraction

Trace elements in coal can be associated with organic and inorganic matter or both (Finkelman, 1981; Swaine, 1990). Inorganic association can be different forms such as silicates, sulfides, carbonates, oxides,

phosphates, selenides, and halides. Understanding the mode of occurrence of trace elements helps to follow these elements during coal preparation, combustion, and waste disposal, as well as during the extraction of valuable metals (Dai et al., 2012; Equeenuddin et al., 2016; Finkelman, 1994, 2004; Zhang et al., 2015). There are different methods to identify the mode of occurrence of trace elements in coal, including scanning electron microscope with energy dispersive X-ray spectroscopy (SEM-EDX) from electron microscope elemental analysis, elemental analysis of fractions obtained from density separation, leaching, and statistical correlation (Creelman & Ward, 1996; Finkelman et al., 1990; Rao & Gluskoter, 1973).

Sequential extraction was first developed to analyze particulate trace metals (Tessier et al., 1979). This procedure was later modified for coal (Finkelman, 1994; Finkelman et al., 1990). Density based sequential extraction procedure for REE in coal was successfully applied by Dai et al. (2002). A similar extraction method was also applied to other trace elements in coal such as arsenic, mercury, and selenium (Bai et al., 2011; Dai et al., 2004; Zhang et al., 2007; Zheng et al., 2008; Zhou et al., 2016). avidson (2000) presented the comparison of sequential extraction procedure used in different national laboratories. Based on these studies, a four-step sequential extraction procedure was used in this study for select samples to understand the REE association into the following five types: the ion-exchangeable REE, Weak acid soluble REE, REE bound to other carbonates and monosulfides, REE associated with disulfides, and REE association with silicates and aluminosilicate form. **Table 1** provides the sequential extraction procedure used in the study.

Table 1. Sequential extraction procedure adopted in this study

Stage	Mode of occurrence	Procedure
1	Ion-Exchangeable REE	A 50g sample was transferred into a 400mL beaker, to which 250mL of 1M ammonium acetate solution was added. The slurry was magnetically stirred for 1 hour at room temperature and filtered using Whatman grade 42 filter papers. The filtered solids residue was dried at 65˚C, weighed, and a small subsample was taken for REE analysis.
2	Weak acid soluble REE	The dried residue from step 1 was mixed with 1M sodium acetate solution at liquid to solid ratio of 5:1 and magnetically stirred for 5 hours at room temperature. The slurry was filtered, dried, weighed and a small subsample was stored for REE analysis.

3	REE bound to other carbonates and monosulfides	The dried residue from step 2 was extracted with 3N Hydrochloric acid at liquid to solid ratio of 5:1 and magnetically stirred for 18 hours at room temperature. The slurry was filtered, dried, weighed and a small subsample was obtained for REE analysis.
4	REE bound to disulfides	The dried residue from step 3 was extracted with 3N Nitric acid at liquid to solid ratio of 5:1 and magnetically stirred for 18 hours at room temperature. The slurry was filtered, dried, weighed and a small subsample was collected for REE analysis.
5	REE bound to silicates & aluminosilicates	REE in the residual solids

3.4 Physical Separation Test Procedure

Separation techniques such as density, magnetic, size, and flotation was employed to understand potential of physically concentrating the REE from the select samples. A brief description of the procedure is given in this section as follows.

3.4.1 Particle Size Separation

Particle size separation of samples was performed using a sieve shaker on select samples. A representative sample of 300 g passing 500 µm was wet sieved to separate ultra fines (-25 µm) from rest of the sample. Both fractions (-25 & +25 µm) were filtered, dried at 65°C, and weighed. Dry screening was conducted on the coarser fraction (+25 µm) using Ro-tap for 20 min and separated into 5 more fractions: +300 µm; -300 µm +212 µm; -212 µm +106 µm; -106 µm +53 µm; -53 µm +25 µm. All the fractions were collected, weighed, and sent for REE analysis in each size fractions using ICP-MS. The mass loss during the experiment was less than 2%.

3.4.2 Density Separation

Density separation of samples was carried out using the traditional float-sink method (ASTM D-4371) for selected samples passing -50 µm with P_{80} of 20 - 25 µm. In a standard float-sink analysis, set amounts of the representative sample are crushed to a specified particle size and placed in liquids of known density or across a range of densities. Four different density liquids were selected for the test: SG 1.3, SG 1.9, SG 2.5, and SG 2.8. The four organic liquids with different densities (kerosene: 0.82 g/cm^3,

perchloroethylene: 1.62 g/cm^3, bromoform: 2.89 g/cm^3, and tetrabromoethane: 2.97 g/cm^3) was used for the preparation of heavy liquid media for the test.

For each test, the sample was placed in the heavy liquid with the lowest specific gravity (SG:1.3) in a 250 mL beaker with cap and mixed. The closed beaker was shaken by hand to ensure thorough dispersion of sample particles in the heavy liquid. The mixture was then centrifuged at 3500 rpm for 20 min to get float-and-sink fraction. The float fraction (<1.3 SG) was decanted into separate beaker and filtered using vacuum pump. The sink fraction (>1.3 SG) was transferred into next heavy liquid (SG;1.9). The process was repeated for all heavy density liquids. All collected fractions were washed with acetone to remove any residual heavy liquid, filtered, dried at 35°C, and weighed. After sample preparation, each of the fractions were also sent for elemental analysis using ICP-MS. The mass loss during the experiment was less than 1.5%. The REE recovery (R) in each fraction was calculated as follows:

$$R = \frac{M_R * C_R}{M_F * C_F} * 100\%$$

Where M_F and M_R is the mass of feed and density fraction, respectively (g); C_F and C_R is concentration of REE in feed and density fraction, respectively (µg/g).

3.4.3 Magnetic Separation

Magnetic separation test was carried out using a bench scale Carpco Wet High Intensity Magnetic Separator, as shown in **Figure 7**. For each test, 50 g sample passing -50 µm with P_{80} of 20 - 25 µm was mixed with 450 mL of water in 1L beaker. The slurry was thoroughly mixed using an overhead stirrer for 10 mins and fed into separator at a feed rate of 2L/min. In this study, sample was subjected to three different magnetic intensity levels (0.5 T, 0.85 T, & 1.1T) to obtain total of 4 products (Three concentrates and final tailings). Initially, the magnetic intensity was adjusted to 0.5T, freshly prepared slurry was passed into the separator producing concentrate (Product 1). The residue from the stage 1 was subjected to higher magnetic intensity of 0.85 T to get second concentrate (Product 2). Finally, residue from stage 2 separation was again subjected to separation at 1.1 T to obtain third concentrate (Product 3) and tailings. **Figure 8** depicts the magnetic separation procedure used in this study. Products and tailings were collected separately, filtered, dried at 70°C, and weighed to obtain yield data. The representative portion of concentrates and tailings were sent for REE analysis to calculate recovery and enrichment factor.

Figure 7 Bench scale high wet magnetic intensity separator used in this study

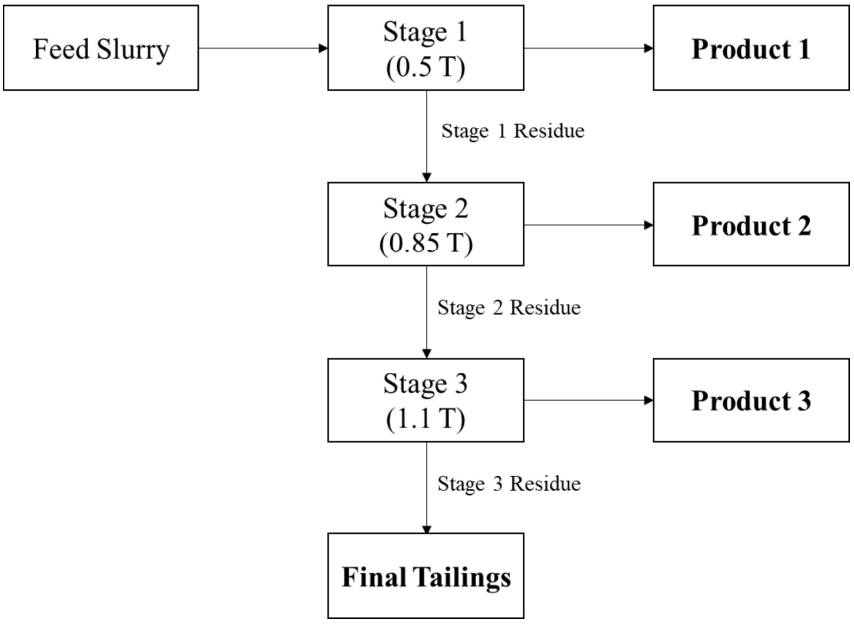

Figure 8. Magnetic separation test procedure adopted in this study

3.4.4 ravity Separation

The gravity separation was conducted using lab scale (FLSmidth Model: KC-MD3) Knelson concentrator as shown in **Figure 9**. For the test, a 1 kg sample (-106 μm) was mixed with water to produce slurry with 60% solid content and was added slowly with fluidization water flow rate of 3 L/min. For each test, the

sample was subjected to separation process at two different levels of applied G force (60 and 90) in a staged recovery to obtain two product concentrates and one final tailings, as depicted in **Figure 10**. At the end of each stage separation test, fluidization water was stopped, followed by concentrate collection chamber motor was turned off to avoid any concentrate loss to the tailings launder. Concentrate and tailings were collected separately, filtered, dried at 70°C, and weighed to obtain yield data. The representative portion of concentrates and tailings were sent for REE analysis to calculate recovery and enrichment factor.

Figure 9. Lab scale Knelson concentrator used in this study

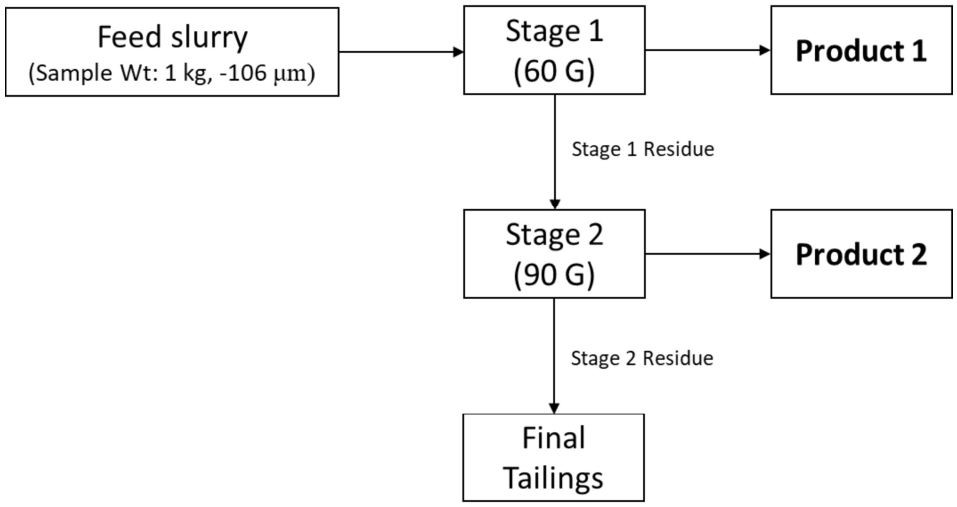

Figure 10. Knelson concentration separation test procedure adopted in this study

3.4.5 REE and Coal Flotation

The samples selected for REE minerals concentration using flotation was crushed to target particle size of below -500 µm with P_{80} of feed samples is 350 - 360 µm. Before conducting REE flotation, feed sample was subjected to coal flotation to remove any excess carbonaceous material present in the feed sample. The feed sample removed of carbon material was later used for REE flotation in all the test.

3.4.5.1 Coal Flotation

For the coal flotation test, standard 10L Denver laboratory cell was used to conduct the batch test, as shown in **Figure 6**. For carbon (coal) removal, flotation test was carried out in two stages.

A representative feed sample was crushed to a target particle size below -500 µm with P_{80} of feed samples is 350 - 360 µm and weighed to obtain 1000 g for each test. The cell was filled to 3/4 height with water and impeller speed was adjusted to 1300 r/min. Feed sample was placed in the cell and conditioned for 5 min to wet the sample completely. Flotation tests were conducted with an initial solid content of 14.3% and pH of the natural slurry was used in the coal (carbon) flotation test without any modification, which was generally in the range of 8 to 8.5.

In the first stage, the reagent emulsion of 240 g/t of kerosene (Collector) and 200 g/t of Methyl isobutyl carbinol (MIBC) (frother) was used for coal concentrate collection. As explained in Section 3.3.2, the reagent emulsion was used for coal flotation. Using a high-speed laboratory blender, the reagent emulsion was prepared separately by pouring 200 mL of water in the blender. The required amount of collector (Kerosene) and one half of the required volume of frother (MIBC) was also added to the blender and mixed at high speed for 30 s. The prepared emulsion was quickly transferred into the cell and conditioned for 15 min. At the end of 15 min conditioning time, the other half of frother volume is introduced to the cell and conditioned for additional 1 more minute. Using an aeration rate of 4.5 L/min of air, the concentrate was collected until the froth was barren, which was usually between 3 to 5 min of froth collection time.

The residual slurry from the first stage is further scavenged for carbonaceous material using second stage addition of reagent emulsion containing 100 g/t of kerosene (Collector) and 200 g/t of MIBC (frother). After the second stage of carbon removal, tailings were pressure filtered and both filtered tailings & concentrate were dried at 65 ˚C. Based on the tailings yield, carbon removal step was carried out to produce enough material for REE flotation tests. After drying, the concentrate (Coal) and rejects (REE flotation feed) collected from different flotation batches were homogenized and used for subsequent REE flotation test.

3.4.5.2 REE Flotation Test

For these tests, flotation was carried out using a standard 3-litre Denver laboratory cell. The feed slurry was prepared by mixing 400 g of sample with 2200 mL of water in the cell at an impeller speed of 1300 rpm and conditioned for 5 min. The slurry pH was adjusted using 0.5 N HCl or NaOH and required amount of collector (sodium oleate or hydroxamate) was added and conditioned for 10 min. After conditioning, frother (DF200) was added and conditioned for additional 1 min. With 4.5 L/min of air bubbling through the slurry, the concentrate was collected for 3 to 5 min or until the froth was barren. After the test, concentrate and tailings left in the cell were filtered, dried at 60 °C and weighed to obtain yield data. Based on the literature review, the flotation test was conducted by varying different process parameter including collector dose, collector type, staged addition of collector dose, particle size, solid density of feed slurry, pH, slurry temperature, and addition of depressant. **Table 2** lists the experimental conditions used for REE flotation test in this study.

3.5 REE Leaching Procedure

The hydrometallurgical extraction of REE from select sample was conducted using two leaching techniques: 1) direct acid leaching (DL) and 2) acid baking and water leaching (ABWL). **Figure 11** shows the reactor setup used in this study. The reactor consists of a 1-litre double-walled glass beaker fitted with various parts, including an impeller, baffle, pH and ORP probes, and a condenser. The temperature of the system can be controlled at a predetermined level up to 90°C using a water bath. To maintain atmospheric pressure, the reactor was equipped with a condenser, and cold water was circulating through the condenser jacket to reduce evaporative loss of water in the reactor. For select experiments, pH and ORP data was recorded using probes connected to the Hach SC 200 controller.

3.5.1 Direct Acid Leaching

To obtain an acid leaching REE extraction value, the leaching test was conducted using 1 M sulfuric acid at the desired temperature for a fixed time. The test was carried out at 2 wt.% solid content, and the slurry was agitated at 500 rpm. Solution samples were also collected at different time intervals to monitor the extraction progress over time. For acid-leach tests, a 1-litre double-walled stirred-glass leach reactor, as shown in **Figure 11**, was used. At the end of the test, the slurry was filtered using Whatman grade 42 filter paper and washed three times with deionized water. The filtered solid cake was dried at 60°C, weighed, and elemental concentrations were determined using ICP-MS.

3.5.2 Acid Baking and Water Leaching

For each ABWL test, 10 g of feed sample was transferred to porcelain crucibles and a known quantity of concentrated sulfuric acid (VWR chemicals BDH, ACS grade, 95–98%) was added to achieve the required acid dose. After the acid addition, the contents were mixed thoroughly, weighed, and placed in a muffle furnace. The muffle furnace used in this study is illustrated in **Figure 12**. The temperature of the muffle furnace was increased at a rate of 5°C/min to a desired value and baked for fixed time. After the set baking time, the resultant baked solids were cooled, weighed, and ground using a mortar and pestle for the water-leach test. **Figure 13** shows the tailings sample before and after being acid baked at 200°C using the muffle furnace.

Table 2. Rare earth element (REE) flotation test conditions used in this study

Test ID	Sample	Particle Size µm	Temperature °C	%Solids	Collector Type	Collector g/t	Frother g/t	pH	Depressant	Depressant kg/t
FT1	RR	-500	20	27.3	Hydroxamate	500	100	9.5	-	
FT2 Stage 1	RR	-500	20	15.4	Hydroxamate	100	50	9.5	-	-
FT2 Stage 2	RR	-500	20	15.4	Hydroxamate	150	100	9.5	-	
FT3	HMC	-500	20	27.3	Hydroxamate	500	100	9.5	-	
FT4 Stage 1	HMC	-500	20	15.4	Hydroxamate	100	50	9.5	-	-
FT4 Stage 2	HMC	-500	20	15.4	Hydroxamate	150	100	9.5	-	
FT5	HMC	-500	20	15.4	Sodium Oleate	500	100	9.5	-	
FT6	RR	-500	20	15.4	Sodium Oleate	500	100	9.5	-	
FT7	RR	-500	20	15.4	Sodium Oleate	500	100	4	-	-
FT8	HMC	-500	20	15.4	Sodium Oleate	500	100	4	-	-
FT9	HMC	-500	20	15.4	Hydroxamate	500	100	7	-	-
FT10	RR	-500	20	15.4	Hydroxamate	500	100	7	-	-
FT11	HMC	-500	20	15.4	Hydroxamate	500	100	9.5	-	
FT12	RR	-500	20	15.4	Hydroxamate	500	100	9.5	-	
FT13	RR	-500	20	15.4	Hydroxamate	1000	100	9.5	-	-
FT14	HMC	-500	20	15.4	Hydroxamate	1000	100	9.5	-	-
FT15	HMC	-500	20	15.4	Hydroxamate	500	100	9.5	Sodium Silicate	25
FT16	RR	-500	20	15.4	Hydroxamate	500	100	9.5	Sodium Silicate	25
FT17	RR	-106	20	15.4	Hydroxamate	500	100	9.5	Sodium Silicate	25
FT18	HMC	-106	20	15.4	Hydroxamate	500	100	9.5	Sodium Silicate	25
FT19 Stage 1	RR	-106	70	15.4	Hydroxamate	500	100	9.5	Sodium Silicate	25
FT19 Stage 2	RR	-106	70	15.4	Hydroxamate	500	100	9.5	Sodium Silicate	25
FT20 Stage 1	HMC	-106	70	15.4	Hydroxamate	500	100	9.5	Sodium Silicate	25
FT20 Stage 2	HMC	-106	70	15.4	Hydroxamate	500	100	9.5	Sodium Silicate	25

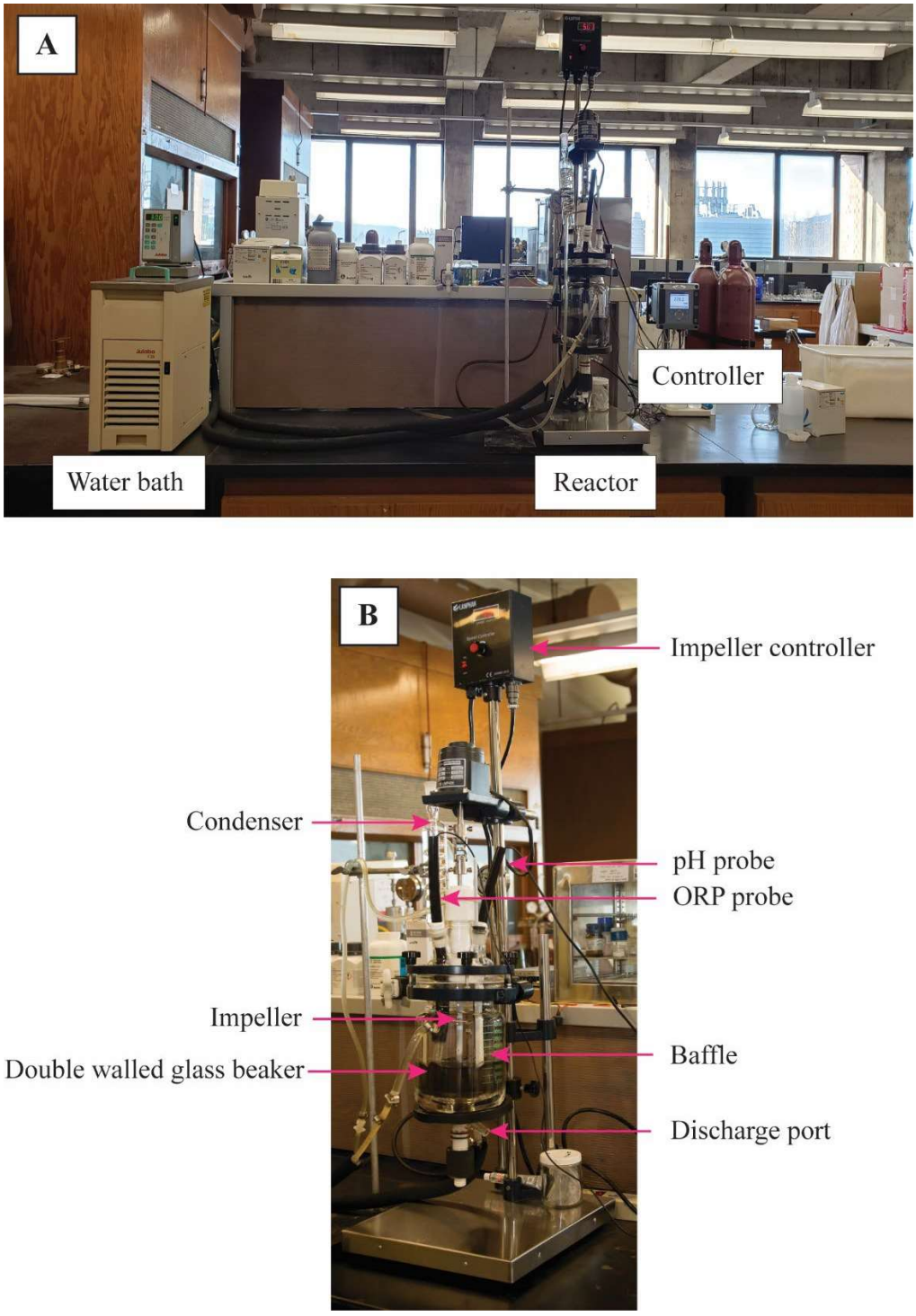

Figure 11. Leaching reactor set-up: A) overview B) details of the reactor

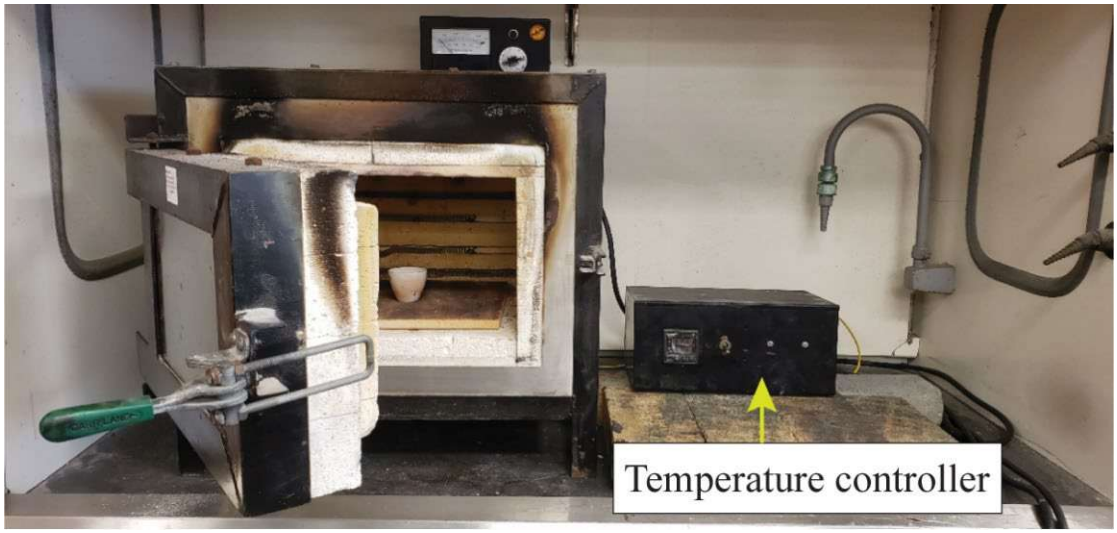

Figure 12. Muffle furnace used for acid baking

Water-leach tests were conducted using the setup shown in **Figure 11**. At a constant 2 wt.% solids concentration and 500 rpm stirrer speed, water-leach experiments were performed using deionized water for a varied time between 1 and 24 hours at 80°C. The lower solid percent was chosen to avoid any potential solubility issues during leaching. At the end of the test, the slurry was filtered using Whatman grade 42 filter paper and washed three times with deionized water. The filtered solid cake was dried at 60°C, weighed, and elemental concentrations were determined with ICP-MS.

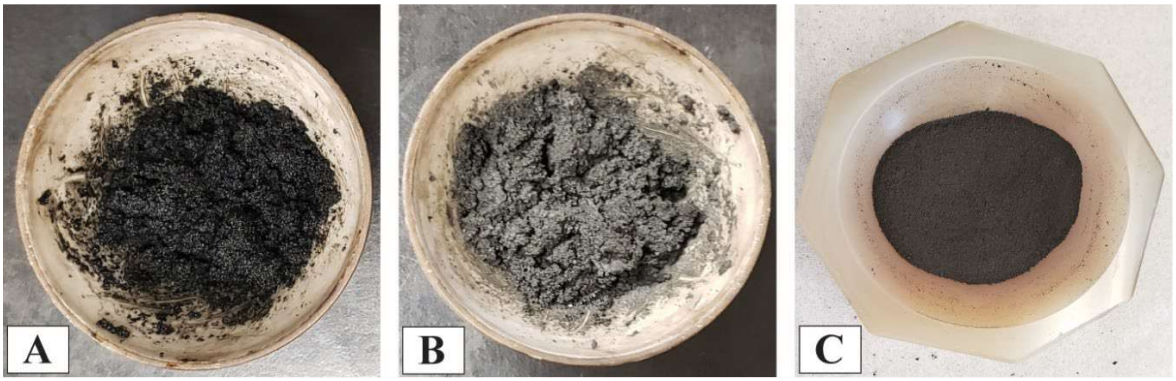

Figure 13. Photos of tailings sample before and after acid baking at 200°C using a muffle furnace: A) tailings mixed with acid, B) acid-baked tailings, and C) de-agglomerated baked tailings before water-leaching stage

3.6 Analytical Methods

3.6.1 REE and Other Elements Analysis

For total REE (TREE) quantification, sample (0.2g) was mixed thoroughly with lithium metaborate and lithium tetraborate flux. The samples were then fused in a furnace at 1025˚C. Finally, the resulting melts were cooled and digested in an acid mixture containing nitric, hydrochloric, and hydrofluoric acids. The digested solutions were then analyzed by inductively coupled plasma–mass spectrometry (ICP-MS). The analytical results were corrected for inter-elemental spectral interference. This analysis was conducted by ALS Geochemistry in North Vancouver, British Columbia. In this study, REE in coal are expressed as follows: whole-coal basis (REE concentration in the coal sample) and ash basis (REE concentration in the ash of the coal sample). To ensure accuracy of the method, the results were compared against reference materials and calibration standards.

Base metals and other minor elements were analyzed by four-acid digestion followed by inductively coupled plasma–emission spectroscopy (ICP-ES). For a few highly reactive samples, aqua-regia digestion was used for the analysis. All the chemical analysis was conducted by ALS-Geochemistry (North Vancouver, BC).

3.6.2 X-Ray Diffraction Analysis

X-ray diffraction analysis was conducted on select four samples (S9, S42, S57, and S81) to understand sample mineralogy. For analysis, samples were reduced to the optimum grain-size range for quantitative X-ray analysis (<10 μm) by grinding under ethanol in a vibratory McCrone XRD Mill (Retsch GmbH, Germany) for 10 min. Continuous-scan X-ray powder-diffraction data were collected over a range 3-80°2θ with CoKα radiation on a Bruker D8 Advance Bragg-Brentano diffractometer equipped with an Fe filter foil, 0.6 mm (0.3°) divergence slit, incident- and diffracted-beam Soller slits and a LynxEye-XE detector. The long fine-focus Co X-ray tube was operated at 35 kV and 40 mA, using a take-off angle of 6°. The X-ray diffractograms were analyzed using the International Centre for Diffraction Database PDF-4 and Search-Match software by Bruker. X-ray powder-diffraction data of the samples were refined with Rietveld program Topas 4.2 (Bruker AXS). The results of quantitative phase analysis by Rietveld refinements represent the relative amounts of crystalline phases normalized to 100%.

3.6.3 Scanning Electron Microscope and Mineral Liberation Analysis

Trace mineral characterization was carried out using scanning electron microscope with energy dispersive X-ray spectroscopy (SEM-EDX). For the analysis, an FEI Company Quanta 650 scanning electron microscope (SEM) was used and operated at 20kV at a working distance of 10mm.

For certain samples, SEM characterization was conducted on low temperature ash (LTA) sample to reduce interference of carbonaceous material during the analysis. To remove residual organic (coal) matter in the sample, low-temperature ashing (LTA) was performed on the representative sample using a PVA TePla Ion 40 plasma system under oxygen atmosphere, fed at a constant pressure of 40 psi until a constant weight was reached. After LTA, samples were mounted on epoxy resin and probed using SEM-EDX at UBC. LTA was performed at CanmetENERGY laboratory at Ottawa, Canada.

For selected samples, mineral liberation analysis (MLA) was also carried out at independent laboratory. MLA is an automated mineral analysis system which can identify minerals in polished sections and is used to quantify grain size, mineral association and liberation. MLA analysis was carried out by Process Mineralogical Consulting Limited, Maple Ridge, BC.

A single Polished Block Section was prepared from each sample and systematically measured with the Hitachi FLEXSEM equipped with the AMICS software to collect information on the deportment of REE-bearing minerals, their modal abundance, degree of liberation and association with gangue minerals. A second measurement with the Tescan Integrated Mineral Analyszer (TIMA) system was completed to validate the results, complete elemental mapping for REE, and generate particle maps.

3.6.4 Performance Indicator

The recovery (R) of REE for physical extraction process was calculated using the following equation

$$R = \frac{M_C * C_C}{M_F * C_F} * 100 \qquad \text{Eq. 3.1}$$

Where M_F and M_C is the mass of the feed and concentrate (product), respectively (g). C_F and C_C is the concentration of REE in the feed and concentrate (product) (µg/g).

Other than recovery, Enrichment Factor (EF) was calculated for physical extraction process, which indicates the quality of the concentrate in terms of REE concentration. EF was calculated as follows:

$$EF = \frac{C_C}{C_F} \qquad \text{Eq. 3.2}$$

C_F and C_C is the concentration of REE in the feed and concentrate (product) (µg/g).

The REE extraction (E) for leaching test was calculated using the following equation:

$$E = \frac{M_F * C_F - M_{SR} * C_{SR}}{M_F * C_F} * 100\% \qquad \text{Eq. 3.3}$$

Where M_F and M_{SR} is the mass of feed and solid residue, respectively (g); C_F and C_{SR} is the concentration of REE in feed and solid residue, respectively (µg/g).

To ensure the reliability of the recovery data, mass balance calculations were performed on selected tests where elemental concentrations of feed was back calculated based on the product concentrates and mass of the feed and products.

4.0 Results and Discussion

4.1 REE Database

A total of 104 samples were collected and analyzed during the period of this study. There were 37 coal samples, 11 rock partings, 25 roof samples, 27 floor samples, 2 rock samples, and 2 tonstein samples were also collected. Data is stored in an MS Access database and contains proximate analysis and trace element analysis.

Results of the proximate analysis of the coal samples are listed in **Table 3**. According to ASTM D388-17 (2017), all the coal samples can be classified as low-to-medium volatile bituminous coal and is known to be of a metallurgical quality. **Figure 14** is a schematic showing the relative locations of parting, roof, and floor samples with respect to the coal seam. Two tonstein samples bands were also collected. All samples were analyzed for REE and multi-element analysis using inductively coupled plasma mass spectrometry (ICP-MS). This method of analysis used in the mining industry because it allows for analysis of multiple elements at one time, has a large analytical range, low detection limit and requires simple sample preparation and low sample volume (Wilschefski & Baxter, 2019).

Analytical results were loaded into an MS Access database and reviewed for trends and relationships in the data. For the database, more than 60 parameters were collected for each sample including type, proximate analysis and major-, minor- and trace-elements data. The complete dataset is provided as a separate file along with this report. Seam ID and the specific locations of the individual samples are not disclosed to uphold a confidentiality agreement.

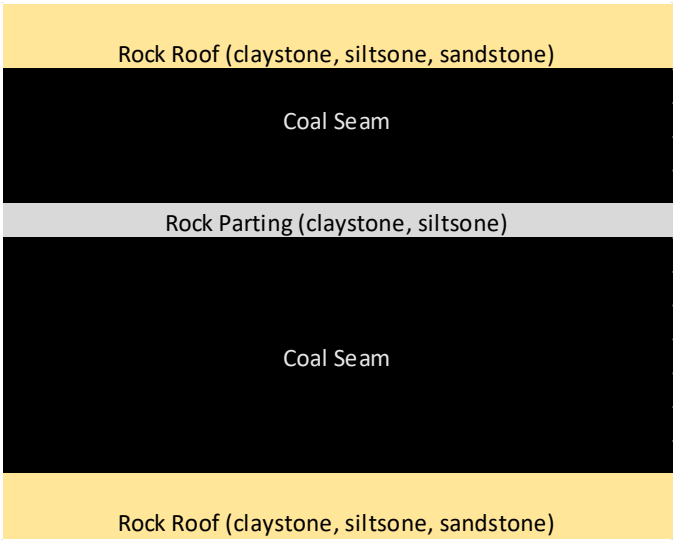

Figure 14 General stratigraphy of a coal seam

Table 4 details the minimum, maximum, and average total REE per sample type. The maximum total REE concentration found was 259 parts per million (ppm) in a coal seam floor sample. Floor samples had the highest average total REE equaling 216 ppm. Coal samples contained the least amount of REE on a whole rock basis. Among the 17 REE, the five elements of Ce, La, Nd, Y and Sc accounted for more than 77% of the total REE present in these samples.

Coal is a rock type known to be made up of mineral matter (known as ash), volatile matter, carbon, and water. The total REE in the ash component of coal was calculated. In this study the highest total REE in a coal seam mineral fraction was 686 ppm, the average was 284 ppm. The average crustal abundance (ACA) (the concentration expected in rocks worldwide on average) of REE is 190 ppm. Therefore, the concentration of REE in the coalfield is enriched relative to the average crustal abundance.

Table 3. Proximate analysis results for coal samples (as-determined basis) from the East Kootenay coalfield, southeastern British Columbia

Sample ID	Type	Moisture content (%)	Ash content (%)	Volatile matter (%)	Fixed carbon (%)
10	Coal	2.4	7.2	22.9	67.5
11	Coal	2.8	10.1	21.9	65.1
12	Coal	2.4	7.7	23.0	67.0
13	Coal	2.4	7.5	22.9	67.1
14	Coal	2.4	7.9	23.0	66.6
15	Coal	2.5	10.5	22.3	64.7
16	Coal	2.6	5.1	24.1	68.2
17	Coal	2.1	5.3	23.7	68.9
18	Coal	2.1	20.2	27.3	50.4
19	Coal	2.8	7.4	25.7	64.2
20	Coal	1.4	12.4	24.7	61.6
22	Coal	0.9	19.1	19.4	60.7
26	Coal	1.3	7.8	22.7	68.2
27	Coal	1.2	13.2	19.3	66.3
41	Coal	1.3	20.7	23.1	54.8
48	Coal	0.7	20.3	20.2	58.9
49	Coal	0.9	15.1	22.2	61.9
53	Coal	1.0	10.6	24.3	64.1
54	Coal	1.4	6.9	28.7	63.1
60	Coal	1.4	10.3	30.7	57.6
61	Coal	1.0	30.3	22.8	45.9
69	Coal	0.8	32.5	20.7	46.1
73	Coal	0.6	12.6	22.8	64.0
74	Coal	0.60	20.89	24.46	54.05
76	Coal	0.62	25.98	21.75	51.65
78	Coal	0.46	7.36	22.29	69.89
81	Coal	1.97	29.88	19.68	48.46
83	Coal	1.51	45.55	18.00	34.94
87	Coal	1.21	4.86	5.57	88.35
89	Coal	1.07	13.37	14.18	71.38
96	Coal	1.03	40.52	15.51	42.94
98	Coal	0.74	13.40	18.39	67.47
99	Coal	0.86	23.48	18.40	57.26
100	Coal	0.75	22.64	22.12	54.50
102	Coal	0.55	19.53	22.57	57.35
103	Coal	0.97	25.60	24.66	48.77
104	Coal	0.94	17.10	26.21	55.75

Table 4. Total REE concentration by sample type

Sample Type	Total REE			Total LREE			Total HREE		
	Min	Max	Average	Min	Max	Average	Min	Max	Average
Roof	62	274	196	53	212	150	9	62	45
Floor	12	259	216	9	200	142	3	59	39
Parting	95	224	162	47	175	125	24	49	37
Coal (whole rock)	10	125	47	7	94	35	2	37	12
Coal Ash	105	686	284	-	-	-	-	-	-
Tonstein	147	164	155	131	131	131	16	32	24

REEs can be grouped into light rare earth elements (LREE) and heavy rare earth elements (HREE). LREEs have lower atomic weights than HREEs and are more abundant. The LREEs are lanthanum, cerium, praseodymium, neodymium, samarium, europium, scandium and gadolinium. and the HREEs are terbium, dysprosium, holmium, erbium, thulium, ytterbium, lutetium, and yttrium. The samples in this dataset contain a higher proportion of LREE than HREE. **Figure 15** summarizes the LREE and HREE contents of all samples, oriented North to South (left to right). The graph shows a light blue horizontal line for the average crustal abundance (ACA) of light rare earth elements (145 ppm) and a light green line for the average crustal abundance of heavy rare earth elements (32ppm). The values for LREE are scattered above and below the corresponding LREE ACA line. The values for the heavy rare earth elements are also scattered above and below the HREE ACA line.

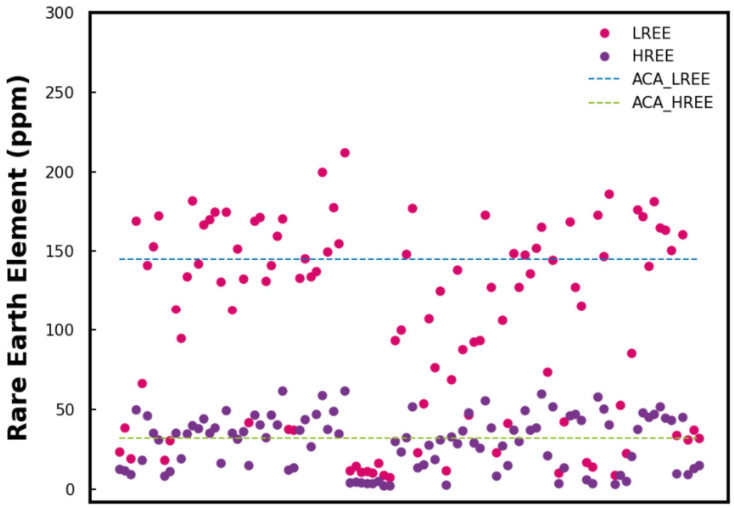

Figure 15. Light rare earth and heavy rare earth element data for all samples

Figure 16 plots heavy rare earth concentration against light rare earth concentration. In this dataset there is a positive relationship between the two groups; where there is an increase in LREE, there is also an increase in HREE.

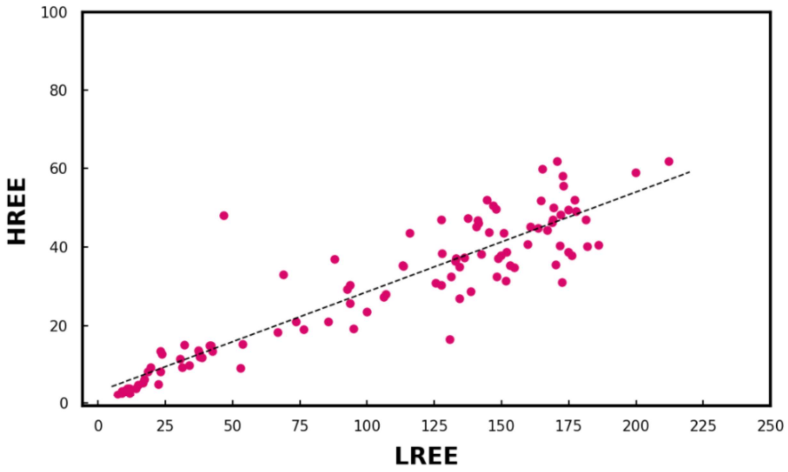

Figure 16. LREE vs HREE for all samples

The database was studied for trends in the data. **Figure 17** to **Figure 21** summarize, by sample type, the total REE sample content from north (left of diagram) to south (right of diagram). In all diagrams, the average crustal abundance of total REE (190 ppm) is illustrated by a horizontal line.

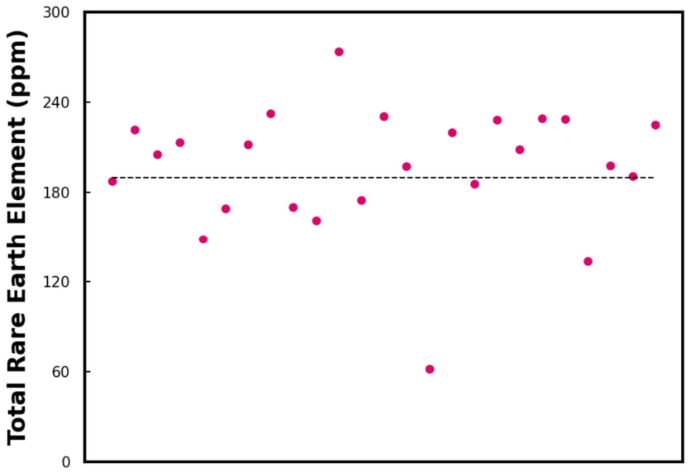

Figure 17. Roof samples running from north to south (Left to Right) across the coalfield

Running from north to south, REE concentrations in coal seam roof samples range between 150 to 250 ppm with the exception of three outliers. We observed no north-to-south trends within the coalfield.

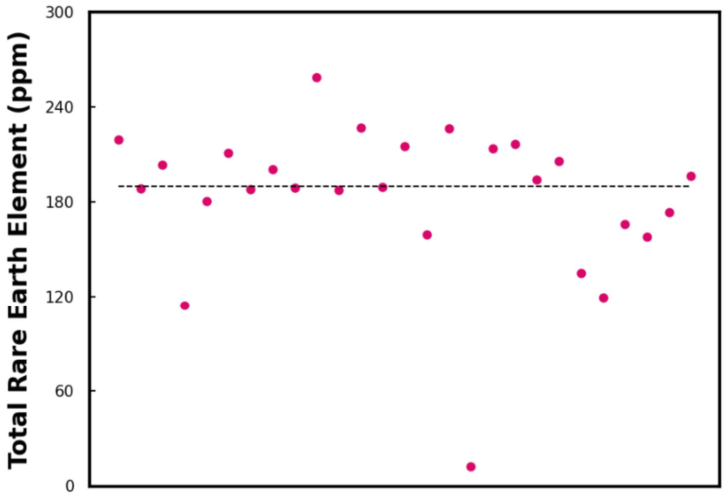

Figure 18. Floor samples running from north to south across the coalfield

Running from north to south, REE concentrations in coal seam floor samples show a larger scatter than the roof samples, ranging between100 to 250ppm with the exception of two outliers. The six floor samples collected in the southern portion of the coalfield have lower total REE values than the average crustal abundance. More data are needed to determine if this is in fact a regional trend in coal seam floor lithologies.

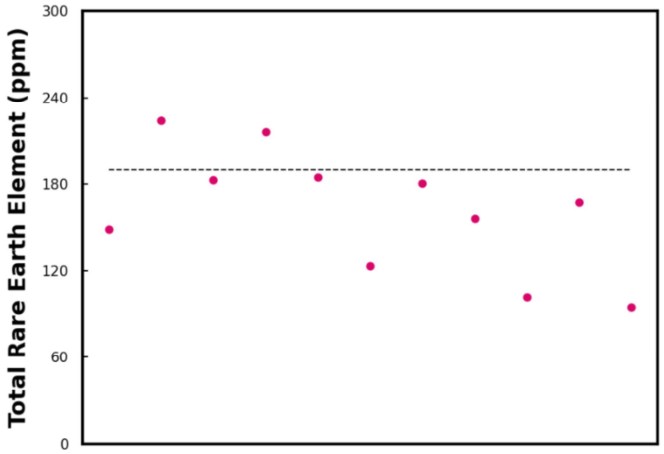

Figure 19. Parting samples running from north to south across the coalfield

Only two coal seam parting samples had total REE values greater than the average crustal abundance. The data available exhibits a trend of decreasing total REE moving from North to South.

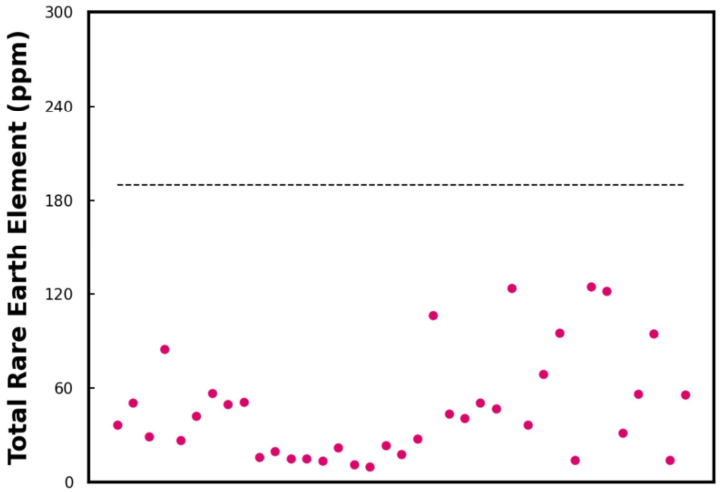

Figure 20. Coal samples running from north to south across the coalfield

The total REE concentration in all of the coal samples in this study was lower than the average crustal abundance. There is a large scatter in the data, with all sample values falling between 10 to 125ppm.

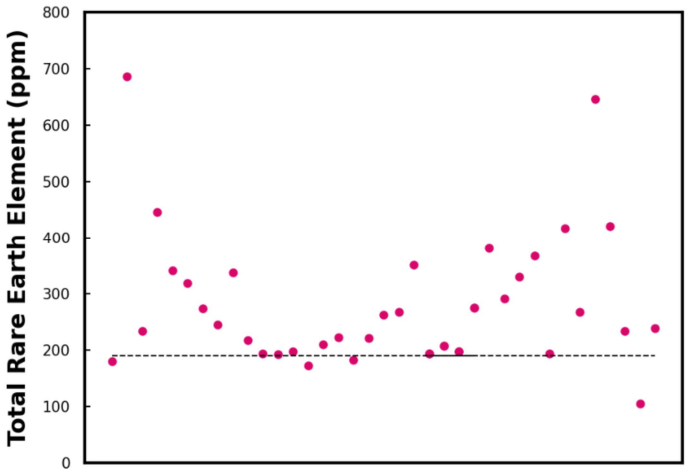

Figure 21. Mineral matter in coal seam samples running from north to south across the coalfield

Once the total REE values are calculated on an "ash basis", assuming all REE are in mineral form, some large values become evident with a maximum of 686ppm. Most values fall between 190 and 400ppm, with the exception of six outliers. No north-south trend is evident.

The two tonstein samples were not anomalously high in REE, with total values of 147 and 164 ppm respectively. Like the rest of the dataset, they show a higher proportion of LREE vs. HREE. Both tonstein bands had anomalously high lithium (140 and 130 ppm), and one of the bands had an anomalous zinc value at 126ppm.

4.2 Source of Rare Earth Elements in SEBC Coalfield

The mineral monazite is a phosphate mineral with the general chemical formula $(REE)PO_4$, where REE = light rare earth ions (Boatner, 2002). Monazite is a common mineral in magmatic, metamorphic, and ore-forming environments (Stein, 2014). It is considered a heavy mineral as its specific gravity is between 5 and 5.5. Monazite and other heavy minerals such as ilmenite, rutile and zircon are resistant to weathering and robust enough to survive fluvial transport. They are concentrated by fluvio-deltaic or shallow marine processes and form placers in those deposits (Wall, 2020).

During the late Jurassic to early Cretaceous periods organic matter was deposited in a foreland basin that now makes up the SEBC coalfield. This foreland basin was an elongate trough that developed between a continental-margin magmatic arc and the North American Craton (Leckie, 1997). A foreland basin is a depression that develops adjacent and parallel to a mountain belt and is formed when the mass created by crustal thickening associated with the creation of the mountain belt causes the lithosphere to bend (Miall, 2009). The Mist Mountain Formation, which hosts the coals of the southeast BC coalfields, was deposited in a deltaic to fluvial/alluvial environment, with intermittent flooding of brackish water during deposition (Leckie, 1997). **Figure 22** illustrates an aerial few of the depositional environment, outlining rivers and streams running down from the mountains in the west through marsh lands and towards the Fernie Sea.

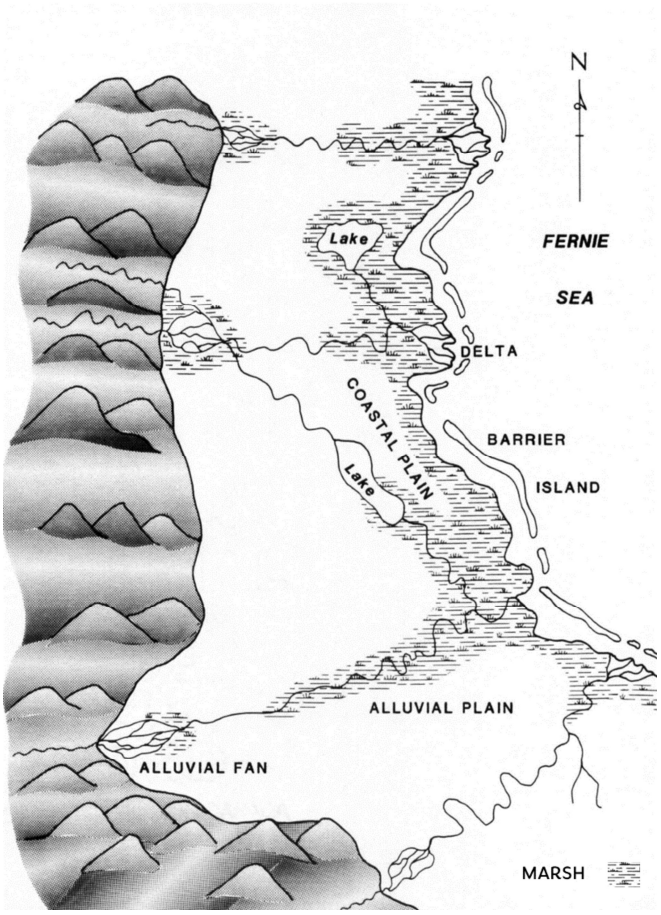

Figure 22. Late Jurassic-Early Cretaceous: rivers and alluvial fans running east and northeast towards the Fernie Sea (Donald, 1984)

Gibson (1985) summarized three theories on the provenance of the sediments in the Mist Mountain Formation. One suggests that the sediments were derived from the Western Ranges of the Rocky Mountains, the Purcell and Selkirk Mountains and the Shuswap Metamorphic Complex in central British Columbia. Another theory suggests that the sediment source area comprised mainly the Main and Front ranges of the Rocky Mountains. Yet another theory suggests that the sediments were derived from rising thrust sheets developing in the Rocky Mountains in the area east of the Rocky Mountain Trench (Gibson, 1985).

4.3 Preliminary Economic Evaluation for BC Coal Samples

Seredin and Dai (2012) estimated that a coal seam with a thickness greater than 5 m may be considered as a potential source of REE if its rare-earth oxide content is above 800–900 ppm on an ash basis. Zhang et al. (2015) estimated the minimum average REE content to be 720 ppm on an ash basis, assuming a valence state of +3 for all of the REE and a relative atomic mass of 132.5. In the United States, coal

seams with an REE content of more than 300 ppm are considered a potential source of REE (U.S. Department of Energy, 2016).

It can be inferred that the REE concentration in the feed samples (see **Figure 23**) did not meet the cut-off grade as proposed by Seredin and Dai (2012), but some of the coal showed significant potential. Using the U.S. Department of Energy's (2016) resource cut-off of 300 ppm of REE, it can be concluded that some of the samples met the cut-off grade requirements.

Outlook coefficient (C_{outl}) is another factor that can be used to assess the quality of the REE present in the coal seam. It is defined as the ratio between the relative amounts of critical REE in the sample to the relative amounts of excessive REE in the sample (Seredin and Dai, 2012). It can be calculated as

$$C_{outl} = \left(\frac{sum\ Nd,Eu,Tb,Dy,Er,Y}{total\ REE}\right)/\left(\frac{sum\ Ce,Ho,Tm,Yb,Lu}{(total\ REE)}\right) \quad \text{Eq. 4.1}$$

A higher value for this index represents a higher market value for the REE in the coal seam since the concentration of critical REE increases with the index. Dai et al. (2017) proposed an evaluation plot using REE concentration and C_{outl}. In this study, a similar plot was used (**Figure 23**) but modified to accommodate the resource cut-off suggested by the U.S. Department of Energy (2016). Accordingly, all of the samples were divided into five categories: unpromising source (REE <300 ppm on ash basis or C_{outl} <0.7); promising resource (300<REE<720 ppm on ash basis and 0.7<C_{outl}<2.4); highly promising resource (300<REE<720 ppm on ash basis and C_{outl} >2.4); promising source (REE >720 ppm on ash basis and 0.7<C_{outl}<2.4); and highly promising source (REE >720 ppm on ash basis and C_{outl} >2.4).

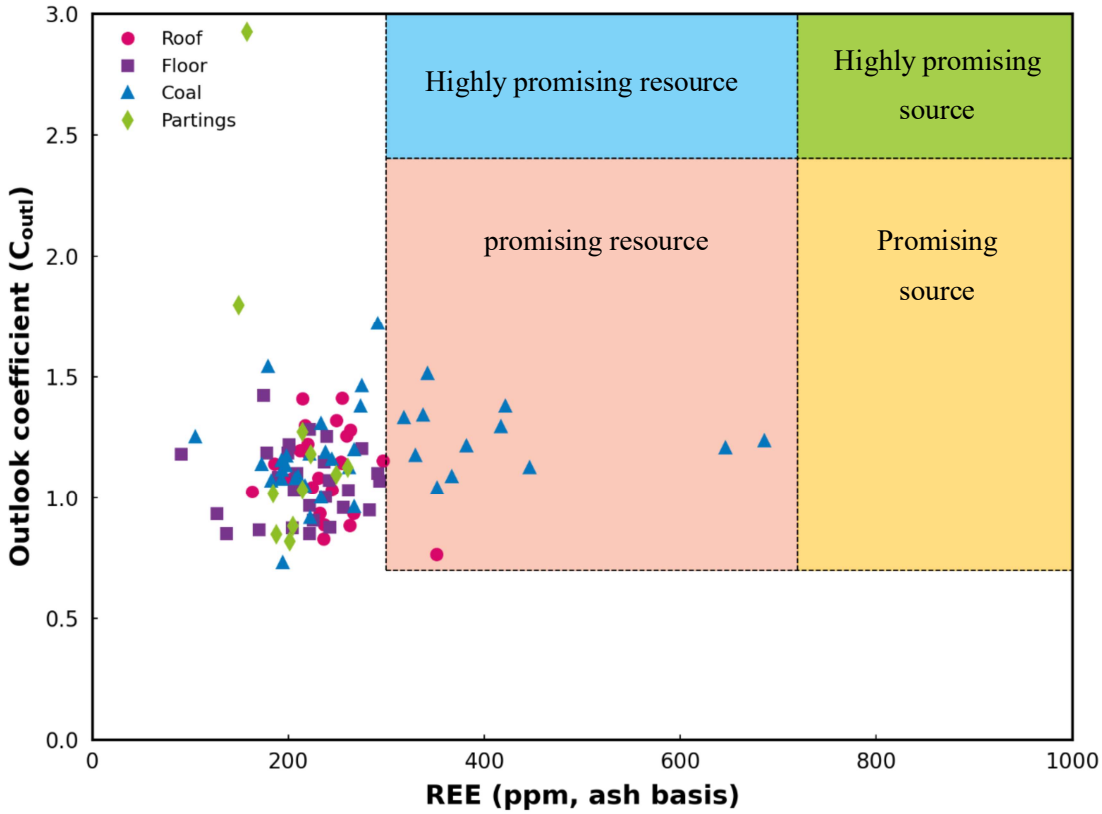

Figure 23 Outlook coefficient (Coutl) versus rare-earth element (REE) concentration for various types of coal samples from the East Kootenay coalfield, southeastern British Columbia. REE resource categories for coal sources: green, highly promising source; yellow, promising source; blue, highly promising resource; light salmon: promising resource.

The C_{outl} values for most of the samples are greater than 1, implying that the critical REE concentration is significant and accounts for, on average, 36% of the total REE. Further, it can be noticed generally from Table 4 that HREE concentrations are more significantly concentrated in coal, in some cases they total more than 50% of total LREE, than in roof, partings and floor materials, which contributes to the better C_{outl} values. The average C_{outl} for the coal samples is found to be 1.2. Additionally, certain partings samples also showed enriched HREE concentration which resulted in highest outlook co-efficient observed among the samples tested. Because of HREE enrichment in few samples, the general statistics of partings were improved and comparable to that of coal values in terms of HREE/LREE ratio and Outlook coefficient. Since the reported C_{outl} for world coal is 0.64 (Zhang et al., 2015, Dai el al., 2017), these results show that BC coal related samples may be a viable source of REE if extraction practices are refined.

4.4 Sample Characterization Results

4.4.1 Preliminary Analysis of REE Deportment during Coal Flotation

REE in coal can occur in different modes, such as ion-adsorbed minerals, aluminosilicate minerals, accessory minerals, authigenic minerals, sub-micron minerals and as elements with organic matter association (Dai et al., 2002; Hower et al., 1999; Hower at al., 2018; Seredin & Dai, 2012; Seredin & Finkelman, 2008; Zhang et al., 2015).

Broadly, REE in coal can be associated with either organic matter (Eskenazy, 1987; Seredin, 1996; Wang et al., 2008;) or inorganic matter (minerals associated with coal) (Dai et al., 2008; Eskenazy, 1987; Birk et al., 1991; Seredin, 1996; Hower et al., 1999). To understand the REE deportment during coal beneficiation, preliminary sample collected from East Kootenay coalfield was subjected to TREE Release analysis as explained in Section 3.3.2.

The tree release analysis provided a separation performance curve achievable under a predetermined set of conditions for flotation of the feed sample. The shape of the performance curve indicates the ability to clean the coal using flotation such as ideal separation, easy cleanability, difficult cleanability, and impossible separation (Laskowski, 2001). As depicted in **Figure 24**, at 10% ash, 83% yield of the clean coal can be achieved for feed coal. It can be seen from **Figure 24** that the sample exhibits easy cleanability using flotation and its combustible recovery exceeded 99%.

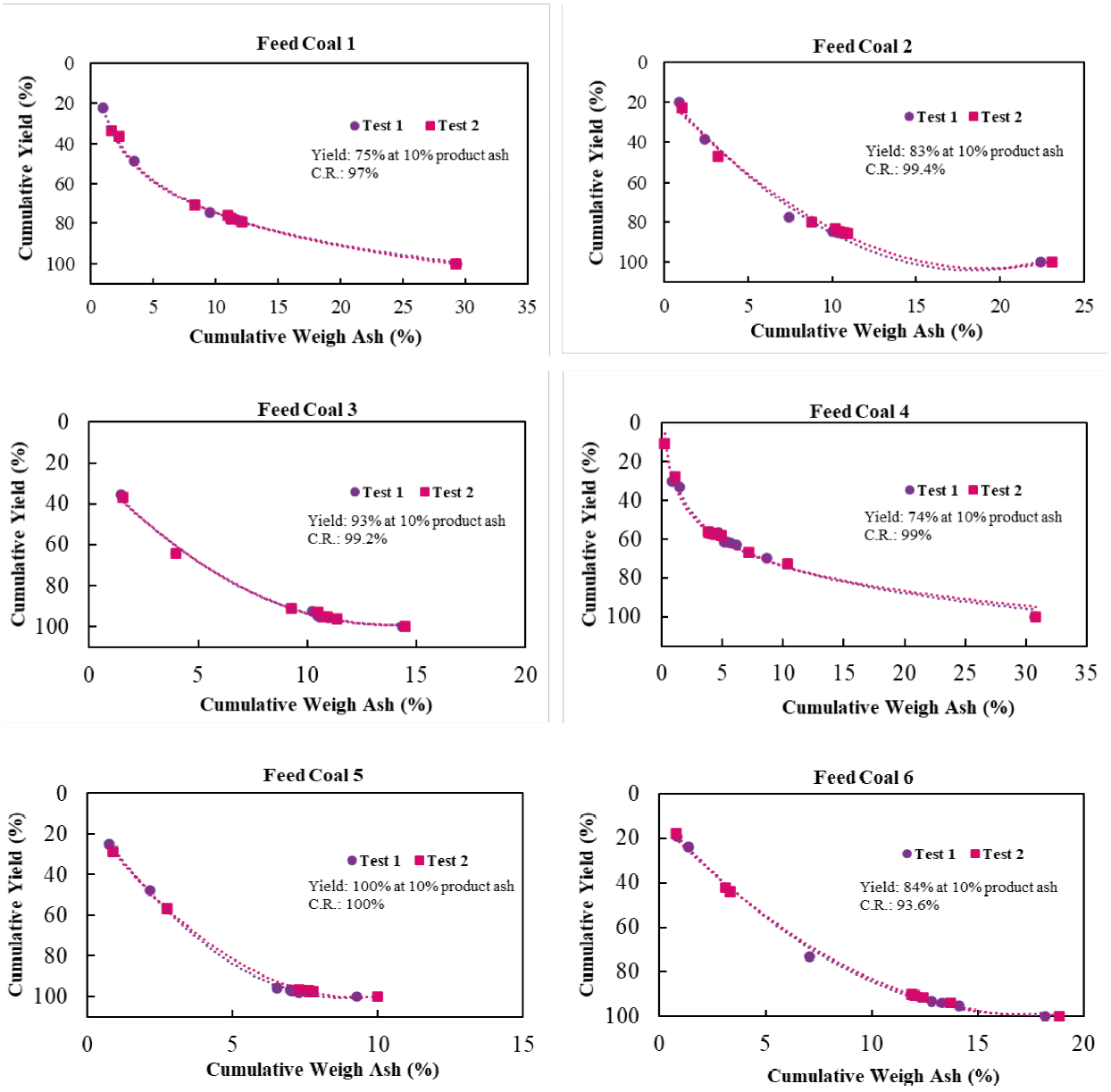

Figure 24. Flotation performance curve obtained from tree analysis of the feed sample. Test was performed in duplicates as represented by Test 1 and Test 2 data

The feed sample and selected three tree release analysis products containing low (<10%)-, medium (10-60%)- and high-ash (>60%) products were analyzed for REE concentrations, the results of which are presented in **Table 5**. The highest concentration of REE on ash basis was reported in the low ash flotation product (550 ppm; see **Table 5**). On whole coal basis, however, the concentration of REE in low ash flotation product (25 ppm; see **Table 5**) was six times lower than tailings (173 ppm). It shows that concentration of REE in the tailings enriched during the flotation process, which indicates the association of REE with mineral matter in the feed coal.

Table 5. REE concentration in feed sample and tree analysis products (ppm, ash basis). Low ash denotes product <10% ash, middlings denote product with 10-60% ash and tailings denote product >60% ash.

Sample ID	Sample Name	Ash (%)	Sc	Ce	Dy	Er	Eu	Gd	Ho	La	Lu	Nd	Pr	Sm	Tb	Tm	Y	Yb	Total REE
A1	Feed Coal 1	30.38	13.	94.14	7.57	4.87	2.60	8.3	1.68	50.69	0.63	44.11	11.39	9.35	1.32	0.76	49.70	4.51	**304.86**
A2	Feed Coal 2	24.82	12.09	89.46	7.50	4.63	2.22	8.50	1.73	47.95	0.64	41.51	10.60	8.10	1.25	0.81	47.95	4.88	**289.82**
A3	Feed Coal 3	15.61	12.81	96.08	8.84	5.57	2.56	10.06	1.92	48.68	0.90	44.84	11.66	9.22	1.60	0.90	53.16	5.25	**314.0**
A4	Feed Coal 4	32.73	12.22	70.58	5.38	3.33	1.71	6.14	1.16	40.33	0.49	33.61	8.7	6.78	0.92	0.55	34.83	3.27	**230.03**
A5	Feed Coal 5	10.54	NA	87.27	8.92	5.12	2.09	7.97	1.90	47.4	0.76	39.84	10.4	8.63	1.42	0.95	52.17	5.22	**280.12**
A6	Feed Coal 6	19.25	15.58	87.77	8.05	5.14	2.0	8.73	1.82	47.26	0.8	42.07	10.65	8.57	1.45	0.78	49.34	4.88	**294.9**
A7	Coal 1 Test 1 FFF	4.24	NA	240.37	19.56	12.49	5.66	23.33	4.48	124.9	1.89	110.7	29.22	23.33	3.53	2.36	127.26	11.5	**740.68**
A8	Coal 1 Test 1 TTF	59.12	10.	76.8	6.12	3.87	1.83	6.80	1.35	41.78	0.58	35.5	9.40	7.27	1.0	0.59	37.72	3.74	**244.59**
A9	Coal 1Test 1 TTT	81.92	7.32	83.2	6.05	3.74	1.90	7.28	1.34	46.02	0.57	38.94	10.20	7.80	1.09	0.5	37.9	3.55	**257.6**
A10	Coal 2 Test 1 FFF	4.50	NA	177.66	14.66	9.55	4.2	15.	3.55	97.7	1.33	82.1	21.1	15.32	2.44	1.33	93.27	9.33	**549.41**
A11	Coal 2 Test 1 TTF	35.92	11.	76.83	6.65	4.29	1.70	7.10	1.45	41.2	0.6	33.96	9.02	6.99	1.17	0.72	42.87	4.29	**249.9**
A12	Coal 2 Test 2 TTT	85.5	7.01	64.8	4.87	3.06	1.43	5.60	1.08	34.95	0.46	30.16	7.87	5.93	0.87	0.46	30.8	2.88	**202.34**
A13	Coal 3 Test 1 FFF	4.06	NA	219.30	20.45	13.31	5.9	21.44	4.68	115.81	2.22	101.0	26.8	19.7	3.45	2.22	128.13	13.55	**698.0**
A14	Coal 3 Test 1 & Test 2 TTF	60.26	9.96	78.49	5.6	3.35	2.02	7.57	1.26	45.30	0.50	37.67	9.44	7.78	1.0	0.56	34.35	3.40	**248.3**
A15	Coal 3 Test 2 TTT	84.93	7.06	71.59	4.6	2.61	1.7	6.76	0.93	39.8	0.39	33.6	8.63	6.8	0.91	0.38	25.79	2.37	**214.10**
A16	Coal 4 Test 2 FFF	2.41	124.25	306.49	21.12	12.84	7.46	26.51	4.56	169.81	2.07	140.82	35.62	27.	3.73	1.66	140.82	12.8	**1038.35**
A17	Coal 4 Test 1 TTFF	35.58	14.05	71.66	5.14	3.54	1.63	5.85	1.18	41.59	0.53	32.0	8.4	6.32	0.87	0.51	34.85	3.43	**231.68**
A18	Coal 4 Test 1 TTTT	74.97	9.3	58.	4.36	2.73	1.39	5.20	0.9	34.02	0.43	27.75	7.26	5.54	0.75	0.45	29.0	2.67	**190.49**
A19	Coal 5 Test 1 FFF	2.91	NA	195.7	17.5	10.9	4.46	15.45	4.12	106.46	1.72	85.85	23.35	15.45	2.75	2.06	113.32	11.33	**610.57**
A20	Coal 5 Test 2 TFF	11.4	17.47	80.	8.56	5.33	2.01	8.39	1.92	42.80	0.79	38.	9.61	8.04	1.48	0.87	50.6	5.42	**282.12**
A21	Coal 5 Test 1 & Test 2 TTT	89.76	7.80	51.25	4.41	2.6	1.37	5.50	0.90	27.2	0.39	27.1	6.64	5.7	0.80	0.39	29.52	2.33	**174.09**
A22	Coal 6 Test 1 FFF	4.42	45.23	160.56	20.35	12.66	3.84	16.96	4.0	92.72	2.04	76.89	19.4	16.0	3.17	2.04	124.38	12.6	**613.0**
A23	Coal 6 Test 1 TFF	28.39	14.	82.08	7.36	4.61	2.11	7.96	1.5	42.62	0.70	38.40	9.79	8.00	1.20	0.74	44.03	4.58	**269.87**
A24	Coal 6 Test 1 TTT	87.91	7.96	70.07	5.08	2.8	1.50	5.85	0.97	38.11	0.45	35.	8.69	6.80	0.9	0.43	30.48	2.83	**218.18**

Total REE = Sc + Ce + Dy +Er + Eu + Gd + Ho + La + Lu + Nd + Pr + Sm + Tb + Tm + Y + Yb

NA = Not Available

Further, REE distribution calculated using the mass balance on the low ash products (<10% ash), middling (10 – 60% ash), and tailings (>60% ash) as obtained from the tree analysis revealed that most of the REE by weight percent reported to the middlings and tailings streams as shown in **Figure 25**. Tailings contained a major portion of REE in feed sample coals 1, 2, and 4, whereas the majority of REE in feed coals 5 and 6 were found in the middlings. Since only three products from the tree analyses were selected for analysis, feed coal 3 did not follow the general trend in **Figure 25**.

Dai et al. (2002) showed that coal samples from the Shitanjing, Shizuishan, and Fenfeng coalfields contain about 90% of REE associated with aluminum silicate minerals, using a sequential extraction procedure. Coal samples from the East Kootenay coalfield in BC contained approximately 65% of REE that were associated with inorganic constituents of the coal. Only 30% of REE, on average, were associated with the organic phase. Further, Hower et al. (2018) differentiated that organic association (chemically bound elements with organics) is principally different from association with organics, which denotes the dispersion of very fine elements within the coal matrix that cannot be removed by float-sink or chemical methods.

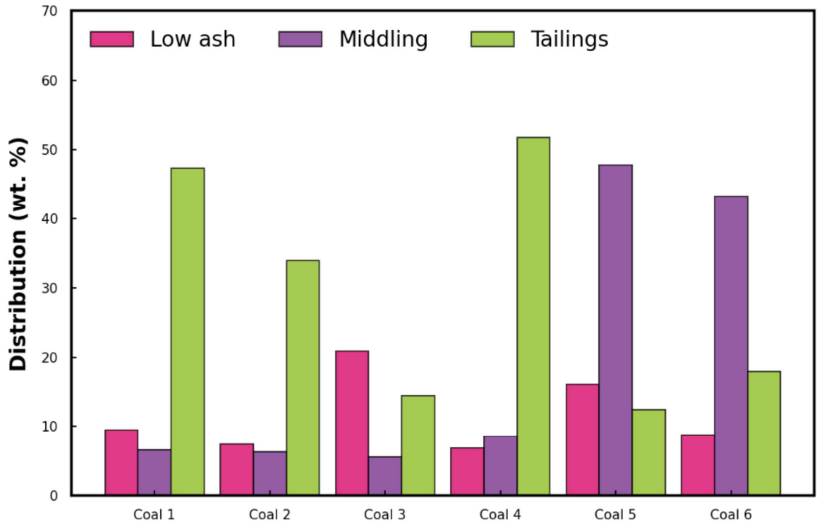

Figure 25. Distribution of REE by weight (%) in the tree analysis flotation products calculated using data shown in **Table 5**. Low ash denotes product <10% ash, middlings denote product 10-60% ash and tailings denote product >60% ash.

Since flotation processes do not account for the fine-grained minerals dispersed within the coal matrix, it may have led to the erroneous assignment of organic-associated REE percentages. Hence, a direct measurement of REE using SEM or other advanced characterization techniques should be incorporated in order to understand the exact nature of organically associated REE in the sample.

The two tree release analysis products with the highest concentration of REE, low-ash product (A16), and tailings (A9), were selected for SEM-EDX characterization in order to find the REE mineral association in the sample.

Figure 26 shows the SEM-EDX images of a low-ash product and tailings. Spot analyses showed that REE were associated with aluminosilicate minerals, likely clays, in both low-ash products and tailings. All of the spots analyzed on low-ash products revealed only the presence of quartz and aluminosilicate minerals, which might be reported to the froth due to the partial entrainment and/or as unliberated mineral phase. REE associated with clays were previously reported in the Jungar coalfield, China; Huaibei coalfield, China; Antaibao mining district, China; Far East deposits, Russia; and in Fire clay coal, United States (Hower et al., 2018 a; Hower et al., 2018 b; Wang et al., 2008; Zhang et al., 2015).

Using transmission electron microscopy, Hower et al. (2018) showed the presence of nanoscale REE minerals in Blue Gem coal from the United States, wherein organically associated REE were previously reported, especially in low-ash and low-rank coals (Dai & Finkelman, 2018; Eskenazy 1999; Eskenazy 1987). Huggins and Huffman (2004) explained the transition of organically associated elements to inorganic associations as a result of the decarboxylation process, which occurs during the coalification of low-rank coal to higher bituminous-rank coal. During the decarboxylation process, the cations associated with carboxyl groups (-COOM, where M represents the cations) undergo decomposition and are eventually incorporated into clays and other minerals, such as oxides and oxyhydroxides. Since the spot analyses on the low-ash product showed REE association with clay, and the coal under study belongs to high ranks, it is likely that not all REE in a low-ash product have an organic association. Hence, the actual amount of organically associated REE in the coal might be less than the reported value in the REE deportment analysis shown in **Figure 25** results. Further advanced characterization would be required in the future to quantify organic associated REE in the sample. It can be further concluded that inorganic association is the dominant mode of REE occurrence in the studied coal samples.

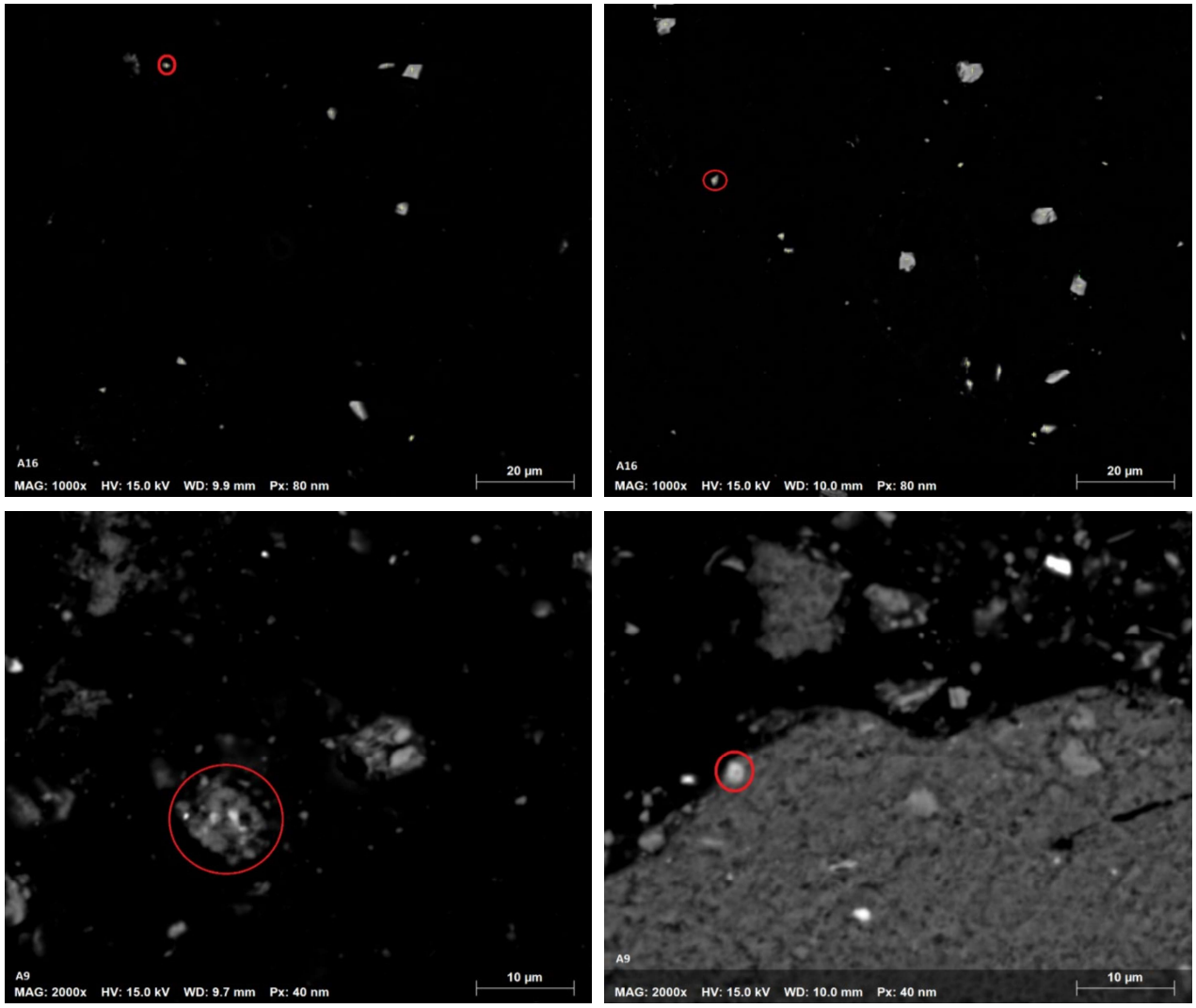

Figure 26. SEM-EDX images of clean coal (A16) and tailings (A9)Elements observed in the highlighted grains are as follows: Top Left (A16): Al, Ba, Ca, Eu, O, P, S, Sr/Top Right (A16): Al, Er, O, Si, Bottom Left (A9): Al, Ba, Br, Ca, Ce, O, P, Si/ Bottom Right (A9): Al, Ba, Br, Ca, Ce, La, O, P, Si

4.4.2 Sequential Extraction Results

Since the preliminary analysis indicated the inorganic REE as dominant mode of REE association in the sample, four samples from the database (S9, S42, S57 and S81) representing different parts of coal seam including coal (S81), roof (S9), floor (S57), and partings (S42) with highest REE concentration was selected for detailed analysis of REE inorganic association using chemical based sequential extraction process, as described in Section 3.3.3. **Figure 27** shows the sequential extraction results for the select samples, which categories the REE association into the following five types: the ion-exchangeable REE (Stage 1), weak acid soluble form (Stage 2), REE bound to other carbonates and monosulfides (Stage 3), REE associated with disulfides (Stage 4), and REE association with silicates and aluminosilicate form

(Stage 5). It can be observed that more than 65% by weight of REE is associated with silicates and aluminosilicate minerals for all the samples. REE association with acid soluble form (Stage 2 & Stage 3) accounts for about 30, 25, 13 and 15% respectively for samples S9, S42, S57, and S81. One of the modes of occurrences of REE in coal is in an ion-exchangeable form. It was previously shown that ion exchangeable REE can be extracted using monovalent salt solutions such as ammonium sulfate (Moldoveanu & Papangelakis, 2012, 2013). The stage 1 extraction using ammonium sulfate indicates that REE in the ion-exchangeable form in samples S42, S57, S81 were insignificant and S9 contains around 3.5% of REE in ion exchangeable form.

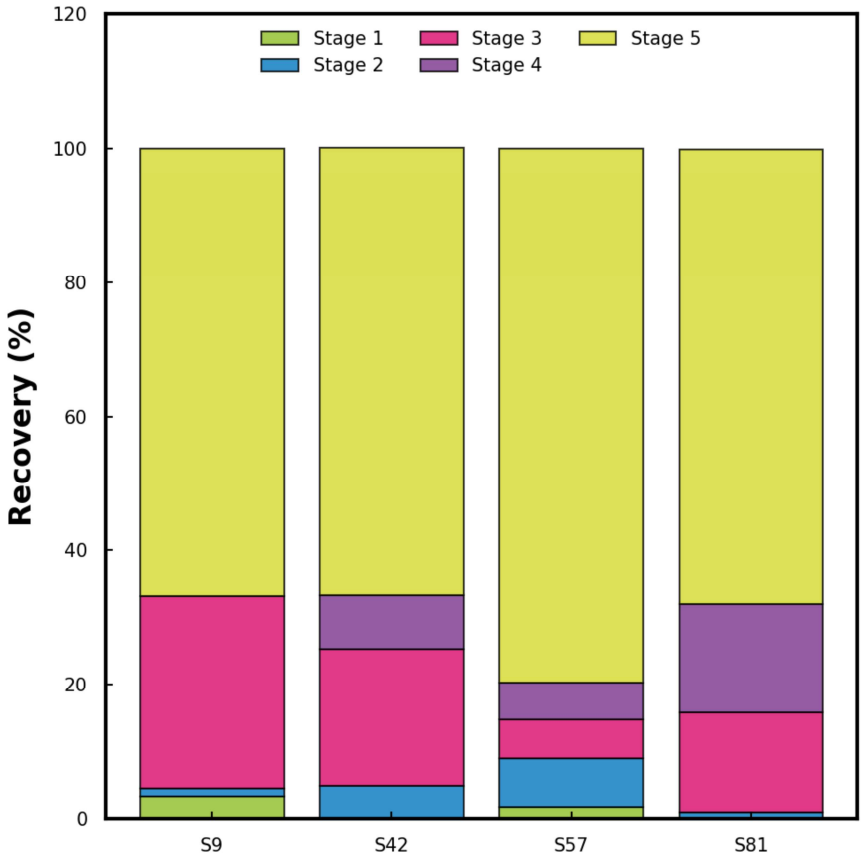

Figure 27. Sequential extraction results of samples (S9, S42, S57, S81) showing the distribution of REE in various modes of occurrences. Missing color indicates the extraction in the certain stage were negligible.

As previously described, fine grained REE minerals locked in the aluminosilicate mineral matrix such as clays would not be reached by reagents used for sequential extraction without proper liberation. **Figure 26** also indicates the presence of fine REE minerals in the clay matrix. Hence, the results presented on quantification should not be considered as an absolute value for the sample. But for all practical purposes,

it can be inferred that REE minerals would behave as though part of clay mineral during physical beneficiation process for the sample studied.

4.4.3 Mineralogical Characterization

Mineralogical analysis using X-ray diffraction (XRD) and SEM-EDX analysis was conducted to identify major mineral phase and REE mineral carrier in the select four samples (S9, S42, S57, and S81). Among the four samples, XRD analysis was conducted only for S9, S42, and S57. Since the sample S81 is coal sample with low ash content, it was not suitable for XRD analysis due to interference from carbonaceous material.

The phase identification results for S9, S42, and S57 are shown in **Figure 28**. It can be observed that the majority of minerals present in all of three samples were clays such as kaolinite and illite, which accounted for around 40 to 50% of the detected crystalline phases in the sample. Quartz contributed about 47 to 58% of the crystalline phase. Other minerals such as anatase, rutile, carbonates, and pyrite were also reported in minor amounts. Since the concentration of REE minerals is below the detection limit for XRD analysis, they were not identified during the analysis.

To identify REE mineral carrier in these samples, SEM-EDX characterization was conducted on all four selected samples (S9, S42, S57 and S81). **Figure 29** shows the REE grains identified in all four sample along with other elements observed during EDX analysis of the grain. REE grains were generally associated with silicate and aluminosilicates, which is expected based on the major minerals identified in the XRD results.

Using the EDX results, REE grains located were zoomed further in the SEM and EDX mapping was conducted on REE grain. The EDX mapping of select grains revealed the presence of apatite, monazite, xenotime, and zircon in the sample. **Figure 30** to **Figure 34** shows the apatite, monazite, xenotime, and zircon mineral identified in the sample. It should be noted that both apatite, monazite and xenotime are REE phosphate minerals, whereas Zircon is silicate mineral, which usually contains minor amounts of Y/REE, P and others.

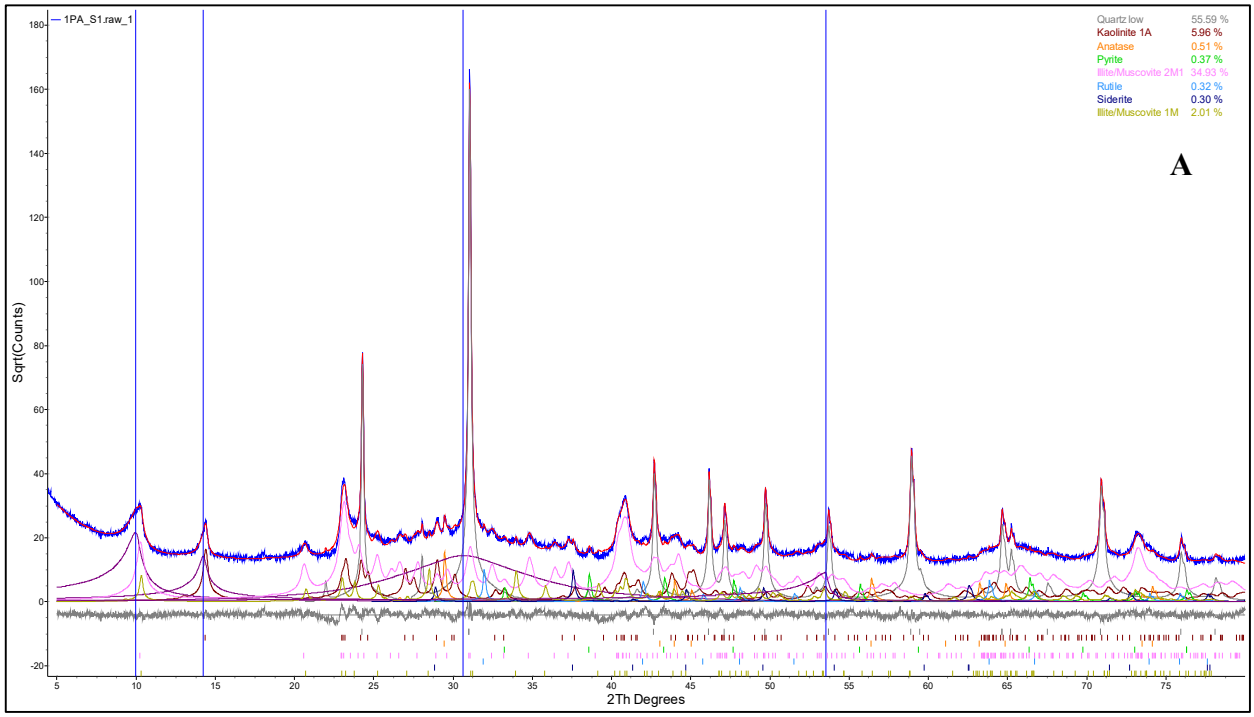
1PA_S1.raw_1
Quartz low 55.59 %
Kaolinite 1A 5.96 %
Anatase 0.51 %
Pyrite 0.37 %
Illite/Muscovite 2M1 34.93 %
Rutile 0.32 %
Siderite 0.30 %
Illite/Muscovite 1M 2.01 %
A
Sqrt(Counts)
2Th Degrees

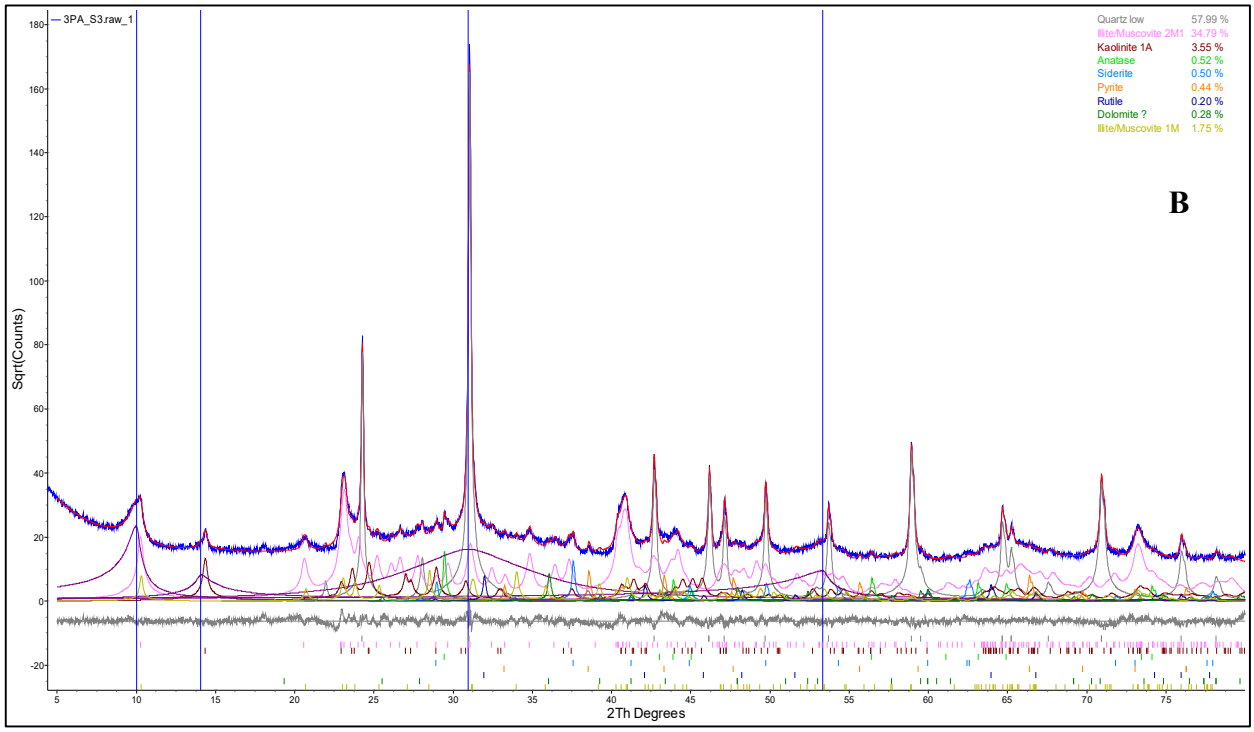
3PA_S3.raw_1
Quartz low 57.99 %
Illite/Muscovite 2M1 34.79 %
Kaolinite 1A 3.55 %
Anatase 0.52 %
Siderite 0.50 %
Pyrite 0.44 %
Rutile 0.20 %
Dolomite ? 0.28 %
Illite/Muscovite 1M 1.75 %
B
Sqrt(Counts)
2Th Degrees

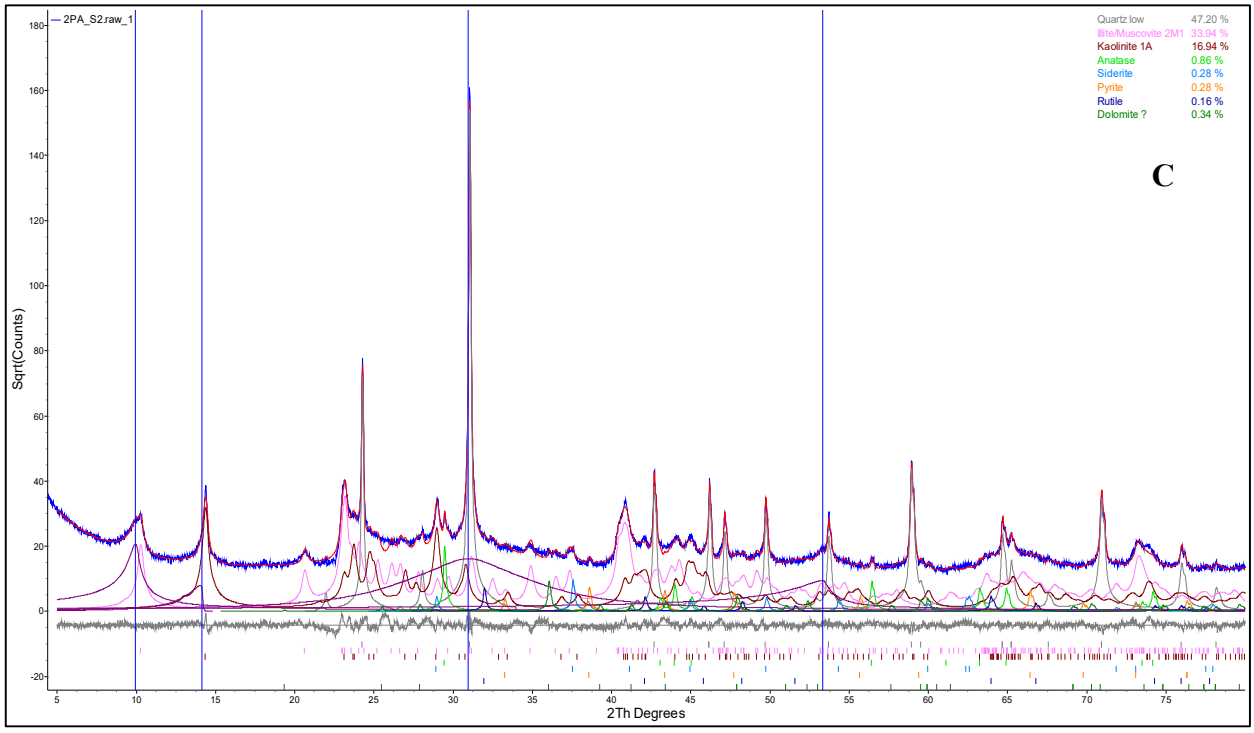

Figure 28. Quantitative X-ray diffraction analysis results for select samples: A) S9 B) S42 C) S57

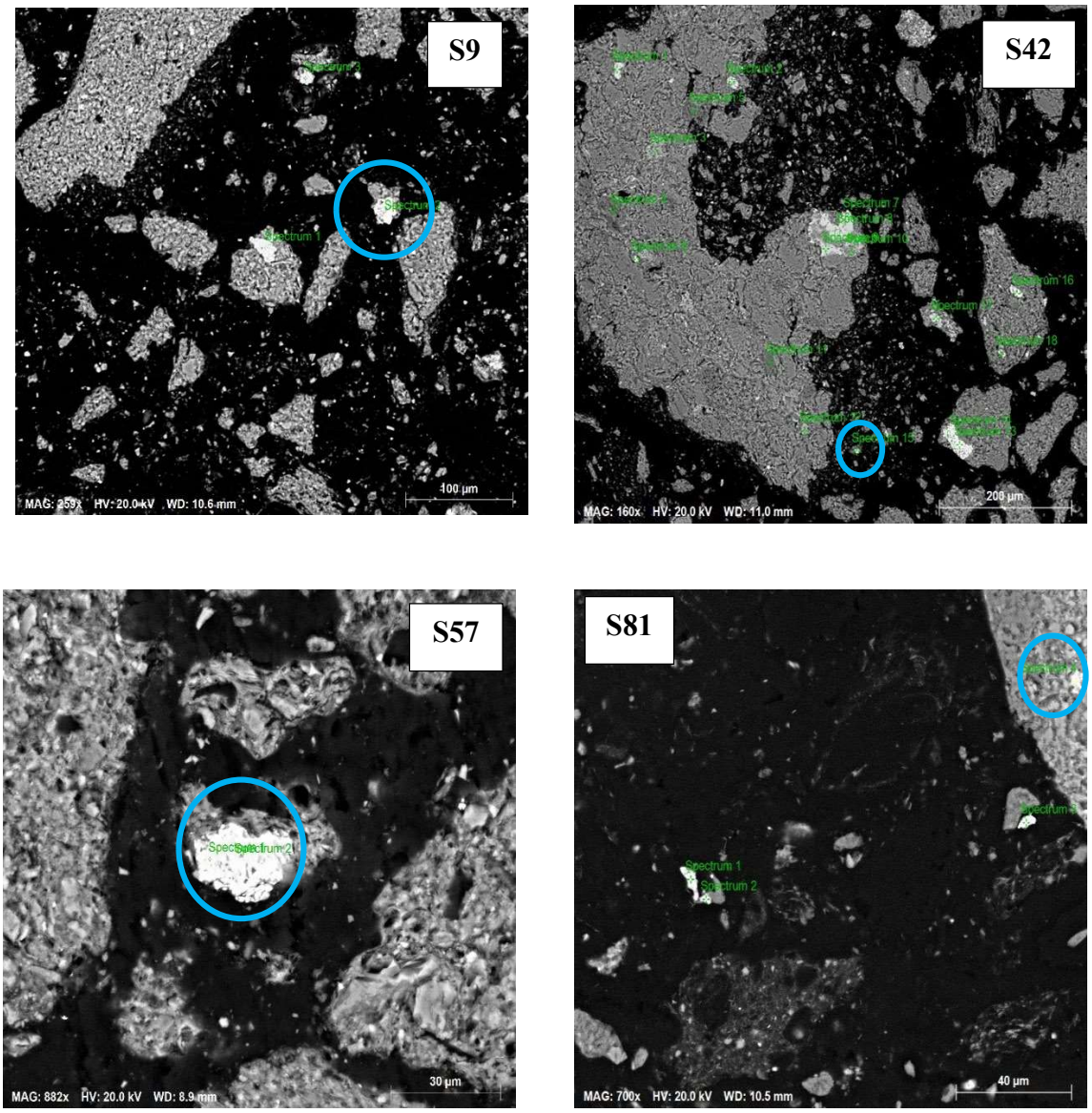

Figure 29. SEM-EDX images of sample S9, S42, S57 and S81. Elements observed in the highlighted grains are as follows: Top Left (S9): Yt, Y, Ca, Si, O; Top Right (S42): (REE) Ba, Fe, Cl, Al, Si, O Bottom Left (S57): La, Ce, Y, Sc, Al, Si, Na, P, O; Bottom Right (S81): Ce, Y, Zr, Ca, K, Al, Si, F, P, O.

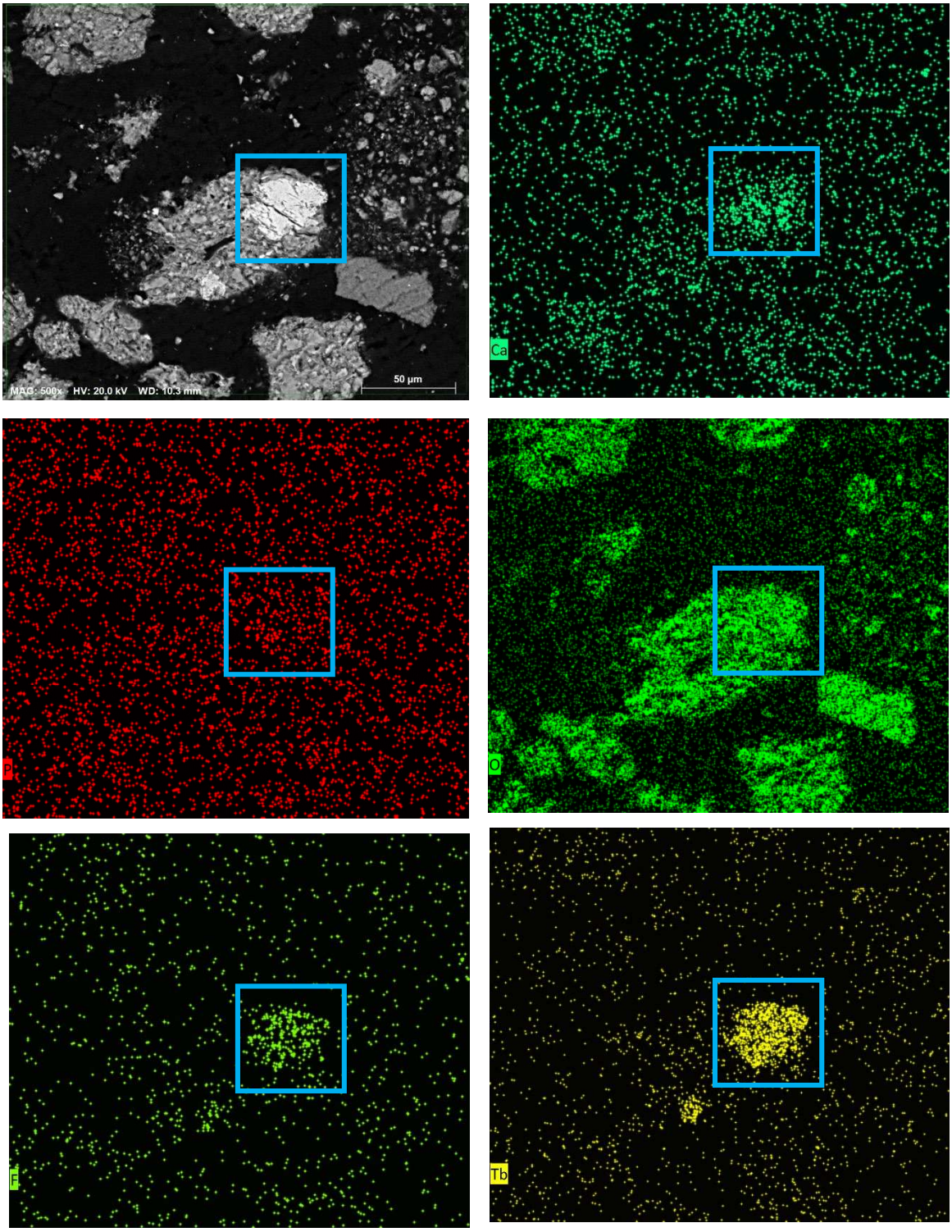

Figure 30 SEM-EDX mapping of Apatite ($Ca_5(PO_4)_3F$) mineral identified in the sample S42

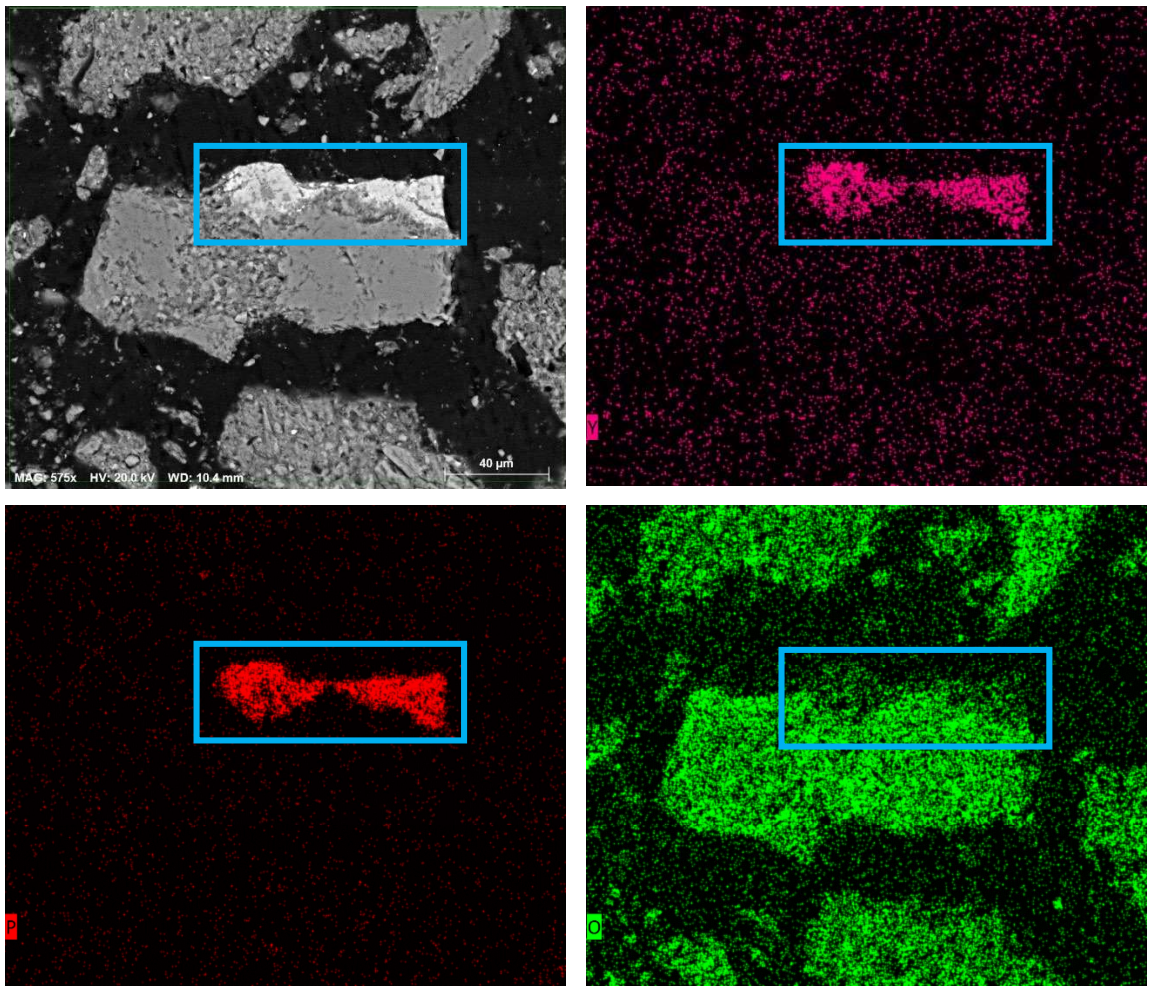

Figure 31 SEM-EDX mapping of Xenotime (YPO_4) mineral identified in the sample S57

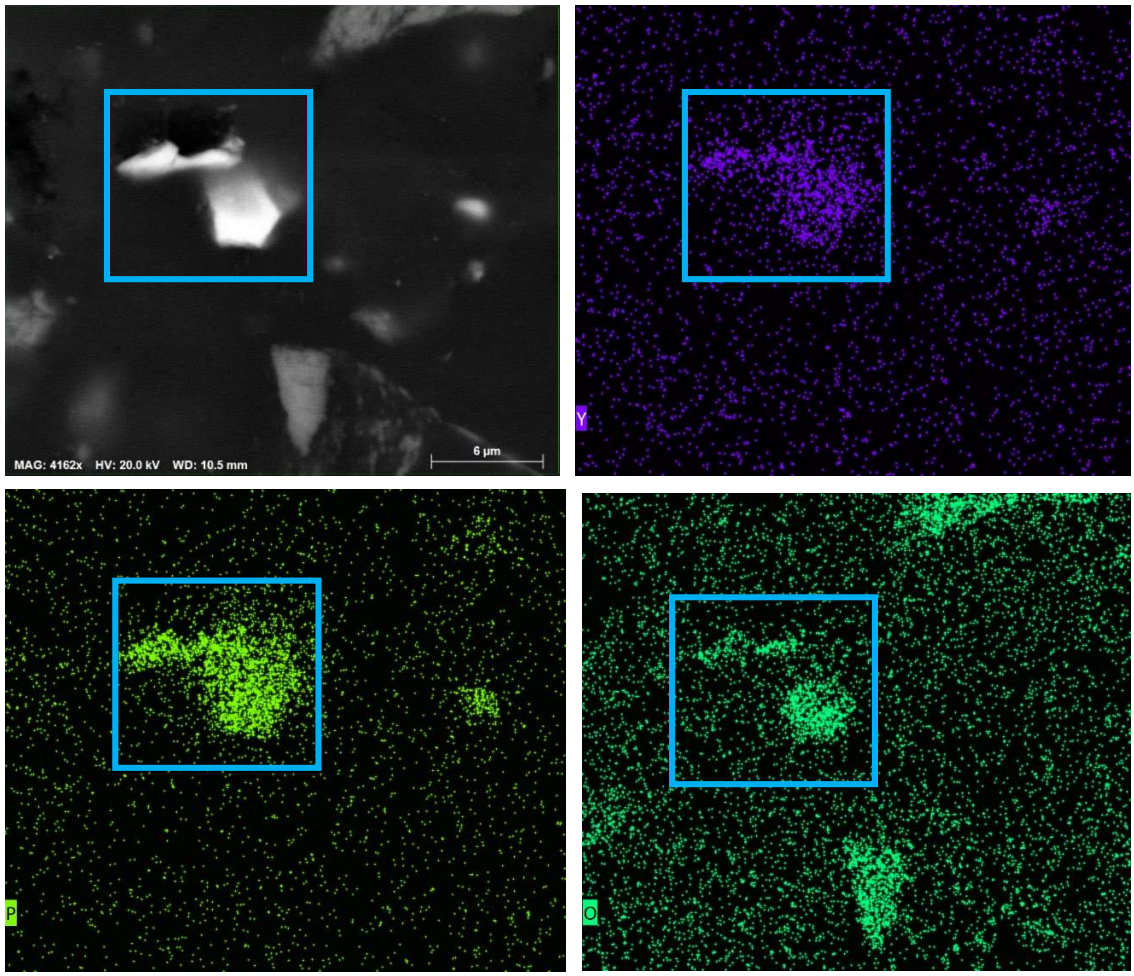

Figure 32. SEM-EDX mapping of Xenotime (YPO_4) mineral identified in the sample S81

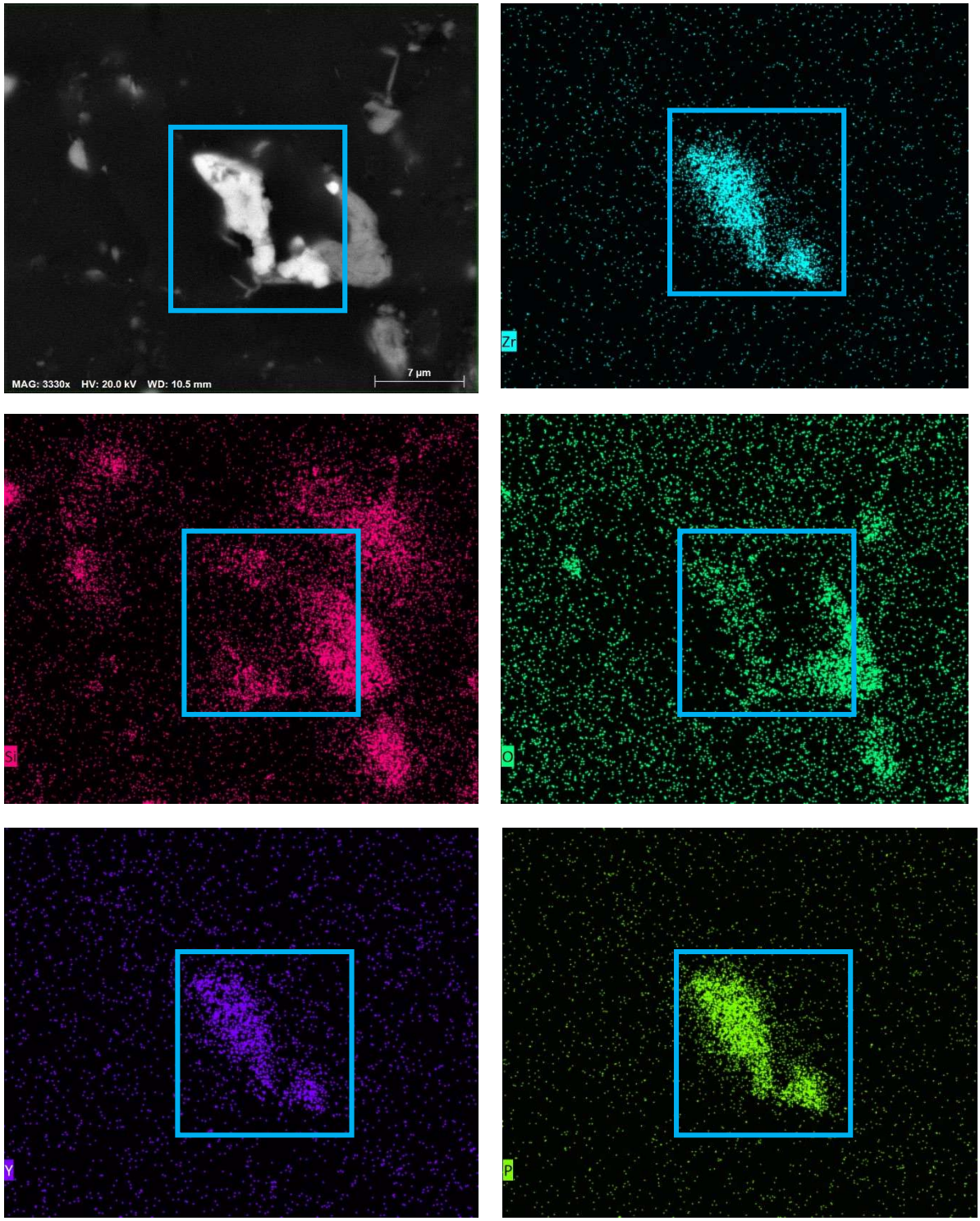

Figure 33. SEM-EDX mapping of Xenotime (YPO_4) mineral identified in the sample S81

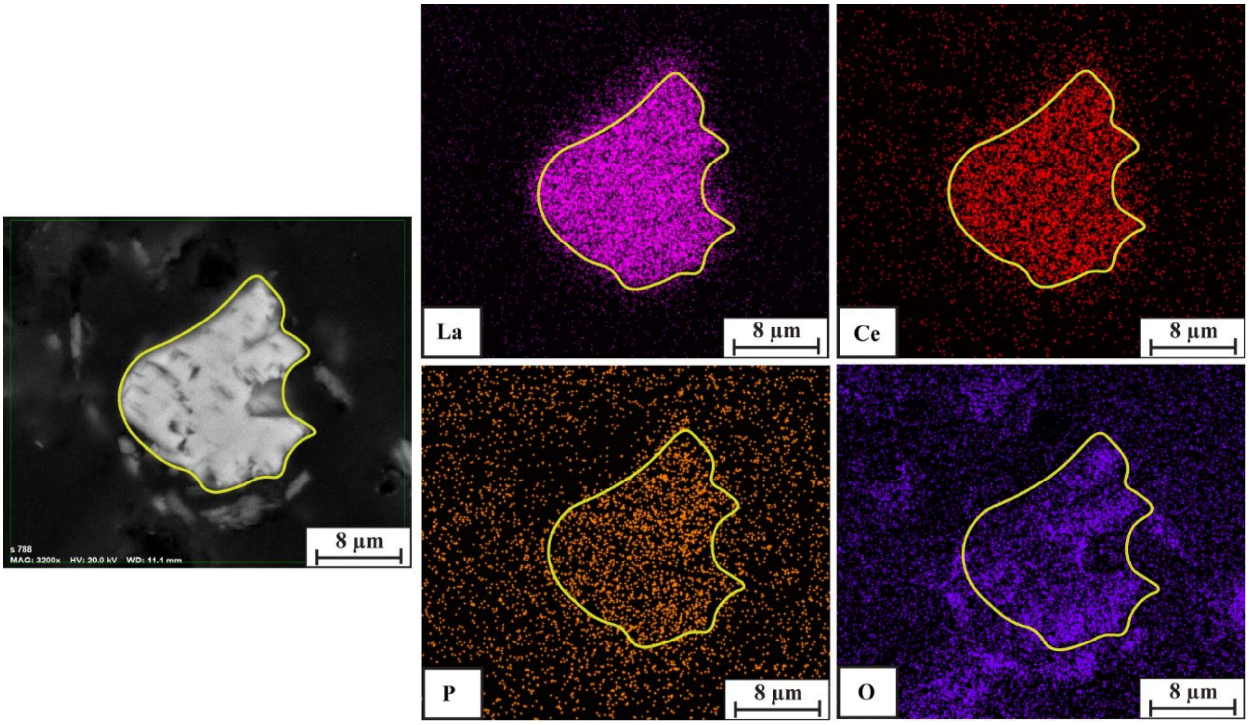

Figure 34. SEM-EDX mapping of monazite (Light Rare Earth Phosphate) mineral identified in the LTA sample of coal 2 tailings

Further, automated liberation analysis was conducted for two samples (S57 and coal 2 tailings). For each sample, two size fractions (-106+75 µm and -53+25 µm) analyzed and results are depicted in **Figure 35** and **Figure 36**.

The two fractions of Sample S57 consists predominantly of quartz (52.9 - 56.5 wt.%) and muscovite/illite (39.3 - 45.6 wt.%) with minor amounts (<5 wt.%) of kaolinite (0.81 - 1.73 wt.%) and carbonates (0.2 - 1.1 wt.%), and trace amounts of (<0.05 wt.%) REE-bearing phases, without a significant difference between the two fractions. A total of 5 monazite grains ranging in size from 5 µm to 25 µm were detected as well as one occurrence of the Y-phosphate xenotime. The majority of the monazite was observed in the +75 fraction in association with quartz and muscovite/illite. The most abundant accessory phase is zircon with 73 observed grains.

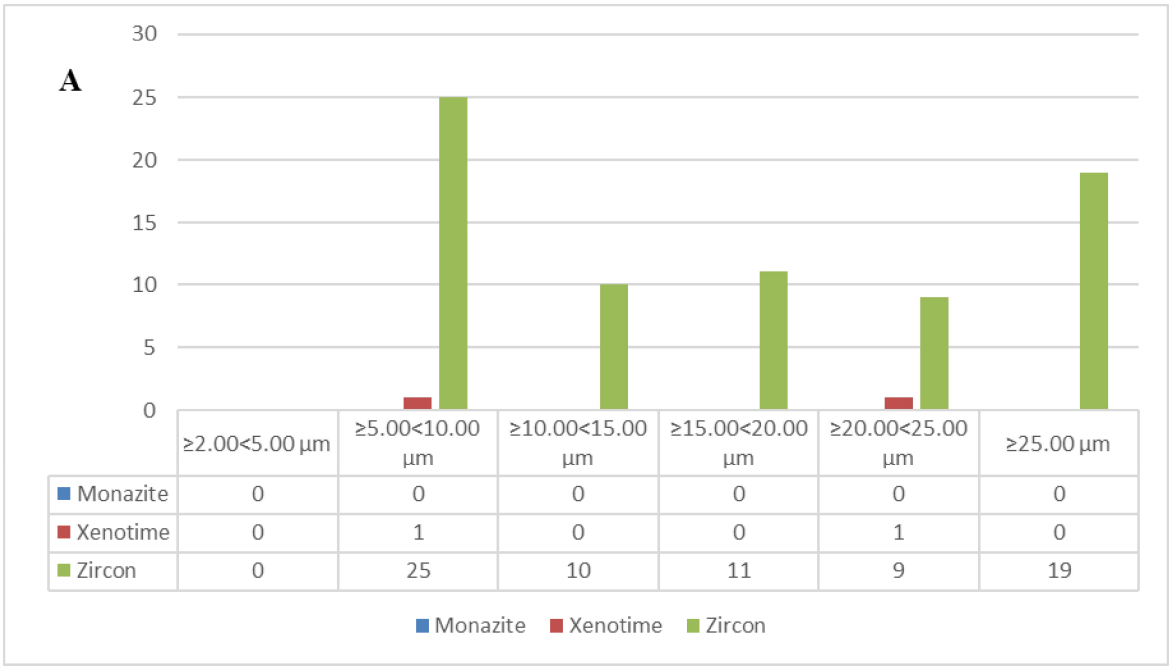

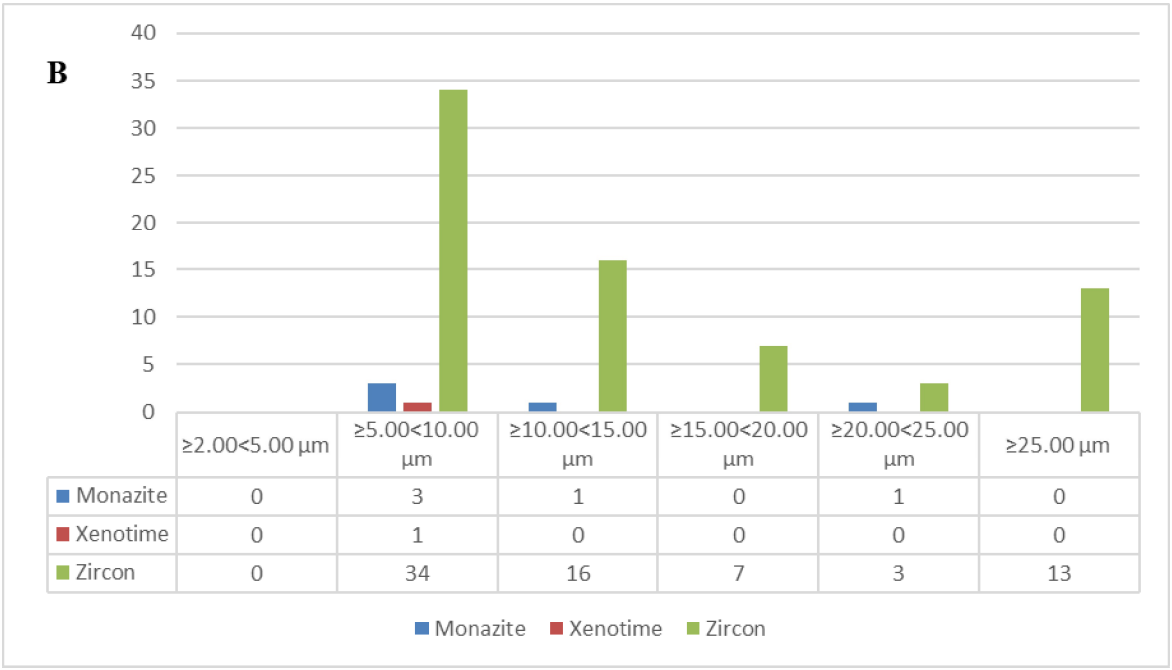

Figure 35. Grain size distribution for different REE bearing minerals in the sample: A) Coal 2 tailings B) S57

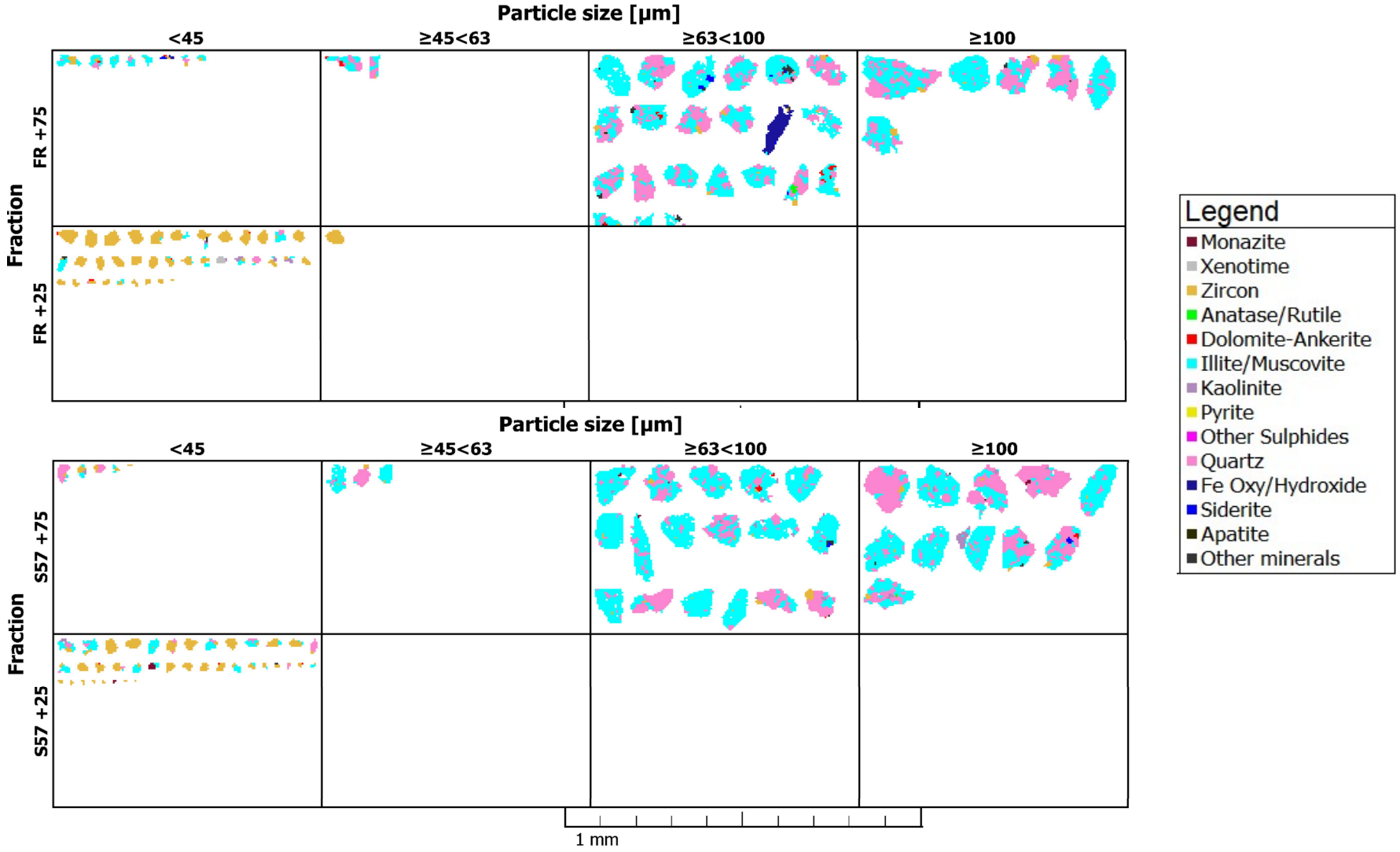

Figure 36 Mineral liberation and association analysis results for select samples: Top: coal 2 tailings and Bottom: S57

The two fractions of Sample coal 2 tailings consist predominantly of quartz (41.8 - 47.2 wt.%) and muscovite/illite (25.7 - 27.6 wt.%), moderate amounts of kaolinte (10.1 wt.%), Fe-oxy/hydroxides (6.5 - 10.5 wt.%), Fe-carbonates (5.2 - 7.8 wt.%) with minor amounts (<5 wt.%) of Ca-Mg carbonates (1.1 - 2.7 wt.%) and carbonates (0.2 - 1. wt.%). The only REE-bearing phase detected was xenotime (HREE) which was observed in 2 occurrences. The most abundant accessory phase is zircon with 74 observed grains. Additional measurements utilizing a REE elemental mapping of particles were employed in order to identify REE-enrichment unrelated to monazite, but analysis results did not find any other minerals. The overall observed grain counts are very, which was expected given the very low REE grade of the samples.

A direct comparison of XRD data obtained from diffraction analyses and the presented automated SEM data reveals discrepancies which are partly related to different sample types (bulk rock versus size fractions) and partly to the inherent advantages and disadvantages of each analytical method. While XRD tends to over-report sheet-silicate and under-report minor phases, automated SEM systems often struggle with clays and very fine-grained/slimes material due to the complex spectra.

4.5 Physical Concentration Test Results

4.5.1 Particle Size Separation Results

All four different sample types (coal, roof, floor, and partings) were sieved to obtain six different size fractions. Each of these size fractions was weighed to obtain weight distribution of sample in each of these size fractions and representative sample was sent for REE analysis. Total REE (15 lanthanides plus Sc and Y, except Pm) distribution in each of these size fractions are shown in **Figure 37** along with the sample weight distribution for each size fractions.

It can be noted that the weight percentage of total REE in each size fraction and sample weight distribution was almost the same for all the size fractions, indicating that REE are evenly distributed between different particle-size fractions, and no significant enrichment of REE was observed in any given size fraction. The even distribution of REE in all the size fraction depicts that particle size reduction was not able to effectively release RE minerals from the gangue matrix.

Further, it can be observed that weight of REE in each size fractions for roof, floor, and partings follows similar trend, except for coal (S81) which generated more finer material for similar sample preparation technique followed for all the samples indicating the soft nature of coal.

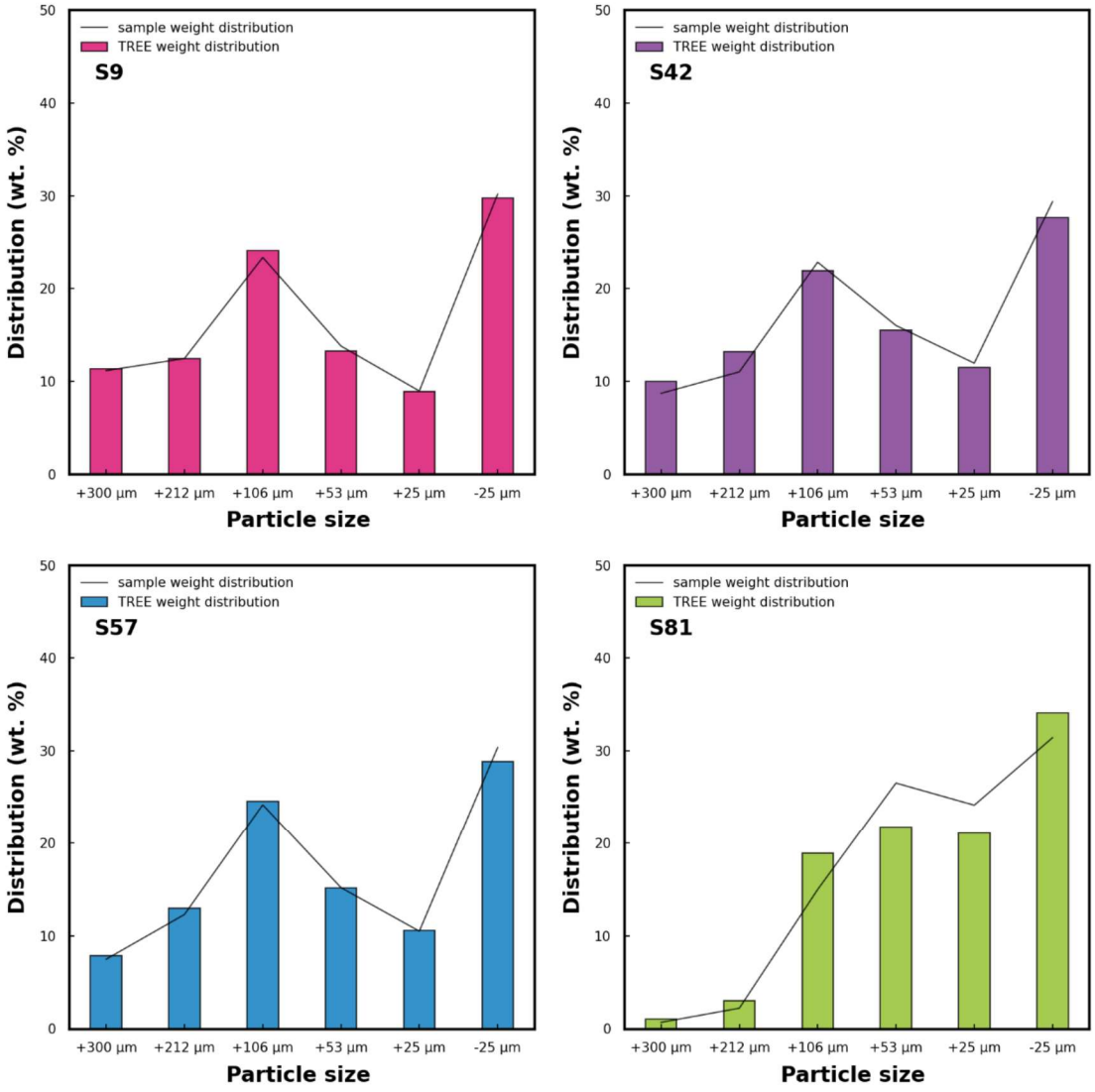

Figure 37. Total REE distribution by wt. (%) in different size fraction for select four (S9, S42, S57 and S81) samples

4.5. Float and Sink Results

Density based separation is predominantly used in coal beneficiation for separating organic material from inorganic matter, which are generally heavier than carbonaceous material. Similarly, density difference between the different minerals is also utilized for concentrating heavier mineral from rest of the sample. The density of monazite, xenotime, and bastnasite, three common RE minerals, are in the range of 4 to 5.5 g/cm^3. The higher density of RE minerals are traditionally uses as technique for concentrating RE

minerals from beach sand deposits (Krishnamurthy & Gupta, 2016). Hence, the potential of concentrating REE using heavy density liquid was tested and results are presented in **Figure 38**.

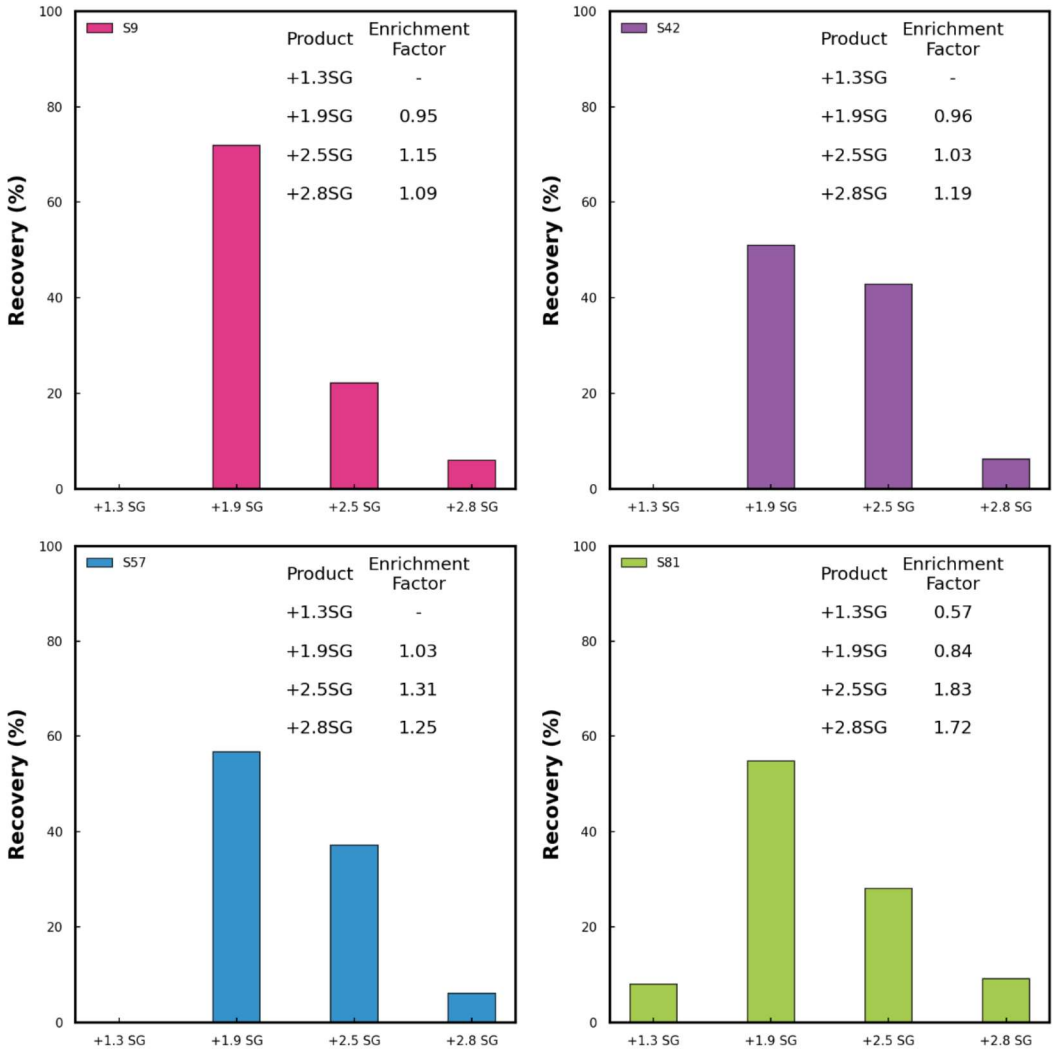

Figure 38. REE recovery and enrichment using density separation for select four (S9, S42, S57 and S81) samples

The results show the REE recovery in each density fraction and the corresponding enrichment factor, which indicates the quality of REE concentrate are also given in the **Figure 38**. The effective density of RE minerals are diluted by presence of lower density mineral matrix components, which reduces the density separation efficiency. It can be noticed that REE recovery in lower density product SG +1.3 and SG +1.9 is still considerable. But any liberated RE mineral have concentrated in the heavier fraction (SG +2.5 and SG +2.8) as indicated by enrichment factor of more than 1 in all the product greater than SG of 2.5. Among all the samples tested, coal (S81) showed the most promising response for REE concentration

by density method. The enrichment factor of almost 2 indicating the concentrate product contains the REE concentration twice that of the feed sample. The lower REE recovery at higher density product could be attributed to poor liberation of RE mineral. Further, it can also be inferred that liberation of REE mineral using grinding would also enhance the REE concentrate quality. Hence, it can be stated that density-based separation is one of the promising methods, which should be studied in detail for REE enrichment in the BC coal related samples.

The density separation for coal beneficiation generally carried out below SG of 2.0. Hence, the reject from the coal preparation plant can be good source material for REE in the study area, which can be processed further to produce REE concentrate for downstream operations.

4.5.3 Wet High Magnetic Intensity Separation Test Results

Monazite and xenotime are paramagnetic rare earth (RE) minerals, which respond to the applied external magnetic field. Magnetic separation is generally used as RE beneficiation for beach sand deposits. Further, it also used to produce separate xenotime from monazite due to difference in magnetic susceptibility (Krishnamurthy & Gupta, 2016). Since mineralogical analysis indicated the presence of both monazite and xenotime in the sample, magnetic separation test was conducted to assess the potential of producing REE concentrate.

Figure 39 shows the REE recovery and concentrate enrichment for magnetically separated products for samples S9, S42, S57, and S81. It can be noted from the figure that on average, more than 80% REE recovered in tailings meaning most of REE reported to non-magnetic fraction. Further, enrichment factor for all the products and tailings streams is roughly equal to 1, which clearly shows that REE did not respond to magnetic separation process for the studied samples.

Further, XRD analysis showed that samples contain quartz and clays as a dominant mineral species and does not contain any major magnetic mineral. Further, fine grain sized REE minerals are not sufficiently liberated for magnetic separation. It is well known that efficiency of magnetic separation drops considerably below 10 μm particle size (Wills, 2015). Hence, it can be concluded that magnetic separation is not a suitable concentration method for the samples studied.

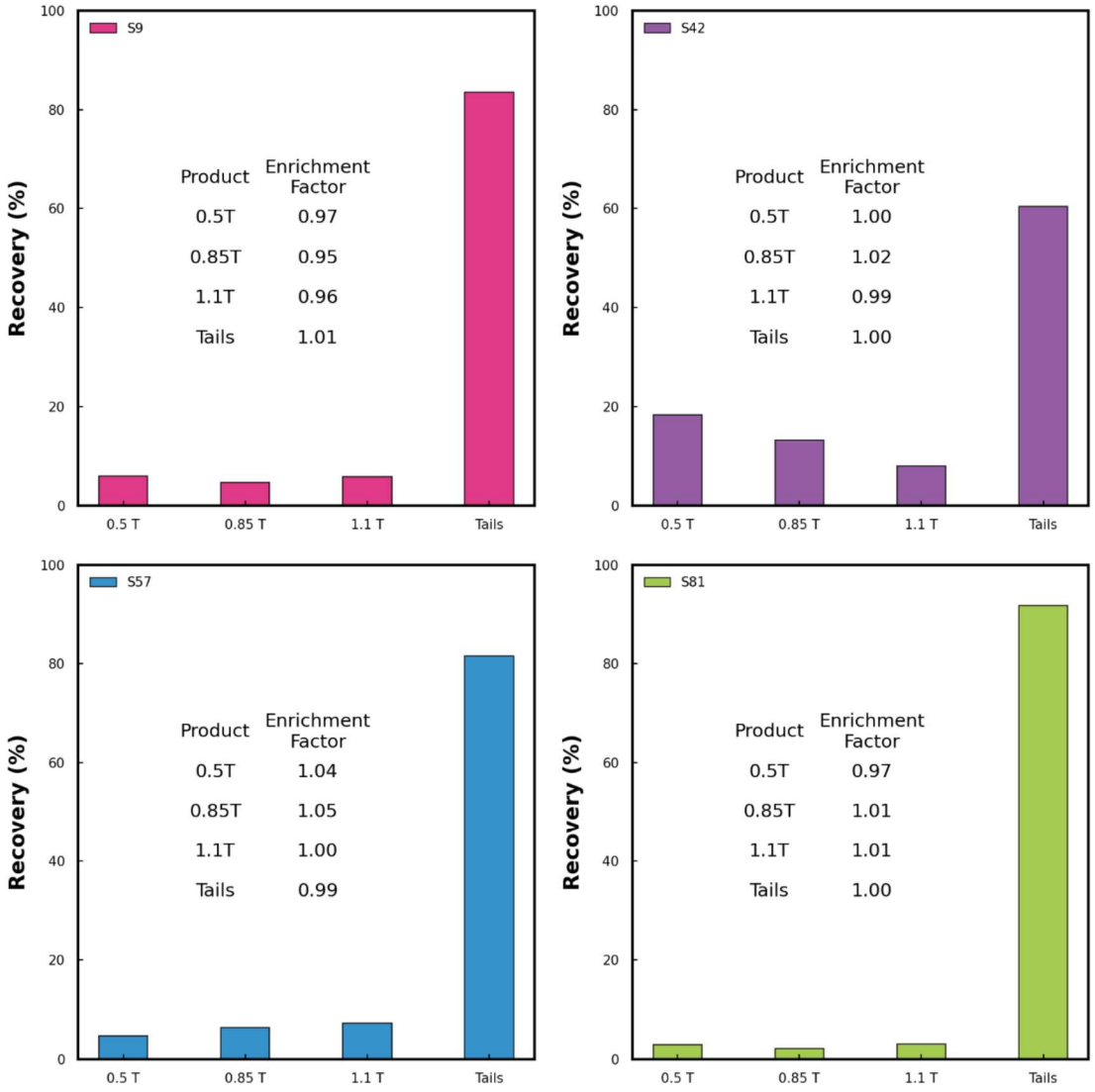

Figure 39. REE recovery and enrichment of magnetically separated products for select four (S9, S42, S57 and S81) samples

4.5. Knelson Concentration Test Results

Gravity based separators such as Knelson concentrator are used in the processing of traditional heavy mineral sands for concentrating REE using higher specific gravity of RE minerals (> 4 g/cm^3) compared to silicates (Krishnamurthy & Gupta, 2016). Knelson concentration test requires at least 2 kg sample, hence, plant reject (Reflux reject and heavy media cyclone tails) collected from operating plant with highest REE concentration were used for test.

The proximate analysis of these samples showed the presence of considerable quantity of carbonaceous materials. Hence, carbon removal flotation was conducted on these two samples, as prescribed in section 3.6.4.1. The tailings from the carbon removal flotation were used as feed for Knelson concentration test and results are shown in **Figure 40**. The concentration test was conducted in two stages with increasing G force at each stage producing two concentrates and final tailings.

The concentrate yields were roughly in the range of 5.5 to 6% for all the samples. The enrichment factor of roughly 1 for all the products depict that no significant upgrading of REE concentration in any of the products. Hence, the Knelson concentration is not a suitable method for REE enrichment in the sample studied. One of the prominent reasons for failure of Knelson concentration could be attributed to non-liberated fine grain nature of REE minerals in the sample.

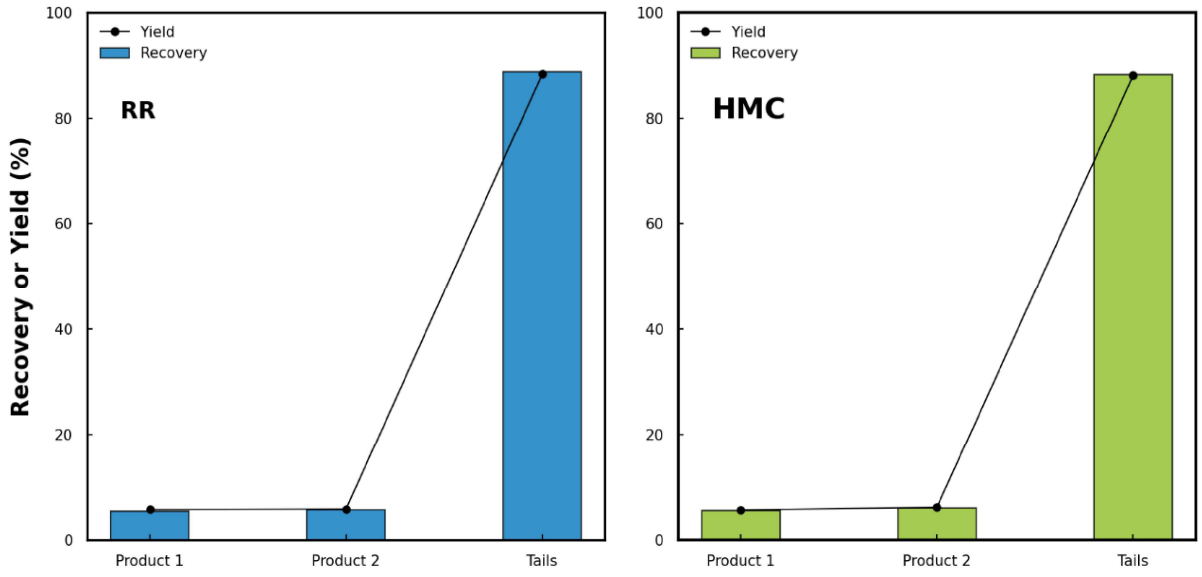

Figure 40. REE recovery and yield for gravity concentrated product for select samples

4.5.5 Flotation Test Results

Froth flotation is one of the commonly applied beneficiation techniques for rare earth ores and can be adapted to deposit's mineralogy. Among the REE minerals, bastnaesite has successfully concentrated using flotation at industrial scale in Bayan Obo (China) and Mountain Pass (USA) deposits (Zhang & Edwards, 2012). Based on the literature review of flotation chemistry, reagent schemes and conditions used for REE mineral flotation, different processing parameters are assessed in this study.

Since there were no sufficient mine samples (S9, S42, S57, and S81) for flotation experiments, plant rejects (Reflux reject, RR and Heavy media cyclone reject, HMC) with highest REE concentration were

selected for REE mineral flotation response in the coal related feed products. The carbon removal flotation was conducted on these two plant samples to remove any residual carbonadoes material. The procedure described in section 3.6.4.1 was used for coal flotation in 1 kg batches. Total of 10 batches of carbon removal flotation were conducted for each sample to produce enough tailings material for REE flotation feed. The ash content of REE flotation feed was around 76% and 81% for RR and HMC tailings, respectively.

REE flotation are generally carried out using oxhydryl collectors such as hydroxamates and carboxylates (Bulatovic, 2010). Hydroxamic acids and their salts, which are referred as hydroxamates, are found to be most effective flotation collectors for bastnaesite and monazite flotation (Bulatovic, 2010; Zhang & Edwards, 2012). Marion et al. (2020) reviewed the flotation reagents used for RE mineral in detail.

To assess the effect of collector dose and type on REE flotation, flotation experiments were conducted using two different types of collectors (Hydroxamate and Sodium Oleate) with varying dose and results are depicted in **Figure 41** and **Figure 42**. It can be observed that enrichment factor for both collector type (Hydroxamate and Sodium Oleate) was roughly 1 and same for HMC tails sample indicating no one collector type is more effective than other for the conditions tested. For RR tails sample, hydroxamate collector produced concentrate with EF of 0.83, which shows that specific mineral lower in REE association in the sample was selectively collected in the concentrate creating reverse REE flotation effect. More mineralogical analysis on flotation products should be carried out in the future to understand reverse flotation strategy.

As the collector dose was increased from 500 g/t to 1000 g/t, there was an additional 14% increase in concentrate yield for RR sample. The concentrate EF increased from 0.83 to 1.05 producing REE enriched concentrate compared to lower collector dose. For HMC sample, there was a modest increase in concentrate EF along with increase in concentrate yield for HMC sample with additional 7% concentrate yield.

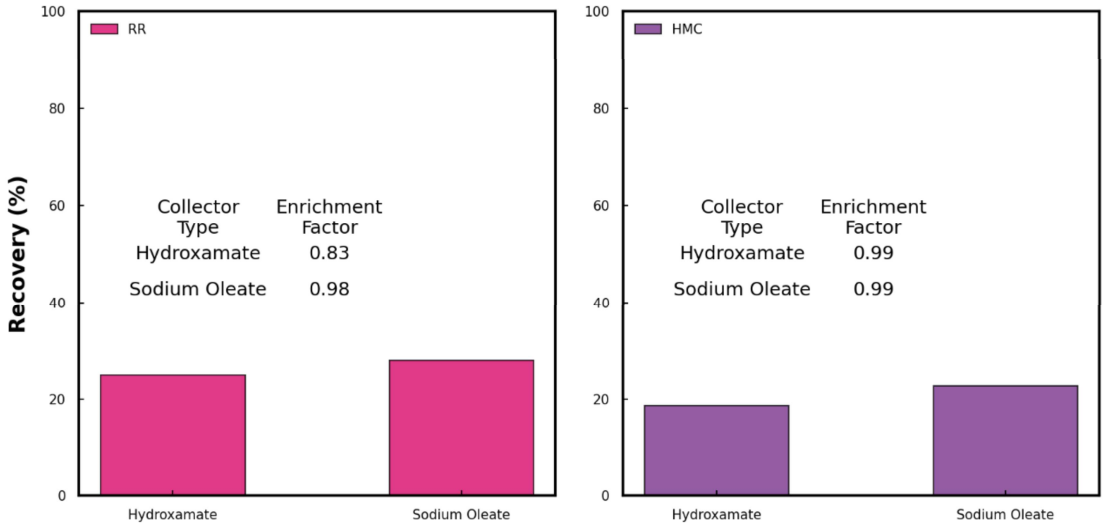

Figure 41. Effect of collector type on REE recovery and enrichment factor on concentrate obtained using froth flotation for select samples (500 g/t collector, 100 g/t frother, 9.5 pH, 15.4% solids, 20°C)

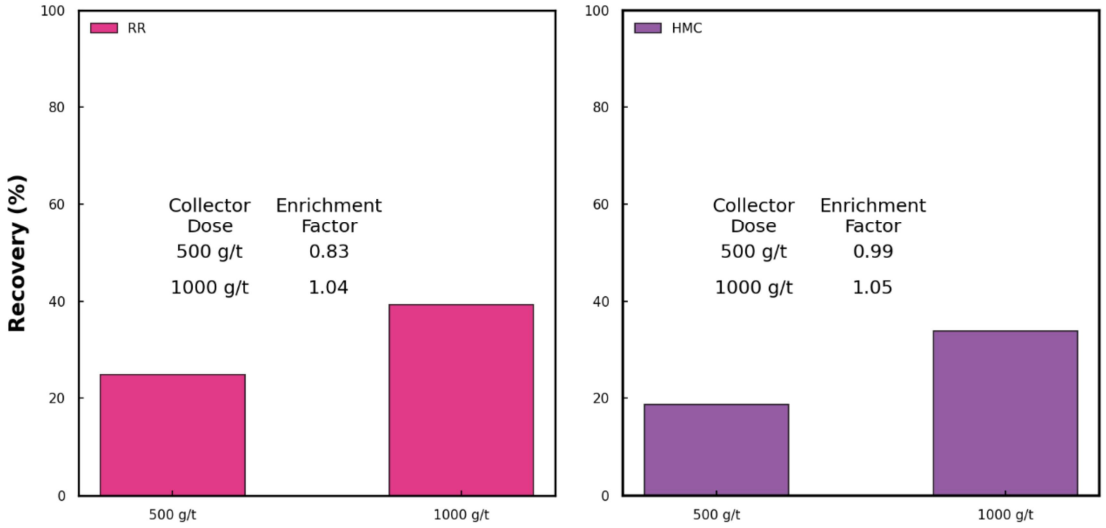

Figure 42. Effect of collector dose on REE recovery and enrichment using froth flotation for select samples (100 g/t frother, 9.5 pH, 15.4% solids, 20°C)

The effect of pH on REE flotation has shown that most optimum pH generally lies around 9 for hydroxamate collector (Marion et al., 2020). In addition, maximum monazite recoveries are reported at lower acid pH of around 3-4 and in the neutral range of 6 to 9 (Pavez et al., 1996). However, optimum pH

would vary for feed, depending on the REE mineral type and reagent dose. Hence, effect of pH on the sample was studied and results are depicted in **Figure 43**.

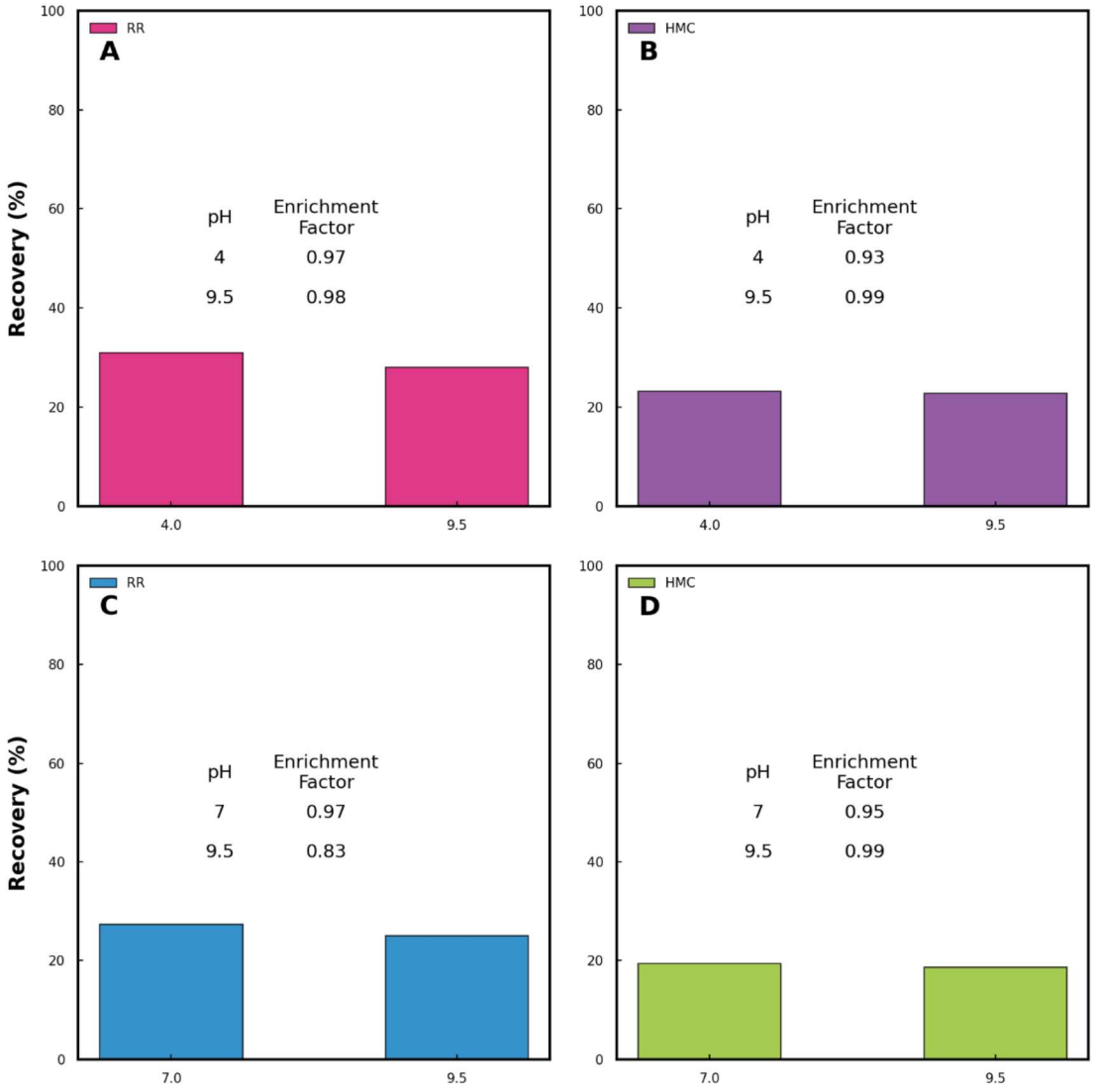

Figure 43. Effect of pH on REE recovery and enrichment using froth flotation for select samples: A) pH effect for sodium oleate collector on reflux reject (RR) tails sample; B) pH effect for sodium oleate collector on heavy media cyclone (HMC) tails sample; C) pH effect for hydroxamate collector on reflux reject (RR) tails sample; D) pH effect for hydroxamate collector on heavy media cyclone (HMC) tails sample

For sodium oleate collector, lower acid pH of 4 did not show any marked difference compared to basic pH of 9 for both samples (RR and HMC), as shown in **Figure 43**A and B. As the pH was decreased from 9.5 to 7 with hydroxamate as collector, the reverse flotation effect seen for RR sample was lost, as noticed

from concentrate EF increase from 0.83 to 0.97 (**Figure 43**C). Whereas for HMC sample, lower pH does not affect the quality of the concentrate (**Figure 43**D).

The feed slurry solid content has also found not to affect the product quality, as shown in **Figure 44**.

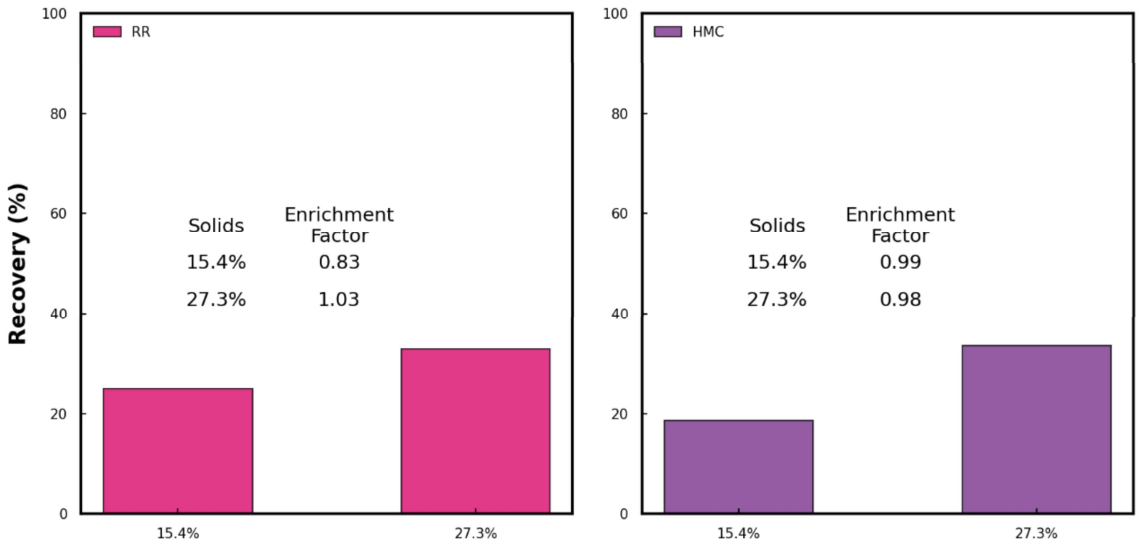

Figure 44. Effect of feed solids content on REE recovery and enrichment using froth flotation for select samples

Since liberation of mineral is one of the factors affecting the flotation concentrating process, the feed particle grind size was decreased from -50 to -106 µm top size. The flotation both coarse and fine feed material does not show any marked improvement in the REE flotation response, as shown in **Figure 45**. However, the particle size of REE mineral grain in the sample are generally less than 25 µm (**Figure 35**). Hence, future study should reduce the grind size further down to p80 of 25 µm or suitably lower and test the response of flotation.

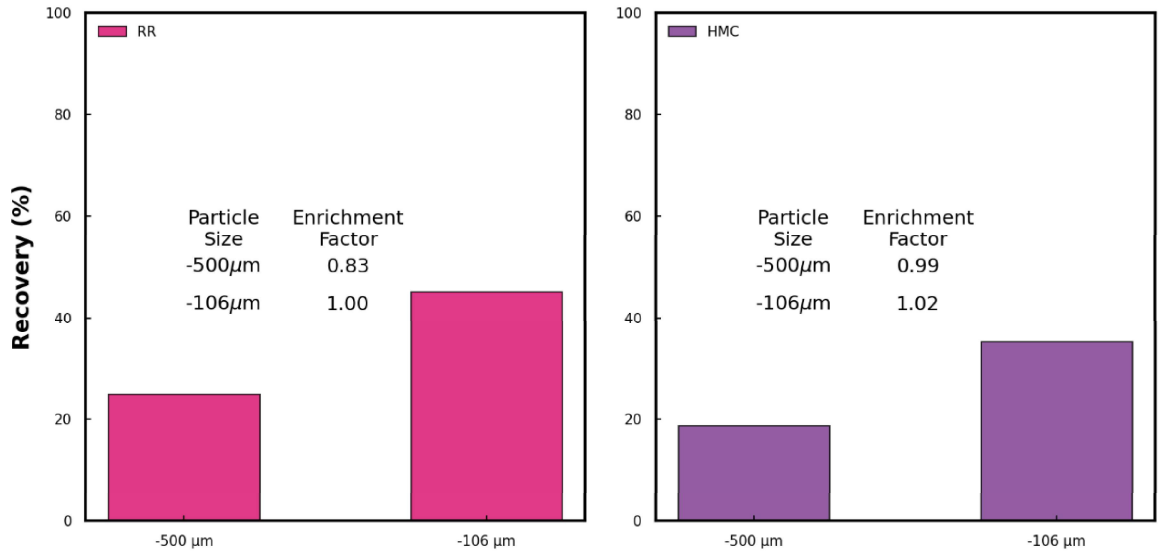

Figure 45. Effect of particle size on REE recovery and enrichment using froth flotation for select samples

The flotation modifiers such as sodium silicate has shown to depress gangue minerals including silicates, carbonates such as dolomite, calcite. However, a very large doses of depressant was needed for successful flotation of REE minerals (Jordens et al., 2013). The effect of depressant on the REE flotation was performed for both samples and results are shown in **Figure 46**. The test was carried out in two stages, where residue from stage 1 was used as feed for second stage with and without depressant. Without depressant, both samples shown a slight improvement in stage 2 concentrate EF. As the depressant dose increased from 0 to 25 g/t, the second stage concentrate EF for both samples shown a marked improvement. With depressant, the concentrate EF of 1.17 and 1.14 has achieved for RR and HMC sample, respectively.

The behaviour of sample to different flotation conditions has indicated that flotation could be one of the techniques shown REE concentrating potential in the sample. However, due to limited scope of this study, further detailed studies are required to optimize conditions to achieve very selective REE flotation for industrial applications.

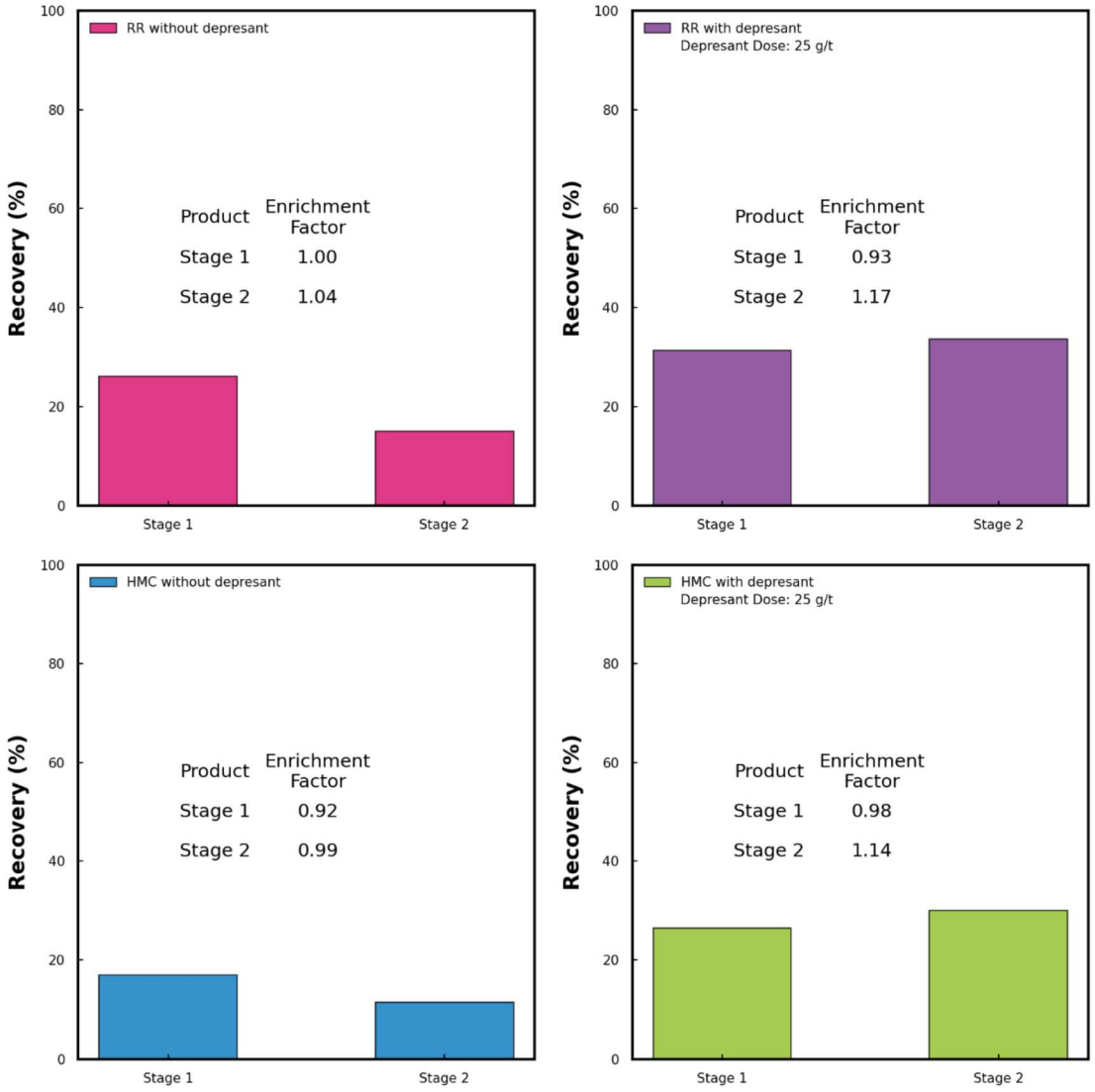

Figure 46. Effect of staged addition of depressant on REE recovery and enrichment using froth flotation for select samples (Conditions: -106 μm, 500 g/t collector, 100 g/t frother, 9.5 pH, 15.4% solids, 20°C)

5.0 REE Leaching Extraction Results

The typical REE extraction flowsheet involves mining, physical concentration, and hydrometallurgical extraction steps including leaching, impurities removal, and a separation and purification process to obtain mixed rare earth oxide (REO) or individual REO. Depending on the type of RE concentrate and its final grade, different leaching techniques are practiced with varied complexity levels for the decomposition of the concentrate/whole ore, including direct leaching, acid roasting, caustic cracking, and chlorination.

In this study, the amenability of REE extraction using leaching was performed using direct acid leaching (DL) and acid baking (ABWL) process for selected sample and results are depicted on **Figure 47**. With direct acid leaching using 1M sulfuric acid, the total REE extraction for the samples varied from 13% to 34%, which was increased significantly using ABWL process. the REE extraction ranges between 45 and 70% for ABWL technique.

Further, REE extraction with direct acid leaching favoured towards HREE (HREE: Tb to Lu + Y) compared to LREE (LREE: La to Gd + Sc). The HREE extraction varied from 25 to 50% among the different samples, which roughly twice the extraction of LREE. Similar extraction behaviour between LREE and HREE was also reported previously in the Illinois basin coal source (Yang et al., 2019). The preferential leaching towards one group was attributed to the different mode of occurrences between these two groups of REE. Finkelman et al. (2018) quantified that in high-rank coals 10–30% of REE can be associated with carbonates. The observation indicates of a roughly 13 to 30% REE association with carbonates in this study, as shown in **Figure 27**, matches the general trend for bituminous coal reported in the literature. This trend of higher HREE leaching capability can significantly impact the economics of the project since it should be noted that Heavy REE generally yield more price in the market compared to LREE. Further detailed studies are required to optimize the process conditions for industrial scale application.

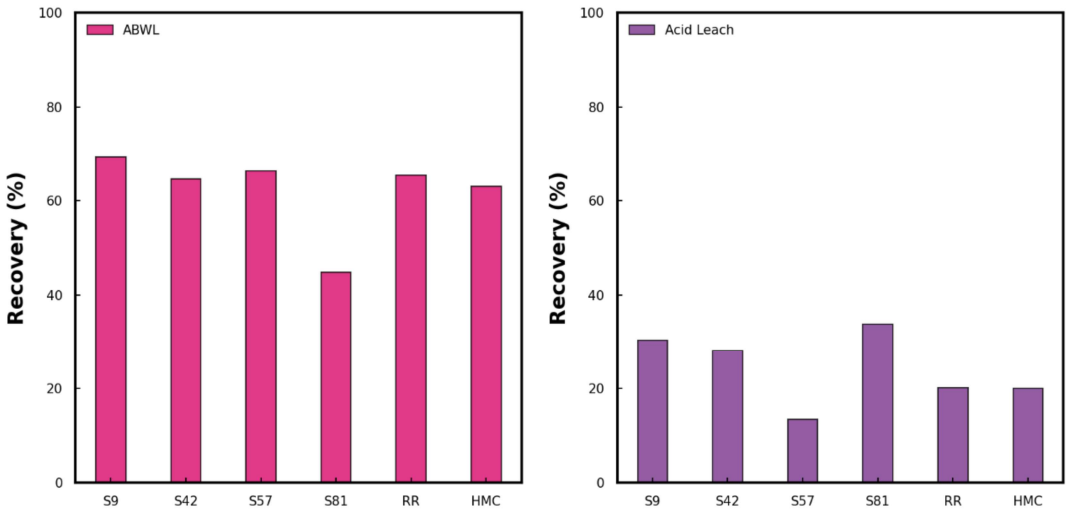

Figure 47 REE leaching extraction for select samples using two different leaching techniques: Direct acid leaching and Acid baking followed by water leaching (ABWL)

6.0 Summary and Conclusions

In this study, REE database from field collected samples was created and the feasibility of concentrating REE from East Kootenay Coalfield samples was explored using conventional separation technologies. The major findings of the research are listed below:

- One of the main objectives of the study was the development of a rare-earth element (REE) database for the East Kootenay coalfield. In this regard, more than 100 coal samples from the East Kootenay coal deposits were tested for the presence of REE and it was found that total REE concentrations on ash basis varied from 91 to 686 ppm.
- The preliminary economic analysis of the database results has shown that East Kootenay coalfield samples could be REE feed source with development of suitable extraction process.
- REE deportment analysis using flotation of coal samples indicated that most of the REE in the sample reports to middlings and tailing streams. Sequential extraction results further explained the inorganic association of REE in the samples.
- Mineralogical analysis of the select samples has shown that monazite, xenotime, and zircon are the dominant REE bearing minerals in the sample and REE minerals were generally locked in the clay matrix.
- Because of the dominant inorganic association (mineral matter) of REE in the given sample, waste streams from the coal processing plant were identified as potential feed sources for extracting REE since cost of mining and preparation would be absorbed with coal process itself. Waste streams from coal plant would also reduce any further land disturbance for REE feed source.
- Preliminary assessment was conducted on concentrating the REE using typical physical separation process used in the conventional REE ore deposits. The results shown that density-based separation and flotation was found to be most suitable enrichment process. However, further detailed focused study needs to be carried out in future for optimizing and industrial scale application. Further, REE concentration using magnetic separation was found to be ineffective due to fine grained nature of REE minerals in the sample studied.
- Direct extraction of REE without physical preconcentration was also performed using direct acid leaching and acid-baking process. With leaching, highest REE extraction of around 70% was achieved for preliminary scoping test.
- With detailed study, the combination of physical concentration and leaching based flowsheet can be developed for successful exploitation of REE from the BC coal-based source.

Acknowledgments

Financial support for the project (N0. 2018-002) from Geoscience BC is greatly appreciated. The authors gratefully acknowledge the scholarship received from Geoscience BC and Mitacs (2017–2020).

References

Alipanah, M., Park, D. M., Middleton, A., Dong, Z., Hsu-Kim, H., Jiao, Y., & Jin, H. (2020). Techno-Economic and Life Cycle Assessments for Sustainable Rare Earth Recovery from Coal Byproducts using Biosorption. *ACS Sustainable Chemistry and Engineering*, *8*(49), 17914–17922. https://doi.org/10.1021/ACSSUSCHEMENG.0C04415

ASTM. (2012a). *D2013/D2013M-12 Standard practice for preparing coal samples for analysis*. ASTM International. https://doi.org/10.1520/D2013_D2013M-12

ASTM. (2012b). *D3174-12 Standard test method for ash in the analysis sample of coal and coke from coal*. ASTM International. https://doi.org/10.1520/D31

ASTM. (2013). *D3172-13 Standard practice for proximate analysis of coal and coke*. ASTM International. https://doi.org/10.1520/D3172

ASTM. (2017a). *D3173/D3173-17a Standard test method for moisture in the analysis sample of coal and coke*. ASTM International. https://doi.org/10.1520/D3173_D3173M-17A

ASTM. (2017b). *D3175-17 Standard test method for volatile matter in the analysis sample of coal and coke*. ASTM International. https://doi.org/10.1520/D3175-17

Bai, J., Wang, Q., Wei, Y., & Liu, T. (2011). Geochemical occurrences of rare earth elements in oil shale from Huadian. *Journal of Fuel Chemistry and Technology*, *39*(7), 489–494. https://doi.org/http://dx.doi.org/10.1016/S1872-5813(11)60032-7

Birk, D., & White, J. C. (1991). Rare earth elements in bituminous coals and underclays of the Sydney Basin, Nova Scotia: Element sites, distribution, mineralogy. *International Journal of Coal Geology*, *19*(1–4), 219–25 https://doi.org/10.1016/0166-5162(91)90022-B

Boatner, L. A. (2002). Synthesis, Structure, and Properties of Monazite, Pretulite, and Xenotime. *Reviews in Mineralogy and Geochemistry*, *48*(1), 87–12 https://doi.org/10.2138/RMG.2002.48.4

Bryan, R. C., Richers, D., Andersen, H. T., & Gray, T. (2015). *Assessment of Rare Earth Elemental Contents in Select United States Coal Basins*. https://doi.org/114-910178X-100-REP-R001-00

Bulatovic, S. M. (2010). Handbook of Flotation Reagents: Chemistry, Theory and Practice. In *Handbook*

of Flotation Reagents: Chemistry, Theory and Practice (Vol. 2). Elsevier. https://doi.org/10.1016/C2009-0-17331-2

Creelman, R. A., & Ward, C. R. (1996). A scanning electron microscope method for automated, quantitative analysis of mineral matter in coal. *International Journal of Coal Geology*, *30*, 249–269. https://ac.els-cdn.com/0166516295000437/1-s2.0-0166516295000437-main.pdf?_tid=021ab356-c4bd-11e7-b94a-0000 aab0f01&acdnat=1510170360_d9ea5e7856c69c57e76ba1f2bc5dc1a5

Dai, S., Chekryzhov, I. Y., Seredin, V. V., Nechaev, V. P., Graham, I. T., Hower, J. C., Ward, C. R., Ren, D., & Wang, X. (2016). Metalliferous coal deposits in East Asia (Primorye of Russia and South China): A review of geodynamic controls and styles of mineralization. *Gondwana Research*, *29*(1), 60–82. https://doi.org/10.1016/J.GR.2015.07.001

Dai, S., & Finkelman, R. B. (2018). Coal as a promising source of critical elements: Progress and future prospects. *International Journal of Coal Geology*, *186*, 155–164. https://doi.org/10.1016/J.COAL.2017.06.005

Dai, S., Li, D., Chou, C. L., Zhao, L., Zhang, Y., Ren, D., Ma, Y., & Sun, Y. (2008). Mineralogy and geochemistry of boehmite-rich coals: New insights from the Haerwusu Surface Mine, Jungar Coalfield, Inner Mongolia, China. *International Journal of Coal Geology*, *74*(3–4), 185–20 https://doi.org/10.1016/j.coal.2008.01.

Dai, S., Li, D., Ren, D., Tang, Y., Shao, L., & Song, H. (2004). Geochemistry of the late Permian No. 30 coal seam, Zhijin Coalfield of Southwest China: Influence of a siliceous low-temperature hydrothermal fluid. *Applied Geochemistry*, *19*(8), 1315–133 https://doi.org/10.1016/j.apgeochem.2003.12.

Dai, S., Ren, D., Chou, C.-L., Finkelman, R. B., Seredin, V. V, & Zhou, Y. (2012). Geochemistry of trace elements in Chinese coals: A review of abundances, genetic types, impacts on human health, and industrial utilization. *International Journal of Coal Geology*, *94*, 3–21. https://doi.org/10.1016/J.COAL.2011.02.0

Dai, S., Ren, D., & Li, S. (2002). Occurrence and sequential chemical extraction of rare earth elements in coals and Seam roofs. *Journal of China University of Mining & Technology*, *31*(5), 349–353.

Dai, S., Zhou, Y. P., Ren, D. Y., Wang, X. B., Li, D., & Zhao, L. (2007). Geochemistry and mineralogy of the Late Permian coals from the Songzo Coalfield, Chongqing, southwestern China. *Science in China, Series D: Earth Sciences*, *50*(5), 678–688. https://doi.org/10.1007/s11430-007-00

Davidson, R. (2000). *Modes of Occurence of Trace Elements in Coal: Results from an International*

Collaborative Programme.

Donald, R. L. (1984). *Sedimentology of the Mist Mountain formation, in the Fording River area, southeastern Canadian Rocky Mountains* [University of British Columbia]. https://doi.org/10.14288/1.0

Equeenuddin, S. M., Tripathy, S., Sahoo, P. K., & Ranjan, A. (2016). Geochemical characteristics and mode of occurrence of trace elements in coal at West Bokaro coalfield. *International Journal of Coal Science & Technology*, *3*(4), 399–406. https://doi.org/10.1007/s40789-016-01 x

Eskenazy, G.M. (1999). Aspects of the geochemistry of rare earth elements in coal: an experimental approach. *International Journal of Coal Geology*, *38*(3), 285–295 https://doi.org/10.1016/S0166-5162(98)00027-5

Eskenazy, Greta M. (1987). Rare earth elements in a sampled coal from the Pirin deposit, Bulgaria. *International Journal of Coal Geology*, *7*(3), 301–314 https://doi.org/10.1016/0166 5162(87)90

Eterigho-Ikelegbe, O., Harrar, H., & Bada, S. (2021). Rare earth elements from coal and coal discard – A review. *Minerals Engineering*, *173*, 107187. https://doi.org/10.1016/J.MINENG.2021.107187

Finkelman, R. B. (1981). *Modes of occurrence of trace elements in coal* [University of Maryland & United States Geological survey]. https://pubs.er.usgs.gov/publication/ofr8199

Finkelman, R. B. (1994). Modes of occurrence of potentially hazardous elements in coal: levels of confidence. *Fuel Processing Technology*, *39*(1–3), 21–34. https://doi.org/10.1016/0378-3820(94)90169-4

Finkelman, R. B. (2004). Potential health impacts of burning coal beds and waste banks. *International Journal of Coal Geology*, *59*, 19–24. https://doi.org/10.1016/j.coal.2003.11.002

Finkelman, R. B., Palmer, C. A., Krasnow, M. R., Aruscavage, P. J., Sellers, G. A., & Dulong, F. T. (1990). Combustion and leaching behavior of elements in the Argonne Premium Coal Samples. *Energy & Fuels*, *4*(6), 755–766. https://doi.org/10.1021/ef00024a024

Finkelman, R. B., Palmer, C. A., & Wang, P. (2018). Quantification of the modes of occurrence of 42 elements in coal. *International Journal of Coal Geology*, *185*, 138–160. https://doi.org/10.1016/J.COAL.2017.09.005

Gibson, D. W. (1985). *Stratigraphy, sedimentology and depositional environments of the coal-bearing Jurassic-Cretaceous Kootenay Group, Alberta and British Columbia* (p. 108). Ministry of Supply and Services Canada. http://publications.gc.ca/collections/collection_2016/rncan-nrcan/M42-357-

eng.pdf

Grieve, D. A. (1993). Geology and rank distribution of the Elk Valley coalfield, southeastern British Columbia (82G115, 82J12, 6, 7, 10, 11). In *British Columbia Ministry of Energy, Mines and Petroleum Resources*. http://www.empr.gov.bc.ca/Mining/Geoscience/PublicationsCatalogue/BulletinInformation/BulletinsAfter1940/Documents/Bull82.pdf

Holuszko, M. E. (1994). *Washability characteristics of British Columbia coals*. http://www.empr.gov.bc.ca/Mining/Geoscience/PublicationsCatalogue/Papers/Documents/Paper1994-2.pdf

Hower, J. C., Berti, D., Hochella, M. F., & Mardon, S. M. (2018). Rare earth minerals in a "no tonstein" section of the Dean (Fire Clay) coal, Knox County, Kentucky. *International Journal of Coal Geology*, *193*, 73–86. https://doi.org/10.1016/J.COAL.2018.05.001

Hower, J. C., Berti, D., Hochella, M. F., Rimmer, S. M., & Taulbee, D. N. (2018). Submicron-scale mineralogy of lithotypes and the implications for trace element associations: Blue Gem coal, Knox County, Kentucky. *International Journal of Coal Geology*, *192*, 73–82. https://doi.org/10.1016/J.COAL.2018.04.

Hower, J. C., Ruppert, L. F., & Eble, C. F. (1999). Lanthanide, yttrium, and zirconium anomalies in the Fire Clay coal bed, Eastern Kentucky. *International Journal of Coal Geology*, *39*(1–3), 141–153. https://doi.org/10.1016/S0166-5162(98)00043-3

Huggins, F. E., & Huffman, G. P. (2004). How do lithophile elements occur in organic association in bituminous coals? *International Journal of Coal Geology*, *58*(3), 193–204. https://doi.org/10.1016/J.COAL.2003.10.009

Jordens, A., Cheng, Y. P., & Waters, K. E. (2013). A review of the beneficiation of rare earth element bearing minerals. *Minerals Engineering*, *41*, 97–114. https://doi.org/10.1016/J.MINENG.2012.10.017

Krishnamurthy, N., & Gupta, C. (2016). *Extractive Metallurgy of Rare Earths* (2nd ed.). CRC Press. https://doi.org/10.1201/b19055

Laskowski, J. (Janusz). (2001). *Coal flotation and fine coal utilization* (1st ed.). Elsevier.

Leckie, D. A. (1997). *Evolution of fluvial landscapes in the Western Canada foreland basin : late Jurassic to the modern*. Geological Survey of Canada.

Marion, C., Lin, R., & Waters, K. E. (2020). A review of reagents applied to rare earth mineral flotation.

Advances in Colloid and Interface Science, *279*(102142), 25. https://doi.org/https://doi.org/10.1016/j.cis.2020.102142

Miall, A. D. (2009). Initiation of the Western Interior foreland basin. *Geology*, *37*(4), 383–38 https://doi.org/10.1130/FOCUS042009.1

Mills, D., Seward, A. J., & Knight, A. J. (2016). *NI 43 - 101 Technical Report on the Mineral Resource and Mineral Reserve Estimates for the Greenhills Operation*. http://www.sedar.com/GetFile.do?lang=EN&docClass=24&issuerNo=00001787&issuerType=03&projectNo=02451483&docId=3874164

Ministry of Energy Mines and Low Carbon. (2021). *British Columbia coal industry overview 2020*. https://www2.gov.bc.ca/gov/content/industry/mineral-exploration-mining/british-columbia-geological-survey/publications

Mohanty, M. K., Honaker, B. Q., Patwardhan, A., & Ho, K. (1998). Coal Flotation Washability : An Evaluation of theTraditional Procedures. *Coal Preparation*, *19*(1–2), 33–49. https://doi.org/10.1080/07349349808945

Moldoveanu, G. A., & Papangelakis, V. G. (2012). Recovery of rare earth elements adsorbed on clay minerals: I. Desorption mechanism. *Hydrometallurgy*, *117–118*, 71–78. https://doi.org/10.1016/j.hydromet.2012.02.007

Moldoveanu, G. A., & Papangelakis, V. G. (2013). Recovery of rare earth elements adsorbed on clay minerals: II. Leaching with ammonium sulfate. *Hydrometallurgy*, *131–132*, 158–166. https://doi.org/10.1016/J.HYDROMET.2012.10.011

Nieto, A., & Zhang, K. Y. (2013). Cutoff grade economic strategy for byproduct mineral commodity operation: rare earth case study. *Mining Technology*, *122*(3), 166–171. https://doi.org/10.1179/1743286312Y.0000000025

Pavel, C. C., Lacal-Arántegui, R., Marmier, A., Schüler, D., Tzimas, E., Buchert, M., Jenseit, W., & Blagoeva, D. (2017). Substitution strategies for reducing the use of rare earths in wind turbines. *Resources Policy*, *52*, 349–357. https://doi.org/10.1016/j.resourpol.2017.04.010

Pavez, O., Brandao, P. R. G., & Peres, A. E. C. (1996). Adsorption of oleate and octyl-hydroxamate on to rare-earths minerals. *Minerals Engineering*, *9*(3), 357–366. https://doi.org/10.1016/0 6875(96)00020-9

Rao, P. C., & Gluskoter, H. J. (1973). *DEPARTMENT OF REGISTRATION AND EDUCATION STATE OF ILLINOIS Occurrence and Distribution of Minerals in llinois Coals*.

https://www.ideals.illinois.edu/bitstream/handle/2142/42747/occurrencedistri476raoc.pdf?sequence=2

Seredin, V. V. (1996). Rare earth element-bearing coals from the Russian Far East deposits. *International Journal of Coal Geology*, *30*(1), 101–129 https://doi.org/10.1016/0166-5162(95)00039-9

Seredin, V. V., & Dai, S. (2012). Coal deposits as potential alternative sources for lanthanides and yttrium. *International Journal of Coal Geology*, *94*, 67–93. https://doi.org/10.1016/j.coal.2011.11.00

Seredin, V. V., & Finkelman, R. B. (2008). Metalliferous coals: A review of the main genetic and geochemical types. *International Journal of Coal Geology*, *76*(4), 253–289 https://doi.org/10.1016/J.COAL.2008.07.016

Standards Australia. (1998). *AS 4156.2.2-1998 (R2013) Coal preparation Higher rank coal - Froth flotation - Sequential procedure* (p. 11). Standards Australia. https://infostore.saiglobal.com/en-us/standards/as-4156-2-2-1998-r2013--311563

Stein, H. J. (2014). Dating and Tracing the History of Ore Formation. *Treatise on Geochemistry: Second Edition*, *13*, 87–118. https://doi.org/10.1016/B978-0-08-095975-7.01104-9

Swaine, D. J. (1990). *Trace elements in coal*. Butterworth.

Tessier, A., Campbell, P. G. C., & Bisson, M. (1979). Sequential Extraction Procedure for the Speciation of Particulate Trace Metals. *Analytical Chemistry*, *51*(7), 844–85 https://doi.org/10.1021/ac50043a017

US Department of Energy. (n.d.). *Critical Minerals Sustainability Program*. Retrieved September 15, 2022, from https://www.netl.doe.gov/coal/rare-earth-elements/program-overview/background

Wall, F. (2020). Rare earth elements. In S. Elias & D. Alderton (Eds.), *Encylopedia of Geology* (Second, pp. 680–693). Elsevier. https://doi.org/10.1016/B978-0-08-102908-4.00101-6

Wang, W., Qin, Y., Sang, S., Zhu, Y., Wang, C., & Weiss, D. J. (2008). Geochemistry of rare earth elements in a marine influenced coal and its organic solvent extracts from the Antaibao mining district, Shanxi, China. *International Journal of Coal Geology*, *76*(4), 309–31 https://doi.org/10.1016/J.COAL.2008.08.01

Wills, B. A. (2015). *Mineral Processing Technology: An Introduction to Practical Aspects of Ore Treatment and Mineral Recovery*. Butterworth-Heinemann.

Wilschefski, S. C., & Baxter, M. R. (2019). Inductively Coupled Plasma Mass Spectrometry: Introduction

to Analytical Aspects. *The Clinical Biochemist Reviews*, *40*(3), 115–133. https://doi.org/10.33176/AACB-19-00024

Yang, X., Werner, J., & Honaker, R. Q. (2019). Leaching of rare Earth elements from an Illinois basin coal source. *Journal of Rare Earths*, *37*(3), 312–321. https://doi.org/10.1016/j.jre.2018.07.003

Zhang, J., & Edwards, C. (2012). A review of rare earth mineral processing technology. *44th Annual Meeting of The Canadian Mineral Processors. CIM, Ottawa*, *79*.

Zhang, W., Noble, A., Yang, X., & Honaker, R. (2020). A Comprehensive Review of Rare Earth Elements Recovery from Coal-Related Materials. *Minerals*, *10*(5), 479. https://doi.org/10.3390/min10050451

Zhang, W., Rezaee, M., Bhagavatula, A., Li, Y., Groppo, J., & Honaker, R. (2015). A review of the occurrence and promising recovery methods of rare earth elements from coal and coal by-products. *International Journal of Coal Preparation and Utilization*, *35*(6), 281–294. https://doi.org/10.1080/19392699.2015.1033097

Zhang, Y., Liu, G., Chou, C.-L., Wang, L., & Kang, Y. (2007). Sequential solvent extraction for the modes of occurrence of selenium in coals of different ranks from the Huaibei Coalfield, China. *Geochemical Transactions*, *8*(1), 14. https://doi.org/10.1186/1467-4866-8-14

Zheng, L., Liu, G., Qi, C., Zhang, Y., & Wong, M. (2008). The use of sequential extraction to determine the distribution and modes of occurrence of mercury in Permian Huaibei coal, Anhui Province, China. *International Journal of Coal Geology*, *73*(2), 139–155. https://doi.org/10.1016/j.coal.2007.04.001

Zhou, C. C., Zhang, N. N., Peng, C. Bin, Cong, L. F., Ouyang, C. H., & Han, R. (2016). Arsenic in Coal: Modes of Occurrence, Distribution in Different Fractions, and Partitioning Behavior during Coal Separation - A Case Study. *Energy and Fuels*, *30*(4), 3233–3240. https://doi.org/10.1021/acs.energyfuels.5b02669